Tearing Mode Dynamics in Tokamak Plasmas

R. Fitzpatrick *
Institute for Fusion Studies,
Department of Physics,
University of Texas at Austin,
Austin TX 78712, USA

Contents

*rfitzp@utexas.edu

1 Introduction

2 Plasma Fluid Theory

2.1 Introduction

The aim of this section is to introduce the fundamental plasma fluid theory that underpins the analysis of tearing mode dynamics in tokamak plasmas.

2.2 Fundamental Quantities

Consider an idealized tokamak plasma consisting of an equal number of electrons, with mass m_e and charge $-e$ (here, e denotes the magnitude of the electron charge), and ions, with mass m_i and charge $+e$. We shall employ the symbol

$$T_s = \frac{1}{3}\, m_s \,\langle v_s^2 \rangle \tag{1}$$

to denote a *kinetic temperature* measured in units of energy. Here, v is a particle speed, and the angular brackets denote an ensemble average (Reif 1965). The kinetic temperature of species s is a measure of the mean kinetic energy of particles of that species. (Here, s represents either e for electrons, or i for ions.)

Quasi-neutrality demands that

$$n_i \simeq n_e, \tag{2}$$

where n_s is the *particle number density* (that is, the number of particles per cubic meter) of species s (Fitzpatrick 2015).

We can estimate typical particle speeds in terms of the so-called *thermal speed*,

$$v_{t\,s} = \left(\frac{2\,T_s}{m_s}\right)^{1/2}. \tag{3}$$

In a tokamak plasma, the ambient magnetic field, $\mathbf{B}$, is strong enough to significantly alter charged particle trajectories. Consequently, tokamak plasmas are highly anisotropic, responding differently to forces that are parallel and perpendicular to the direction of $\mathbf{B}$. As is well known, charged particles react to the Lorentz force by freely streaming in the direction of $\mathbf{B}$, while executing circular *gyro-orbits* in the plane perpendicular to $\mathbf{B}$ (Fitzpatrick 2008). The typical *gyroradius* of a charged particle gyrating in a magnetic field is given by

$$\rho_s = \frac{v_{t\,s}}{\Omega_s}, \tag{4}$$

where

$$\Omega_s = \frac{e\,B}{m_s} \tag{5}$$

is the *gyrofrequency* associated with the gyration.

The electron-ion and ion-ion *collision times* are written

$$\tau_e = \frac{6\sqrt{2}\pi^{3/2}\,\epsilon_0^2\,\sqrt{m_e}\;T_e^{3/2}}{\ln\Lambda_c\,e^4\,n_e}, \tag{6}$$

and

$$\tau_i = \frac{12\pi^{3/2}\,\epsilon_0^2\,\sqrt{m_i}\;T_i^{3/2}}{\ln\Lambda_c\,e^4\,n_e}, \tag{7}$$

respectively (Fitzpatrick 2015). Here, $\ln\Lambda_c \simeq 15$ is the *Coulomb logarithm* (Richardson 2019). Note that τ_e is the typical time required for the cumulative effect of electron-ion collisions to deviate the path of an electron through 90°. Likewise, τ_i is the typical time required for the cumulative effect of ion-ion collisions to deviate the path of an ion through 90°.

2.3 Braginskii Equations

The electron and ion fluid equations in a collisional plasma take the form:

$$\frac{d_e n}{dt} + n\,\nabla\cdot\mathbf{V}_e = 0, \tag{8}$$

$$m_e\,n\,\frac{d_e\mathbf{V}_e}{dt} + \nabla p_e + \nabla\cdot\boldsymbol{\pi}_e + e\,n\,(\mathbf{E}+\mathbf{V}_e\times\mathbf{B}) = \mathbf{F}, \tag{9}$$

$$\frac{3}{2}\frac{d_e p_e}{dt} + \frac{5}{2}\,p_e\,\nabla\cdot\mathbf{V}_e + \boldsymbol{\pi}_e : \nabla\mathbf{V}_e + \nabla\cdot\mathbf{q}_e = w_e, \tag{10}$$

and

$$\frac{d_i n}{dt} + n\,\nabla\cdot\mathbf{V}_i = 0, \tag{11}$$

$$m_i\,n\,\frac{d_i\mathbf{V}_i}{dt} + \nabla p_i + \nabla\cdot\boldsymbol{\pi}_i - e\,n\,(\mathbf{E}+\mathbf{V}_i\times\mathbf{B}) = -\mathbf{F}, \tag{12}$$

$$\frac{3}{2}\frac{d_i p_i}{dt} + \frac{5}{2}\,p_i\,\nabla\cdot\mathbf{V}_i + \boldsymbol{\pi}_i : \nabla\mathbf{V}_i + \nabla\cdot\mathbf{q}_i = w_i, \tag{13}$$

respectively. Equations (8)–(13) are called the *Braginskii equations*, because they were first obtained in a celebrated article by S.I. Braginskii (Braginskii 1965). Here, n is the electron number density, $\mathbf{V}_s$ the species-s flow velocity, $p_s = n\,T_s$ the species-s scalar pressure, $\boldsymbol{\pi}_s$ the species-s viscosity tensor, $\mathbf{F}$ the collisional friction force density, $\mathbf{q}_s$ the species-s heat flux density, w_s the species-s collisional heating rate density, and $\mathbf{E}$ the ambient electric field-strength. Moreover, $d_e/dt \equiv \partial/\partial t + \mathbf{V}_e\cdot\nabla$ and $d_i/dt \equiv \partial/\partial t + \mathbf{V}_i\cdot\nabla$.

A tokamak plasma is *highly magnetized*. In other words,

$$\Omega_i\,\tau_i, \quad \Omega_e\,\tau_e \gg 1, \tag{14}$$

which implies that the electron and ion gyroradii are much smaller than the corresponding mean-free-paths between 90° collisional scattering events. In this limit, a standard two-Laguerre-polynomial Chapman-Enskog closure scheme (Chapman & Cowling 1953; Braginskii 1965) yields

$$\mathbf{F} = n\,e\left(\frac{\mathbf{j}_\parallel}{\sigma_\parallel} + \frac{\mathbf{j}_\perp}{\sigma_\perp}\right) - 0.71\,n\,\nabla_\parallel T_e - \frac{3\,n}{2\,\Omega_e\,\tau_e}\,\mathbf{b}\times\nabla_\perp T_e, \tag{15}$$

$$w_i = \frac{3\,m_e}{m_i}\frac{n\,(T_e - T_i)}{\tau_e}, \tag{16}$$

$$w_e = -w_i + \frac{\mathbf{j}\cdot\mathbf{F}}{n\,e}. \tag{17}$$

Here, $\mathbf{b} = \mathbf{B}/B$ is a unit vector parallel to the magnetic field, and $\mathbf{j} = n\,e\,(\mathbf{V}_i - \mathbf{V}_e)$ is the plasma current density. Moreover, the *parallel electrical conductivity* is given by

$$\sigma_\parallel = 1.96\,\frac{n\,e^2\,\tau_e}{m_e}. \tag{18}$$

whereas the *perpendicular electrical conductivity* takes the form

$$\sigma_\perp = 0.51\,\sigma_\parallel = \frac{n\,e^2\,\tau_e}{m_e}. \tag{19}$$

Note that $\nabla_\parallel(\cdots) \equiv [\mathbf{b}\cdot\nabla(\cdots)]\,\mathbf{b}$ denotes a gradient parallel to the magnetic field, whereas $\nabla_\perp \equiv \nabla - \nabla_\parallel$ denotes a gradient perpendicular to the magnetic field. Likewise, $\mathbf{j}_\parallel \equiv (\mathbf{b}\cdot\mathbf{j})\,\mathbf{b}$ represents the component of the plasma current density flowing parallel to the magnetic field, whereas $\mathbf{j}_\perp \equiv \mathbf{j} - \mathbf{j}_\parallel$ represents the perpendicular component of the plasma current density.

In a highly magnetized plasma, the electron and ion heat flux densities are written

$$\mathbf{q}_e = -\kappa_{\parallel\,e}\,\nabla_\parallel T_e - \kappa_{\perp\,e}\,\nabla_\perp T_e - \kappa_{\times\,e}\,\mathbf{b}\times\nabla_\perp T_e - 0.71\,\frac{T_e}{e}\,\mathbf{j}_\parallel - \frac{3\,T_e}{2\,\Omega_e\,\tau_e\,e}\,\mathbf{b}\times\mathbf{j}_\perp, \tag{20}$$

$$\mathbf{q}_i = -\kappa_{\parallel\,i}\,\nabla_\parallel T_i - \kappa_{\perp\,i}\,\nabla_\perp T_i + \kappa_{\times\,i}\,\mathbf{b}\times\nabla_\perp T_i, \tag{21}$$

respectively. Here, the *parallel thermal conductivities*, which control the diffusion of heat parallel to magnetic field-lines, are given by

$$\kappa_{\parallel\,e} = 3.2\;\frac{n\,\tau_e\,T_e}{m_e}, \tag{22}$$

$$\kappa_{\parallel\,i} = 3.9\;\frac{n\,\tau_i\,T_i}{m_i}, \tag{23}$$

whereas the *perpendicular thermal conductivities*, which control the diffusion of heat perpendicular to magnetic flux-surfaces, take the form

$$\kappa_{\perp\,e} = 4.7\,\frac{n\,T_e}{m_e\,\Omega_e^2\,\tau_e}, \tag{24}$$

$$\kappa_{\perp\, i} = 2\,\frac{n\,T_i}{m_i\,\Omega_i^2\,\tau_i}. \tag{25}$$

Finally, the *cross thermal conductivities*, which control the flow of heat within magnetic flux-surfaces, are written

$$\kappa_{\times\, e} = \frac{5\,n\,T_e}{2\,m_e\,\Omega_e}, \tag{26}$$

$$\kappa_{\times\, i} = \frac{5\,n\,T_i}{2\,m_i\,\Omega_i}. \tag{27}$$

In order to describe the viscosity tensor in a magnetized plasma, it is helpful to define the *rate-of-strain tensor*

$$W_{\alpha\beta} = \frac{\partial V_\alpha}{\partial r_\beta} + \frac{\partial V_\beta}{\partial r_\alpha} - \frac{2}{3}\,\nabla\cdot\mathbf{V}\,\delta_{\alpha\beta}. \tag{28}$$

Obviously, there is a separate rate-of-strain tensor for the electron and ion fluids. It is easily demonstrated that this tensor is zero if the fluid translates, or rotates as a rigid body, or if it undergoes isotropic compression. Thus, the rate-of-strain tensor measures the deformation of fluid volume elements.

In a highly magnetized plasma, the viscosity tensor is conveniently described as the sum of five component tensors,

$$\boldsymbol{\pi} = \sum_{n=0,4} \boldsymbol{\pi}_n, \tag{29}$$

where

$$\boldsymbol{\pi}_0 = -3\,\eta_0\,\left(\mathbf{bb} - \frac{1}{3}\,\mathbf{I}\right)\left(\mathbf{bb} - \frac{1}{3}\,\mathbf{I}\right) : \nabla\mathbf{V}, \tag{30}$$

with

$$\boldsymbol{\pi}_1 = -\eta_1\left[\mathbf{I}_\perp\cdot\mathbf{W}\cdot\mathbf{I}_\perp + \frac{1}{2}\,\mathbf{I}_\perp\,(\mathbf{b}\cdot\mathbf{W}\cdot\mathbf{b})\right], \tag{31}$$

and

$$\boldsymbol{\pi}_2 = -4\,\eta_1\,\left(\mathbf{I}_\perp\cdot\mathbf{W}\cdot\mathbf{bb} + \mathbf{bb}\cdot\mathbf{W}\cdot\mathbf{I}_\perp\right). \tag{32}$$

plus

$$\boldsymbol{\pi}_3 = \frac{\eta_3}{2}\,\left(\mathbf{b}\times\mathbf{W}\cdot\mathbf{I}_\perp - \mathbf{I}_\perp\cdot\mathbf{W}\times\mathbf{b}\right), \tag{33}$$

and

$$\boldsymbol{\pi}_4 = 2\,\eta_3\,\left(\mathbf{b}\times\mathbf{W}\cdot\mathbf{bb} - \mathbf{bb}\cdot\mathbf{W}\times\mathbf{b}\right). \tag{34}$$

Here, $\mathbf{I}$ is the identity tensor, and $\mathbf{I}_\perp = \mathbf{I} - \mathbf{bb}$. The previous expressions are valid for both electrons and ions.

The tensor $\boldsymbol{\pi}_0$ describes what is known as *parallel viscosity*. This is a viscosity that controls the variation along magnetic field-lines of the velocity component parallel to field-lines. The parallel viscosity coefficients are given by

$$\eta_{0\, e} = 0.73\,n\,\tau_e\,T_e, \tag{35}$$

$$\eta_{0\,i} = 0.96\, n\, \tau_i\, T_i. \tag{36}$$

The tensors $\boldsymbol{\pi}_1$ and $\boldsymbol{\pi}_2$ describe what is known as *perpendicular viscosity*. This is a viscosity that controls the variation perpendicular to magnetic field-lines of the velocity components perpendicular to field-lines. The perpendicular viscosity coefficients are given by

$$\eta_{1\,e} = 0.51\, \frac{n\, T_e}{\Omega_e^2\, \tau_e}, \tag{37}$$

$$\eta_{1\,i} = \frac{3\, n\, T_i}{10\, \Omega_i^2\, \tau_i}. \tag{38}$$

Finally, the tensors $\boldsymbol{\pi}_3$ and $\boldsymbol{\pi}_4$ describe what is known as *gyroviscosity*. This is not really viscosity at all, because the associated viscous stresses are always perpendicular to the velocity, implying that there is no dissipation (i.e., viscous heating) associated with this effect. The gyroviscosity coefficients are given by

$$\eta_{3\,e} = -\frac{n\, T_e}{2\, \Omega_e}, \tag{39}$$

$$\eta_{3\,i} = \frac{n\, T_i}{2\, \Omega_i}. \tag{40}$$

2.4 Normalization of Braginskii Equations

As we have just seen, the Braginskii equations contain terms that describe a very wide range of different physical phenomena. For this reason, they are extremely complicated in nature. Fortunately, however, it is not generally necessary to retain all of the terms in these equations when investigating tearing mode dynamics in tokamak plasmas. In this section, we shall construct a systematic normalization scheme for the Braginskii equations that will enable us to determine which terms to keep, and which to discard, when investigating tearing mode dynamics.

It is convenient to split the friction force density, $\mathbf{F}$, into a component, $\mathbf{F}_U$, corresponding to resistivity, and a component, $\mathbf{F}_T$, corresponding to the so-called *thermal force density*. Thus,

$$\mathbf{F} = \mathbf{F}_U + \mathbf{F}_T, \tag{41}$$

where

$$\mathbf{F}_U = n\, e \left(\frac{\mathbf{j}_\parallel}{\sigma_\parallel} + \frac{\mathbf{j}_\perp}{\sigma_\perp} \right), \tag{42}$$

$$\mathbf{F}_T = -0.71\, n\, \nabla_\parallel T_e - \frac{3\, n}{2\, \Omega_e\, \tau_e}\, \mathbf{b} \times \nabla_\perp T_e. \tag{43}$$

Likewise, the electron collisional energy gain term, w_e, is split into a component, $-w_i$, corresponding to the energy lost per unit volume to the ions (in the ion rest frame), a component,

w_U, corresponding to work done by the friction force density, $\mathbf{F}_U$, and a component, w_T, corresponding to work done by the thermal force density, $\mathbf{F}_T$. Thus,

$$w_e = -w_i + w_U + w_T, \tag{44}$$

where

$$w_U = \frac{\mathbf{j}\cdot\mathbf{F}_U}{n\,e}, \tag{45}$$

$$w_T = \frac{\mathbf{j}\cdot\mathbf{F}_T}{n\,e}. \tag{46}$$

Finally, it is helpful to split the electron heat flux density, $\mathbf{q}_e$, into a diffusive component, $\mathbf{q}_{Te}$, and a convective component, $\mathbf{q}_{Ue}$. Thus,

$$\mathbf{q}_e = \mathbf{q}_{Te} + \mathbf{q}_{Ue}, \tag{47}$$

where

$$\mathbf{q}_{Te} = -\kappa_{\parallel\, e}\,\nabla_\parallel T_e - \kappa_{\perp\, e}\,\nabla_\perp T_e - \kappa_{\times\, e}\,\mathbf{b}\times\nabla_\perp T_e, \tag{48}$$

$$\mathbf{q}_{Ue} = 0.71\,\frac{T_e}{e}\,\mathbf{j}_\parallel - \frac{3\,T_e}{2\,\Omega_e\,\tau_e\,e}\,\mathbf{b}\times\mathbf{j}_\perp. \tag{49}$$

Let us, first of all, consider the electron fluid equations, which can be written:

$$\frac{d_e n}{dt} + n\,\nabla\cdot\mathbf{V}_e = 0, \tag{50}$$

$$m_e\,n\,\frac{d_e\mathbf{V}_e}{dt} + \nabla p_e + \nabla\cdot\boldsymbol{\pi}_e + e\,n\,(\mathbf{E}+\mathbf{V}_e\times\mathbf{B}) = \mathbf{F}_U + \mathbf{F}_T, \tag{51}$$

$$\frac{3}{2}\frac{d_e p_e}{dt} + \frac{5}{2}\,p_e\,\nabla\cdot\mathbf{V}_e + \boldsymbol{\pi}_e : \nabla\mathbf{V}_e + \nabla\cdot\mathbf{q}_{Te} + \nabla\cdot\mathbf{q}_{Ue} = -w_i + w_U + w_T. \tag{52}$$

Let $\bar{n}$, $\bar{v}_e$, $\bar{\tau}_e$, $\bar{l}_e = \bar{v}_e\,\bar{\tau}_e$, $\bar{B}$, and $\bar{\rho}_e = \bar{v}_e/(e\bar{B}/m_e)$ be typical values of the particle density, the electron thermal velocity, the electron collision time, the electron mean-free-path between collisions, the magnetic field-strength, and the electron gyroradius, respectively. Suppose that the typical spatial variation lengthscale of fluid variables is L. Let

$$\delta_e = \frac{\bar{\rho}_e}{L}, \tag{53}$$

$$\zeta_e = \frac{\bar{\rho}_e}{\bar{l}_e}, \tag{54}$$

$$\mu = \sqrt{\frac{m_e}{m_i}}. \tag{55}$$

All three of these parameters are assumed to be small compared to unity. Finally, the typical electron flow velocity is assumed to be of order $\delta_e\,\bar{v}_e$. This corresponds to the so-called *drift*

ordering in which the flow velocity is comparable to the curvature and grad-B particle drift velocities (Fitzpatrick 2015). The drift ordering is appropriate to tearing modes in tokamak plasmas, which are comparatively slowly growing instabilities.

We define the following normalized quantities:

$$\hat{n} = \frac{n}{\bar{n}}, \qquad \hat{v}_e = \frac{v_e}{\bar{v}_e}, \qquad \hat{\mathbf{r}} = \frac{\mathbf{r}}{L},$$

$$\widehat{\nabla} = L\,\nabla, \qquad \hat{t} = \frac{\delta_e\,\bar{v}_e\,t}{L}, \qquad \widehat{\mathbf{V}}_e = \frac{\mathbf{V}_e}{\delta_e\,\bar{v}_e},$$

$$\widehat{\mathbf{B}} = \frac{\mathbf{B}}{\bar{B}}, \qquad \widehat{\mathbf{E}} = \frac{\mathbf{E}}{\delta_e\,\bar{v}_e\,\bar{B}}, \qquad \widehat{\mathbf{j}} = \frac{\mathbf{j}}{n\,e\,\delta_e\,\bar{v}_e},$$

$$\hat{p}_e = \frac{p_e}{m_e\,\bar{n}\,\bar{v}_e^2}, \qquad \widehat{\boldsymbol{\pi}}_e = \frac{\boldsymbol{\pi}_e}{\delta_e^2\,\zeta_e^{-1}\,m_e\,\bar{n}\,\bar{v}_e^2}, \qquad \widehat{\mathbf{q}}_{Te} = \frac{\mathbf{q}_{Te}}{\delta_e\,\zeta_e^{-1}\,m_e\,\bar{n}\,\bar{v}_e^3},$$

$$\widehat{\mathbf{q}}_{Ue} = \frac{\mathbf{q}_{Ue}}{\delta_e\,m_e\,\bar{n}\,\bar{v}_e^3}, \qquad \widehat{\mathbf{F}}_U = \frac{\mathbf{F}_U}{\zeta_e\,m_e\,\bar{n}\,\bar{v}_e^2/L}, \qquad \widehat{\mathbf{F}}_T = \frac{\mathbf{F}_T}{m_e\,\bar{n}\,\bar{v}_e^2/L},$$

$$\widehat{w}_i = \frac{w_i}{\delta_e^{-1}\,\zeta_e\,\mu^2\,m_e\,\bar{n}\,\bar{v}_e^3/L}, \qquad \widehat{w}_U = \frac{w_U}{\delta_e\,\zeta_e\,m_e\,\bar{n}\,\bar{v}_e^3/L}, \qquad \widehat{w}_T = \frac{w_T}{\delta_e\,m_e\,\bar{n}\,\bar{v}_e^3/L}.$$

The normalization procedure is designed to make all hatted quantities $\mathcal{O}(1)$. The normalization of the electric field is chosen such that the $\mathbf{E}\times\mathbf{B}$ velocity is of similar magnitude to the electron diamagnetic velocity. (See Section 2.5.) Note that the parallel viscosity makes an $\mathcal{O}(1)$ contribution to $\widehat{\boldsymbol{\pi}}_e$, whereas the gyroviscosity makes an $\mathcal{O}(\zeta_e)$ contribution, and the perpendicular viscosity only makes an $\mathcal{O}(\zeta_e^2)$ contribution. Likewise, the parallel thermal conductivity makes an $\mathcal{O}(1)$ contribution to $\widehat{\mathbf{q}}_{Te}$, whereas the cross conductivity makes an $\mathcal{O}(\zeta_e)$ contribution, and the perpendicular conductivity only makes an $\mathcal{O}(\zeta_e^2)$ contribution. Similarly, the parallel components of $\mathbf{F}_T$ and $\mathbf{q}_{Ue}$ are $\mathcal{O}(1)$, whereas the perpendicular components are $\mathcal{O}(\zeta_e)$.

The normalized electron fluid equations take the form:

$$\frac{d_e\hat{n}}{d\hat{t}} + \hat{n}\,\widehat{\nabla}\cdot\widehat{\mathbf{V}}_e = 0, \tag{56}$$

$$\hat{n}\,\frac{d_e\widehat{\mathbf{V}}_e}{d\hat{t}} + \delta_e^{-2}\,\widehat{\nabla}\hat{p}_e + \zeta_e^{-1}\,\widehat{\nabla}\cdot\widehat{\boldsymbol{\pi}}_e + \delta_e^{-2}\,\hat{n}\,(\widehat{\mathbf{E}} + \widehat{\mathbf{V}}_e\times\widehat{\mathbf{B}}) = \delta_e^{-2}\,\zeta_e\,\widehat{\mathbf{F}}_U + \delta_e^{-2}\,\widehat{\mathbf{F}}_T, \tag{57}$$

$$\frac{3}{2}\frac{d_e\hat{p}_e}{d\hat{t}} + \frac{5}{2}\,\hat{p}_e\,\widehat{\nabla}\cdot\widehat{\mathbf{V}}_e + \delta_e^2\,\zeta_e^{-1}\,\widehat{\boldsymbol{\pi}}_e : \widehat{\nabla}\cdot\widehat{\mathbf{V}}_e + \zeta_e^{-1}\,\widehat{\nabla}\cdot\widehat{\mathbf{q}}_{Te} + \widehat{\nabla}\cdot\widehat{\mathbf{q}}_{Ue} = -\delta_e^{-2}\,\zeta_e\,\mu^2\,\widehat{w}_i + \zeta_e\,\widehat{w}_U + \widehat{w}_T. \tag{58}$$

The only large or small (compared to unity) quantities in these equations are the parameters δ_e, ζ_e, and μ. Here, $d_e/d\hat{t} \equiv \partial/\partial\hat{t} + \widehat{\mathbf{V}}_e\cdot\widehat{\nabla}$. It is assumed that $T_e \sim T_i$.

Let us now consider the ion fluid equations, which can be written:

$$\frac{d_i n}{dt} + n\,\nabla\cdot\mathbf{V}_i = 0, \tag{59}$$

$$m_i\, n\, \frac{d_i \mathbf{V}_i}{dt} + \nabla p_i + \nabla\cdot\boldsymbol{\pi}_i - e\, n\, (\mathbf{E} + \mathbf{V}_i\times\mathbf{B}) = -\mathbf{F}_U - \mathbf{F}_T, \tag{60}$$

$$\frac{3}{2}\frac{d_i p_i}{dt} + \frac{5}{2}\, p_i\, \nabla\cdot\mathbf{V}_i + \boldsymbol{\pi}_i : \nabla\mathbf{V}_i + \nabla\cdot\mathbf{q}_i = w_i. \tag{61}$$

It is convenient to adopt a normalization scheme for the ion equations which is similar to, but independent of, that employed to normalize the electron equations. Let $\bar{n}$, $\bar{v}_i$, $\bar{l}_i$, $\bar{B}$, and $\bar{\rho}_i = \bar{v}_i/(e\bar{B}/m_i)$ be typical values of the particle density, the ion thermal velocity, the ion mean-free-path between collisions, the magnetic field-strength, and the ion gyroradius, respectively. Suppose that the typical spatial variation lengthscale of fluid quantities is L. Let

$$\delta_i = \frac{\bar{\rho}_i}{L}, \tag{62}$$

$$\zeta_i = \frac{\bar{\rho}_i}{\bar{l}_i}, \tag{63}$$

$$\mu = \sqrt{\frac{m_e}{m_i}}. \tag{64}$$

All three of these parameters are assumed to be small compared to unity. As before, we adopt the drift ordering in which the typical ion flow velocity is assumed to be of order $\delta_i\,\bar{v}_i$.

We define the following normalized quantities:

$$\hat{n} = \frac{n}{\bar{n}}, \qquad \hat{v}_i = \frac{v_i}{\bar{v}_i}, \qquad \hat{\mathbf{r}} = \frac{\mathbf{r}}{L},$$

$$\widehat{\nabla} = L\,\nabla, \qquad \hat{t} = \frac{\delta_i\,\bar{v}_i\, t}{L}, \qquad \widehat{\mathbf{V}}_i = \frac{\mathbf{V}_i}{\delta_i\,\bar{v}_i},$$

$$\widehat{\mathbf{B}} = \frac{\mathbf{B}}{\bar{B}}, \qquad \widehat{\mathbf{E}} = \frac{\mathbf{E}}{\delta_i\,\bar{v}_i\,\bar{B}}, \qquad \widehat{\mathbf{j}} = \frac{\mathbf{j}}{n\, e\,\delta_i\,\bar{v}_i},$$

$$\hat{p}_i = \frac{p_i}{m_i\,\bar{n}\,\bar{v}_i^2}, \qquad \widehat{\boldsymbol{\pi}}_i = \frac{\boldsymbol{\pi}_i}{\delta_i^2\,\zeta_i^{-1}\, m_i\,\bar{n}\,\bar{v}_i^2}, \qquad \widehat{\mathbf{q}}_i = \frac{\mathbf{q}_i}{\delta_i\,\zeta_i^{-1}\, m_i\,\bar{n}\,\bar{v}_i^3},$$

$$\widehat{\mathbf{F}}_U = \frac{\mathbf{F}_U}{\zeta_i\,\mu\, m_i\,\bar{n}\,\bar{v}_i^2/L}, \qquad \widehat{\mathbf{F}}_T = \frac{\mathbf{F}_T}{m_i\,\bar{n}\,\bar{v}_i^2/L}, \qquad \widehat{w}_i = \frac{w_i}{\delta_i^{-1}\,\zeta_i\,\mu\, m_i\,\bar{n}\,\bar{v}_i^3/L}.$$

As before, the normalization procedure is designed to make all hatted quantities $\mathcal{O}(1)$. The normalization of the electric field is chosen such that the $\mathbf{E}\times\mathbf{B}$ velocity is of similar magnitude to the ion diamagnetic velocity. Note that the parallel viscosity makes an $\mathcal{O}(1)$ contribution to $\widehat{\boldsymbol{\pi}}_i$, whereas the gyroviscosity makes an $\mathcal{O}(\zeta_i)$ contribution, and the perpendicular viscosity only makes an $\mathcal{O}(\zeta_i^2)$ contribution. Likewise, the parallel thermal conductivity makes an $\mathcal{O}(1)$ contribution to $\widehat{\mathbf{q}}_i$, whereas the cross conductivity makes an $\mathcal{O}(\zeta_i)$ contribution, and the perpendicular conductivity only makes an $\mathcal{O}(\zeta_i^2)$ contribution. Similarly, the parallel component of $\mathbf{F}_T$ is $\mathcal{O}(1)$, whereas the perpendicular component is $\mathcal{O}(\zeta_i\,\mu)$.

The normalized ion fluid equations take the form:

$$\frac{d_i\hat{n}}{d\hat{t}} + \hat{n}\,\widehat{\nabla}\cdot\widehat{\mathbf{V}}_i = 0, \tag{65}$$

$$\hat{n}\,\frac{d_i\widehat{\mathbf{V}}_i}{d\hat{t}} + \delta_i^{-2}\,\widehat{\nabla}\hat{p}_i + \zeta_i^{-1}\,\widehat{\nabla}\cdot\widehat{\boldsymbol{\pi}}_i - \delta_i^{-2}\,\hat{n}\,(\widehat{\mathbf{E}} + \widehat{\mathbf{V}}_i\times\widehat{\mathbf{B}}) = -\delta_i^{-2}\,\zeta_i\,\mu\,\widehat{\mathbf{F}}_U - \delta_i^{-2}\,\widehat{\mathbf{F}}_T, \tag{66}$$

$$\frac{3}{2}\frac{d_i\hat{p}_i}{d\hat{t}} + \frac{5}{2}\,\hat{p}_i\,\widehat{\nabla}\cdot\widehat{\mathbf{V}}_i + \delta_i^2\,\zeta_i^{-1}\,\widehat{\boldsymbol{\pi}}_i : \widehat{\nabla}\cdot\widehat{\mathbf{V}}_i + \zeta_i^{-1}\,\widehat{\nabla}\cdot\widehat{\mathbf{q}}_i = \delta_i^{-2}\,\zeta_i\,\mu\,\widehat{w}_i. \tag{67}$$

The only large or small (compared to unity) quantities in these equations are the parameters δ_i, ζ_i, and μ. Here, $d_i/d\hat{t} \equiv \partial/\partial\hat{t} + \widehat{\mathbf{V}}_i\cdot\widehat{\nabla}$.

2.5 Lowest-Order Fluid Equations

If we restore dimensions to the Braginskii equations then we can write them in the form

$$\frac{\partial n}{\partial t} + \nabla\cdot(n\,\mathbf{V}_e) = 0, \tag{68}$$

$$m_e\,n\,\frac{\partial\mathbf{V}_e}{\partial t} + m_e\,n\,(\mathbf{V}_e\cdot\nabla)\mathbf{V}_e + [\delta_e^{-2}]\,\nabla p_e + [\zeta_e^{-1}]\,\nabla\cdot\boldsymbol{\pi}_e + [\delta_e^{-2}]\,e\,n\,(\mathbf{E} + \mathbf{V}_e\times\mathbf{B}) = [\delta_e^{-2}\,\zeta_e]\,\mathbf{F}_U + [\delta_e^{-2}]\,\mathbf{F}_T, \tag{69}$$

$$\frac{3}{2}\frac{\partial p_e}{\partial t} + \frac{3}{2}\,\mathbf{V}_e\cdot\nabla p_e + \frac{5}{2}\,p_e\,\nabla\cdot\mathbf{V}_e + [\delta_e^2\,\zeta_e^{-1}]\,\boldsymbol{\pi}_e : \nabla\mathbf{V}_e + [\zeta_e^{-1}]\,\nabla\cdot\mathbf{q}_{Te} + \nabla\cdot\mathbf{q}_{Ue} = -[\delta_e^{-2}\,\zeta_e\,\mu^2]\,w_i + [\zeta_e]\,w_U + w_T, \tag{70}$$

and

$$\frac{\partial n}{\partial t} + \nabla\cdot(n\,\mathbf{V}_i) = 0, \tag{71}$$

$$m_i\,n\,\frac{\partial\mathbf{V}_i}{\partial t} + m_i\,n\,(\mathbf{V}_i\cdot\nabla)\mathbf{V}_i + [\delta_i^{-2}]\,\nabla p_i + [\zeta_i^{-1}]\,\nabla\cdot\boldsymbol{\pi}_i - [\delta_i^{-2}]\,e\,n\,(\mathbf{E} + \mathbf{V}_i\times\mathbf{B}) = -[\delta_i^{-2}\,\zeta_i\,\mu]\,\mathbf{F}_U - [\delta_i^{-2}]\,\mathbf{F}_T, \tag{72}$$

$$\frac{3}{2}\frac{\partial p_i}{\partial t} + \frac{3}{2}\,\mathbf{V}_i\cdot\nabla p_i + \frac{5}{2}\,p_i\,\nabla\cdot\mathbf{V}_i + [\delta_i^2\,\zeta_i^{-1}]\,\boldsymbol{\pi}_i : \nabla\mathbf{V}_i + [\zeta_i^{-1}]\,\nabla\cdot\mathbf{q}_i = [\delta_i^{-2}\,\zeta_i\,\mu]\,w_i. \tag{73}$$

The factors in square brackets are there to remind us that the terms they precede are smaller or larger than the other terms in the equations (by the corresponding factors within the brackets).

If we assume that $\delta_e \sim \zeta_e \sim \mu \ll 1$ then the dominant term in the electron energy conservation equation (70) yields

$$\nabla\cdot\mathbf{q}_{Te} \simeq \nabla\cdot(-\kappa_{\parallel e}\,\nabla_\parallel T_e) \simeq 0, \tag{74}$$

which implies that

$$\mathbf{B}\cdot\nabla T_e = 0. \tag{75}$$

In other words, the parallel electron heat conductivity in a tokamak plasma is usually sufficiently large that it forces the electron temperature to be constant on magnetic flux-surfaces. Likewise, if we assume that $\delta_i \sim \zeta_i \sim \mu \ll 1$ then the dominant term in the ion energy conservation equation (73) yields

$$\nabla\cdot\mathbf{q}_{T_i} \simeq \nabla\cdot(-\kappa_{\parallel\, i}\,\nabla_\parallel T_i) \simeq 0, \tag{76}$$

which implies that

$$\mathbf{B}\cdot\nabla T_i = 0. \tag{77}$$

In other words, the parallel ion heat conductivity in a tokamak plasma is usually sufficiently large that it forces the ion temperature to be constant on magnetic flux-surfaces.

The dominant terms in the electron and ion momentum conservation equations, (69) and (72), respectively, yield

$$\nabla p_e + n\,e\,(\mathbf{E}+\mathbf{V}_e\times\mathbf{B}) \simeq 0, \tag{78}$$

$$\nabla p_i - n\,e\,(\mathbf{E}+\mathbf{V}_i\times\mathbf{B}) \simeq 0. \tag{79}$$

The sum of the preceding two equations gives

$$\mathbf{j}\times\mathbf{B} \simeq \nabla p, \tag{80}$$

where $p = p_e + p_i$. In other words, a conventional tokamak plasma exists in a state in which the magnetic force density exactly balances the total scalar pressure force density. It follows from the previous equation that

$$\mathbf{B}\cdot\nabla p \simeq 0. \tag{81}$$

In other words, the total pressure in a conventional tokamak plasma is constant on magnetic flux-surfaces. However, given that $p = n\,(T_e + T_i)$, and making use of Eqs. (75) and (77), we deduce that

$$\mathbf{B}\cdot\nabla n \simeq 0. \tag{82}$$

In other words, the electron number density in a conventional tokamak plasma is also constant on magnetic flux-surfaces.

Let us make the reasonable assumption that Equation (81) implies that $\mathbf{B}\cdot\nabla p_e = \mathbf{B}\cdot\nabla p_i = 0$. In other words, the electron and ion pressures are separately constant on magnetic flux-surfaces. If we assume that, to lowest order, $\mathbf{E} = -\nabla\Phi$, where Φ is the electrostatic potential, then Equations (78) and (79) yield

$$\mathbf{B}\cdot\nabla\Phi = 0. \tag{83}$$

In other words, the electrostatic potential is also constant on magnetic flux-surfaces.

Taking the difference of the electron and ion particle conservation equations, (68) and (71), respectively, we obtain

$$\nabla \cdot \mathbf{j} = 0. \tag{84}$$

Equations (80) and (84) can be combined to give

$$(\mathbf{B} \cdot \nabla)\, \mathbf{j} - (\mathbf{j} \cdot \nabla)\, \mathbf{B} \simeq \mathbf{0}. \tag{85}$$

Here, we have made use of the fact that $\nabla \cdot \mathbf{B} = 0$.

Finally, Equations (78) and (79) imply that

$$\mathbf{V}_{\perp e} \simeq \mathbf{V}_E + \mathbf{V}_{*e}, \tag{86}$$

$$\mathbf{V}_{\perp i} \simeq \mathbf{V}_E + \mathbf{V}_{*i}, \tag{87}$$

where

$$\mathbf{V}_E = \frac{\mathbf{E} \times \mathbf{B}}{B^2} \tag{88}$$

is the *E-cross-B drift velocity* (otherwise known as the $\mathbf{E} \times \mathbf{B}$ velocity), and

$$\mathbf{V}_{*e} = \frac{\nabla p_e \times \mathbf{B}}{e\, n\, B^2}, \tag{89}$$

$$\mathbf{V}_{*i} = -\frac{\nabla p_i \times \mathbf{B}}{e\, n\, B^2}, \tag{90}$$

are termed the *electron diamagnetic velocity* and the *ion diamagnetic velocity*, respectively (Fitzpatrick 2015).

3 Cylindrical Tearing Mode Theory

3.1 Introduction

The aim of this section is to describe the simplest theory of tearing mode dynamics in tokamak plasmas, according to which the plasma equilibrium is approximated as a periodic cylinder.

3.2 Tokamak Equilibrium

Consider a large aspect-ratio, toroidal, tokamak plasma equilibrium whose magnetic flux-surfaces map out (almost) concentric circles in the poloidal plane. Such an equilibrium can be approximated as a periodic cylinder (Wesson 1978). Let us employ a conventional set of right-handed cylindrical coordinates, r, θ, z. The equilibrium magnetic flux-surfaces lie on surfaces of constant r. The system is assumed to be periodic in the z ('toroidal') direction, with periodicity length $2\pi\, R_0$, where R_0 is the simulated *major radius* of the plasma. The *safety-factor* profile takes the form

$$q(r) = \frac{r\, B_z}{R_0\, B_\theta(r)}, \tag{91}$$

where B_z is the constant 'toroidal' magnetic field-strength, and $B_\theta(r)$ is the poloidal magnetic field-strength. It is assumed that $q \sim \mathcal{O}(1)$. The equilibrium 'toroidal' current density satisfies

$$\mu_0\, j_z(r) = \frac{(r\, B_\theta)'}{r}, \tag{92}$$

where $'$ denotes d/dr. Finally, the standard large aspect-ratio tokamak orderings,

$$\frac{r}{R_0} \ll 1, \quad \frac{B_\theta}{B_z} \ll 1, \tag{93}$$

are adopted (Fitzpatrick 1993).

3.3 Perturbed Magnetic Field

Consider a tearing mode perturbation that has m periods in the poloidal direction, and n periods in the toroidal direction, where $m/n \sim \mathcal{O}(1)$. We can write the perturbed magnetic field in the divergence-free form

$$\delta\mathbf{B} \simeq \nabla \times (\psi\, \mathbf{e}_z), \tag{94}$$

where

$$\psi(r,\theta,\varphi,t) = \psi(r,t)\, \exp[\mathrm{i}\,(m\,\theta - n\,\varphi)]. \tag{95}$$

Here, $\varphi = z/R_0$ is a simulated toroidal angle. The perturbed current density becomes

$$\mu_0\, \delta\mathbf{j} \simeq -\nabla^2\psi\, \mathbf{e}_z. \tag{96}$$

It is assumed that $|\delta\mathbf{B}| \ll |\mathbf{B}|$.

3.4 Cylindrical Tearing Mode Equation

To lowest order, the tearing perturbation is governed by the linearized version of Equation (85), which yields

$$(\delta\mathbf{B}\cdot\nabla)\,\mathbf{j} + (\mathbf{B}\cdot\nabla)\,\delta\mathbf{j} - (\delta\mathbf{j}\cdot\nabla)\,\mathbf{B} - (\mathbf{j}\cdot\nabla)\,\delta\mathbf{B} \simeq \mathbf{0}. \tag{97}$$

Making use of Equations (91)–(96), the z-component of the previous equation gives the *cylindrical tearing mode equation* (Wesson 1978; Fitzpatrick 1993),

$$\frac{\partial^2\psi}{\partial r^2} + \frac{1}{r}\,\frac{\partial\psi}{\partial r} - \frac{m^2}{r^2}\,\psi - \frac{J_z'\,\psi}{r\,(1/q - n/m)} = 0, \tag{98}$$

where

$$J_z(r) = \frac{R_0\,\mu_0\, j_z(r)}{B_z}. \tag{99}$$

3.5 Solution in Presence of Perfectly-Conducting Wall

Suppose that the plasma occupies the region $0 \leq r \leq a$, where a is the plasma *minor radius*. (By definition, $a \ll R_0$ in a large aspect-ratio tokamak.) It follows that $J_z(r) = 0$ for $r > a$. Let the plasma be surrounded by a concentric, rigid, radially-thin, perfectly-conducting, wall of radius $r_w > a$. (In most circumstances, the wall represents the metal vacuum vessel that surrounds the plasma.) An appropriate physical solution of the cylindrical tearing mode equation takes the separable form

$$\psi(r,t) = \Psi_s(t)\,\hat{\psi}_s(r), \tag{100}$$

where the real function $\hat{\psi}_s(r)$ is a solution of

$$\frac{d^2\hat{\psi}_s}{dr^2} + \frac{1}{r}\,\frac{d\hat{\psi}_s}{dr} - \frac{m^2}{r^2}\,\hat{\psi}_s - \frac{J_z'\,\hat{\psi}_s}{r\,(1/q - n/m)} = 0 \tag{101}$$

that satisfies

$$\hat{\psi}_s(0) = 0, \tag{102}$$

$$\hat{\psi}_s(r_s) = 1, \tag{103}$$

$$\hat{\psi}_s(r \geq r_w) = 0. \tag{104}$$

Note that Equation (101) is singular at the so-called *resonant* magnetic flux-surface, radius $r = r_s$, at which

$$q(r_s) = \frac{m}{n}. \tag{105}$$

At the resonant surface, $\mathbf{k}\cdot\mathbf{B} = 0$, where $\mathbf{k} = (0,\, m/r,\, -n/R_0)$ is the wavevector of the tearing perturbation. The value of $\psi(r,t)$ at the resonant surface—namely, $\Psi_s(t)$—is known as the *reconnected magnetic flux* (Fitzpatrick 1993). (See Section 5.9.) Note that Ψ_s is, in general, a complex quantity. Let $\rho = (r - r_s)/r_s$. The solution of Equation (101) in the vicinity of the resonant surface is

$$\hat{\psi}_s(\rho) = 1 + \Delta_{s+}\,\rho + \alpha_s\,\rho\,\ln|\rho| + \mathcal{O}(\rho^2) \tag{106}$$

for $\rho > 0$, and

$$\hat{\psi}_s(\rho) = 1 + \Delta_{s-}\,\rho + \alpha_s\,\rho\,\ln|\rho| + \mathcal{O}(\rho^2) \tag{107}$$

for $\rho < 0$. Here,

$$\alpha_s = -\left(\frac{r\,q\,J_z'}{s}\right)_{r=r_s}, \tag{108}$$

$$s(r) = \frac{r\,q'}{q}. \tag{109}$$

Moreover, the real parameters Δ_{s+} and Δ_{s-} are fully determined by Equation (101) and the boundary conditions (102)–(104). Note that, in general, ψ is continuous across the resonant surface (in accordance with Maxwell's equations), whereas $\partial\psi/\partial r$ is discontinuous. The discontinuity in $\partial\psi/\partial r$ implies the presence of a radially-thin, helical, current sheet at the resonant surface. This current sheet can only be resolved by retaining more terms in the perturbed plasma equation of motion, (97). (See Section 5.)

The complex quantity

$$\Delta\Psi_s = \left[r\,\frac{\partial\psi}{\partial r}\right]_{r_{s-}}^{r_{s+}} \tag{110}$$

parameterizes the amplitude and phase of the current sheet flowing at the resonant surface. Matching the solutions in the so-called *inner region* (i.e., the region of the plasma in the immediate vicinity of the resonant surface) and the so-called *outer region* (i.e., everywhere in the plasma other than the inner region) with the help of Equations (100), (106), and (107), we obtain

$$\Delta\Psi_s = E_{ss}\,\Psi_s, \tag{111}$$

where $E_{ss} = \Delta_{s+} - \Delta_{s-}$ is a real dimensionless quantity that is known as the *tearing stability index* (Furth, Killeen & Rosenbluth 1963).

3.6 Solution in Presence of Resistive Wall

Suppose, now, that the wall at $r = r_w$ possesses a finite electrical resistivity, but is surrounded by a second perfectly-conducting wall located at radius $r_c > r_w$. The solution in the outer region can be written

$$\psi(r,t) = \Psi_s(t)\,\hat{\psi}_s(r) + \Psi_w(t)\,\hat{\psi}_w(r), \tag{112}$$

where the real function $\hat{\psi}_s(r)$ is specified in Section 3.5, and the real function $\hat{\psi}_w(r)$ is a solution of

$$\frac{d^2\hat{\psi}_w}{dr^2} + \frac{1}{r}\,\frac{d\hat{\psi}_w}{dr} - \frac{m^2}{r^2}\,\hat{\psi}_w - \frac{J_z'\,\hat{\psi}_w}{r\,(1/q - n/m)} = 0 \tag{113}$$

that satisfies

$$\hat{\psi}_w(r \leq r_s) = 0, \tag{114}$$

$$\hat{\psi}_w(r_w) = 1, \tag{115}$$

$$\hat{\psi}_w(r \geq r_c) = 0. \tag{116}$$

It is easily seen that

$$\hat{\psi}_w(r_w < r < r_c) = \frac{(r/r_c)^{-m} - (r/r_c)^m}{(r_w/r_c)^{-m} - (r_w/r_c)^m}. \tag{117}$$

In general, ψ is continuous across the wall (in accordance with Maxwell's equations), whereas $\partial\psi/\partial r$ is discontinuous. The discontinuity in $\partial\psi/\partial r$ is caused by a helical current

sheet induced in the wall. The complex quantity $\Psi_w(t)$ determines the amplitude and phase of the perturbed magnetic flux that penetrates the wall. The complex quantity

$$\Delta\Psi_w = \left[r \, \frac{\partial \psi}{\partial r} \right]_{r_{w-}}^{r_{w+}} \tag{118}$$

parameterizes the amplitude and phase of the helical current sheet flowing in the wall. Simultaneously matching the outer solution (112) across the resonant surface and the wall yields

$$\Delta\Psi_s = E_{ss}\,\Psi_s + E_{sw}\,\Psi_w, \tag{119}$$

$$\Delta\Psi_w = E_{ws}\,\Psi_s + E_{ww}\,\Psi_w \tag{120}$$

(Fitzpatrick 1993). Here,

$$E_{ww} = \left[r \, \frac{d\hat{\psi}_w}{dr} \right]_{r_{w-}}^{r_{w+}}, \tag{121}$$

$$E_{sw} = \left[r \, \frac{d\hat{\psi}_w}{dr} \right]_{r=r_{s+}}, \tag{122}$$

$$E_{ws} = -\left[r \, \frac{d\hat{\psi}_s}{dr} \right]_{r=r_{w-}} \tag{123}$$

are real quantities determined by the solutions of Equations (101) and (113) in the outer region.

Equations (101) and (113) can be combined to give

$$\frac{d}{dr}\left(\hat{\psi}_s \, r \, \frac{d\hat{\psi}_w}{dr} - \hat{\psi}_w \, r \, \frac{d\hat{\psi}_s}{dr} \right) = 0. \tag{124}$$

If we integrate the previous equation from $r = r_{s+}$ to $r = r_{w-}$, making use of Equations (103), (104), (114), (115), (122), and (123), then we obtain

$$E_{sw} = E_{ws} \tag{125}$$

(Fitzpatrick 1993).

3.7 Resistive Wall Physics

It is clear from Equation (94) that

$$\delta\mathbf{A} \simeq \psi \, \mathbf{e}_z, \tag{126}$$

where $\delta\mathbf{A}$ is the perturbed magnetic vector potential. Hence, the perturbed electric field can be written

$$\delta\mathbf{E} \simeq -\nabla\delta\Phi - \frac{\partial\psi}{\partial t}\,\mathbf{e}_z, \tag{127}$$

where $\delta\Phi$ is the perturbed electric scalar potential. Assuming that $|\nabla\delta\Phi| \sim |\partial\psi/\partial t|$, the z-component of the previous equation yields

$$\delta E_z \simeq -\frac{\partial\psi}{\partial t}, \tag{128}$$

where use has been made of the large aspect-ratio orderings (93). Within the wall, we can write

$$\delta E_z \simeq -\frac{d\Psi_w}{dt}. \tag{129}$$

Here, we are making use of the so-called *thin wall approximation*, according to which ψ is assumed to only vary weakly in r across the wall. Ohm's law implies that

$$\delta j_z = \frac{\delta E_z}{\eta_w} = -\frac{1}{\eta_w}\,\frac{d\Psi_w}{dt} \tag{130}$$

within the wall, where η_w is the wall resistivity. Equations (96) and (118) yield

$$\Delta\Psi_w = -\mu_0 \int_{r_{w-}}^{r_{w+}} r\,\delta j_z\,dr. \tag{131}$$

Suppose that the radial thickness of the wall is $\delta_w \ll r_w$. The previous two equations give

$$\Delta\Psi_w = \tau_w\,\frac{d\Psi_w}{dt}, \tag{132}$$

where

$$\tau_w = \frac{\mu_0\,r_w\,\delta_w}{\eta_w} \tag{133}$$

is the so-called *time constant* of the wall (Nave & Wesson 1990; Fitzpatrick 1993). The thin wall approximation is valid as long as

$$\frac{r_w}{\delta_w} \gg \tau_w \left|\frac{d\ln\Psi_w}{dt}\right|. \tag{134}$$

3.8 Resonant Layer Physics

By analogy with Equation (132), we can write

$$\Delta\Psi_s = \tau_s\left(\frac{d\Psi_s}{dt} + \mathrm{i}\,\omega\,\Psi_s\right). \tag{135}$$

Here, τ_s is the *reconnection time* (i.e., the typical timescale on which magnetic reconnection takes place in the resonant layer surrounding the resonant surface), whereas ω is the phase velocity of the tearing mode when the wall is perfectly conducting. The phase velocity is non-zero because the reconnected flux in the resonant layer is convected by the local plasma flow (Fitzpatrick 1993). (See Sections 6.2 and 9.4.)

3.9 Solution in Presence of External Magnetic Field-Coil

Suppose that the perfectly-conducting wall at $r = r_c$ is replaced by a radially-thin, magnetic field-coil that carries a helical current possessing m periods in the poloidal direction, and n periods in the toroidal direction. Let the current density in the field-coil take the form

$$\delta j_z = \frac{I_c(t)}{r_c}\,\delta(r - r_c)\,\mathrm{e}^{\,\mathrm{i}\,(m\,\theta - n\,\varphi)}. \tag{136}$$

Here, the complex quantity $I_c(t)$ parameterizes the amplitude and phase of the helical current flowing in the field-coil.

The solution in the outer region can be written

$$\psi(r,t) = \Psi_s(t)\,\hat{\psi}_s(r) + \Psi_w(t)\,\hat{\psi}_w(r) + \Psi_c\,\hat{\psi}_c(r), \tag{137}$$

where the real functions $\hat{\psi}_s(r)$ and $\hat{\psi}_w(r)$ are specified in Sections 3.5 and 3.6, respectively. Moreover, the real function $\hat{\psi}_c(r)$ is a solution of

$$\frac{d^2\hat{\psi}_c}{dr^2} + \frac{1}{r}\,\frac{d\hat{\psi}_c}{dr} - \frac{m^2}{r^2}\,\hat{\psi}_c = 0 \tag{138}$$

that satisfies

$$\hat{\psi}_c(r \leq r_w) = 0, \tag{139}$$

$$\hat{\psi}_c(r_c) = 1, \tag{140}$$

$$\hat{\psi}_c(\infty) = 0. \tag{141}$$

It is easily seen that

$$\hat{\psi}_c(r \leq r_w) = 0, \tag{142}$$

$$\hat{\psi}_c(r_w < r \leq r_c) = \frac{(r/r_w)^m - (r/r_w)^{-m}}{(r_c/r_w)^m - (r_c/r_w)^{-m}}, \tag{143}$$

$$\hat{\psi}_c(r > r_c) = \left(\frac{r}{r_c}\right)^{-m}. \tag{144}$$

In general, ψ is continuous across the field-coil (in accordance with Maxwell's equations), whereas $\partial\psi/\partial r$ is discontinuous. The discontinuity in $\partial\psi/\partial r$ is caused by the helical current flowing in the coil. The complex quantity $\Psi_c(t)$ determines the amplitude and phase of the perturbed magnetic flux at the coil. The complex quantity

$$\Delta\Psi_c = \left[r\,\frac{\partial\psi}{\partial r}\right]_{r_{c-}}^{r_{c+}} \tag{145}$$

parameterizes the amplitude and phase of the helical current sheet flowing in the coil. It follows from Equations (95), (96), and (136) that

$$\Delta\Psi_c = -\mu_0\,I_c. \tag{146}$$

Simultaneously matching the outer solution across the resonant surface, the wall, and the field-coil, we obtain

$$\Delta\Psi_s = E_{ss}\,\Psi_s + E_{sw}\,\Psi_w, \tag{147}$$

$$\Delta\Psi_w = E_{ws}\,\Psi_s + E_{ww}\,\Psi_w + E_{wc}\,\Psi_c, \tag{148}$$

$$\Delta\Psi_c = E_{cw}\,\Psi_w + E_{cc}\,\Psi_c. \tag{149}$$

Here,

$$E_{cc} = \left[r\,\frac{d\hat{\psi}_c}{dr}\right]_{r_{c-}}^{r_{c+}} = -\frac{2m}{1-(r_w/r_c)^{2m}}, \tag{150}$$

$$E_{wc} = \left[r\,\frac{d\hat{\psi}_c}{dr}\right]_{r_{w+}} = \frac{2m\,(r_w/r_c)^m}{1-(r_w/r_c)^{2m}}, \tag{151}$$

$$E_{cw} = -\left[r\,\frac{d\hat{\psi}_w}{dr}\right]_{r_{c-}} = \frac{2m\,(r_w/r_c)^m}{1-(r_w/r_c)^{2m}}, \tag{152}$$

where use has been made of Equations (117), (143), and (144).

3.10 Electromagnetic Torques

The flux-surface integrated poloidal and toroidal electromagnetic torque densities acting on the plasma can be written

$$T_\theta(r) = \{r\,\mathbf{j}\times\mathbf{B}\cdot\mathbf{e}_\theta\} \tag{153}$$

$$T_\varphi(r) = \{R_0\,\mathbf{j}\times\mathbf{B}\cdot\mathbf{e}_z\}\,, \tag{154}$$

respectively, where

$$\{\cdots\} \equiv \oint\oint r\,R_0\,\cdots\,d\theta\,d\varphi \tag{155}$$

is a flux-surface integration operator. However, according to Equation (80),

$$\mathbf{j}\times\mathbf{B} \simeq \nabla p. \tag{156}$$

Given that the scalar pressure is a single-valued function of θ and φ, it immediately follows that $T_\theta = T_\varphi = 0$ throughout the plasma (Fitzpatrick 1993). The only exception to this rule occurs in the immediate vicinity of the resonant surface, where Equation (156) breaks down. It follows that we can write

$$T_\theta(r) = T_{\theta\,s}\,\delta(r-r_s), \tag{157}$$

$$T_\varphi(r) = T_{\varphi\,s}\,\delta(r-r_s), \tag{158}$$

where

$$T_{\theta\,s} = \frac{1}{4}\int_{r_{s-}}^{r_{s+}} \oint\oint R_0\, r^{\,2}\,(\delta j_z\,\delta B_r^* + \delta j_z^*\,\delta B_r)\,dr\,d\theta\,d\varphi, \tag{159}$$

$$T_{\varphi\,s} = -\frac{1}{4}\int_{r_{s-}}^{r_{s+}} \oint\oint R_0^2\, r\,(\delta j_\theta\,\delta B_r^* + \delta j_\theta^*\,\delta B_r)\,dr\,d\theta\,d\varphi \tag{160}$$

are the net poloidal and toroidal torques, respectively, acting at the resonant surface. Note that the zeroth-order (in perturbed quantities) torques are zero because $B_r = 0$. Furthermore, the linear (in perturbed quantities) torques average to zero over the flux-surface. Hence, the largest non-zero torques are *quadratic* in perturbed quantities. According to Equation (84),

$$\nabla\cdot\delta\mathbf{j} = \mathrm{i}\left(\frac{m}{r}\,\delta j_\theta - \frac{n}{R_0}\,\delta j_z\right) = 0, \tag{161}$$

where $\delta\mathbf{j}$ is the density of the current sheet flowing at the resonant surface, and we have made use of the fact that δj_r is negligible in a radially-thin current sheet (Fitzpatrick 1993). It follows from the previous three equations that

$$T_{\varphi\,s} = -\frac{n}{m}\,T_{\theta\,s}. \tag{162}$$

Finally, Equations (94), (96), (159), and (162) imply that

$$T_{\theta\,s} = -\frac{2\pi^2\,R_0\,m}{\mu_0}\,\mathrm{Im}(\Delta\Psi_s\,\Psi_s^*), \tag{163}$$

$$T_{\varphi\,s} = \frac{2\pi^2\,R_0\,n}{\mu_0}\,\mathrm{Im}(\Delta\Psi_s\,\Psi_s^*) \tag{164}$$

(Fitzpatrick 1993).

By analogy with the previous analysis, the net poloidal and toroidal electromagnetic torques acting on the resistive wall are

$$T_{\theta\,w} = -\frac{2\pi^2\,R_0\,m}{\mu_0}\,\mathrm{Im}(\Delta\Psi_w\,\Psi_w^*), \tag{165}$$

$$T_{\varphi\,w} = \frac{2\pi^2\,R_0\,n}{\mu_0}\,\mathrm{Im}(\Delta\Psi_w\,\Psi_w^*), \tag{166}$$

respectively. Finally, the net poloidal and toroidal electromagnetic torques acting on the magnetic field-coil are

$$T_{\theta\,c} = -\frac{2\pi^2\,R_0\,m}{\mu_0}\,\mathrm{Im}(\Delta\Psi_c\,\Psi_c^*), \tag{167}$$

$$T_{\varphi\,c} = \frac{2\pi^2\,R_0\,n}{\mu_0}\,\mathrm{Im}(\Delta\Psi_c\,\Psi_c^*), \tag{168}$$

respectively.

It follows from Equations (147)–(149) that

$$\mathrm{Im}(\Delta\Psi_s\,\Psi_s^*) = E_{sw}\,\mathrm{Im}(\Psi_w\,\Psi_s^*), \tag{169}$$

$$\mathrm{Im}(\Delta\Psi_w\,\Psi_w^*) = E_{ws}\,\mathrm{Im}(\Psi_s\,\Psi_w^*) + E_{wc}\,\mathrm{Im}(\Psi_c\,\Psi_w^*), \tag{170}$$

$$\mathrm{Im}(\Delta\Psi_c\,\Psi_c^*) = E_{cw}\,\mathrm{Im}(\Psi_w\,\Psi_c^*). \tag{171}$$

Thus,

$$\mathrm{Im}(\Delta\Psi_s\,\Psi_s^*) + \mathrm{Im}(\Delta\Psi_w\,\Psi_w^*) + \mathrm{Im}(\Delta\Psi_c\,\Psi_c^*) = (E_{sw} - E_{ws})\,\mathrm{Im}(\Psi_w\,\Psi_s^*) + (E_{wc} - E_{cw})\,\mathrm{Im}(\Psi_c\,\Psi_w^*). \tag{172}$$

However, according to Equations (125), (151), and (152), $E_{sw} = E_{ws}$ and $E_{wc} = E_{cw}$. We deduce that

$$\mathrm{Im}(\Delta\Psi_s\,\Psi_s^*) + \mathrm{Im}(\Delta\Psi_w\,\Psi_w^*) + \mathrm{Im}(\Delta\Psi_c\,\Psi_c^*) = 0. \tag{173}$$

Hence, Equations (163)–(168) yield

$$T_{\theta\,s} + T_{\theta\,w} + T_{\theta\,c} = 0, \tag{174}$$

$$T_{\varphi\,s} + T_{\varphi\,w} + T_{\varphi\,c} = 0. \tag{175}$$

In other words, the plasma/wall/field-coil system exerts zero net poloidal electromagnetic torque, and zero net toroidal electromagnetic torque, on itself.

3.11 Plasma Angular Equations of Motion

The sum of the electron fluid equation of motion, (69), and the ion fluid equation of motion, (72), yields the plasma equation of motion,

$$\rho\,\frac{\partial \mathbf{V}_i}{\partial t} + \rho\,(\mathbf{V}_i\cdot\nabla)\mathbf{V}_i + [\delta_i^{-2}]\,\nabla p + [\zeta_i^{-1}]\,\nabla\cdot\boldsymbol{\pi}_i - [\delta_i^{-2}]\,\mathbf{j}\times\mathbf{B} = 0, \tag{176}$$

where $\rho = m_i\,n$ is the plasma mass density. Here, we have neglected electron inertial terms with respect to ion inertial terms (because the former are order m_e/m_i smaller than the latter). We have also neglected electron viscosity terms with respect to ion viscosity terms (because the former are order $\sqrt{m_e/m_i}$ smaller than the latter). (See Sections 2.3 and 2.4.) Recall that the factors in square brackets are there to remind us that the terms they precede are larger than the other terms in the equation (by the corresponding factors within the brackets).

Taking the scalar product of $r\,\mathbf{e}_\theta$ with the plasma equation of motion, (176), and integrating around magnetic flux-surfaces, we obtain

$$\left\{\rho\,\frac{\partial(r\,V_{\theta\,i})}{\partial t}\right\} + \left\{\rho\left[V_{r\,i}\,\frac{\partial(r\,V_{\theta\,i})}{\partial r} + V_{z\,i}\,\frac{\partial(r\,V_{\theta\,i})}{\partial z}\right]\right\} + [\zeta_i^{-1}]\,\{r\,\nabla\cdot\boldsymbol{\pi}_i\cdot\mathbf{e}_\theta\} = [\delta_i^{-2}]\,T_{\theta\,s}\,\delta(r-r_s), \tag{177}$$

where use has been made of Equations (153) and (157). Note that the dominant ∇p term has averaged to zero. Moreover, because $T_{\theta\,s}$ is quadratic in perturbed quantities (see Section 3.10), it is plausible that the right-hand side of the previous equation is no longer a dominant term [i.e., it is not $\mathcal{O}(\delta_i^{-2})$ larger than the other terms in the equation]. To be more exact, if $|\delta\mathbf{B}|/|\mathbf{B}| \sim \delta_i$ then the right-hand side ceases to be a dominant term in the equation.

The largest contribution to $\{r\,\nabla\cdot\boldsymbol{\pi}_i\cdot\mathbf{e}_\theta\}$ comes from the ion parallel viscosity tensor acting on the zeroth-order (in perturbed quantities) ion flow. (See Section 2.3.) However, this contribution averages to zero in a cylindrical plasma, in which B_z is constant on magnetic flux-surfaces. Of course, in reality, in a large aspect-ratio tokamak plasma, B_z varies slightly around magnetic flux-surfaces, being larger on the inboard side of the torus than on the outboard side (Wesson 2011). This variation gives rise to a residual contribution to $\{r\,\nabla\cdot\boldsymbol{\pi}_i\cdot\mathbf{e}_\theta\}$. It is plausible that this contribution is not a dominant term in Equation (177) [i.e., it is not $\mathcal{O}(\zeta_i^{-1})$ larger than the other terms in the equation]. To be more exact, if the residual contribution is $\mathcal{O}(\zeta_i)$ times smaller than the non-averaged contribution then $\{r\,\nabla\cdot\boldsymbol{\pi}_i\cdot\mathbf{e}_\theta\}$ ceases to be a dominant term in the equation.

According to the previous discussion, it is plausible that all terms appearing in Equation (177) are of approximately equal magnitude when the inertial and viscous terms are evaluated with the zeroth-order ion flow, which can be written

$$\mathbf{V}_i = r\,\Omega_\theta(r,t)\,\mathbf{e}_\theta + R_0\,\Omega_\varphi(r,t)\,\mathbf{e}_z. \tag{178}$$

Here, $\Omega_\theta(r,t)$ and $\Omega_\varphi(r,t)$ are the ion poloidal and toroidal angular velocity profiles, respectively. When $\{r\,\nabla\cdot\boldsymbol{\pi}_i\cdot\mathbf{e}_\theta\}$ is evaluated with the ion parallel viscosity tensor, and the zeroth-order ion flow, it gives rise to a term that acts to relax the ion poloidal angular velocity profile toward a so-called *neoclassical profile* determined by ion density and temperature gradients (Stix 1973; Hirshman & Sigmar 1981). In principle, the contribution of the ion perpendicular viscosity tensor to $\{r\,\nabla\cdot\boldsymbol{\pi}_i\cdot\mathbf{e}_\theta\}$ is $\mathcal{O}(\zeta_i^{\,2})$ smaller than the contribution of the ion parallel viscosity tensor. (See Section 2.3.) In practice, the magnitude of the ion perpendicular viscosity tensor is greatly enhanced above the value predicted by the Braginskii equations by the action of small-scale plasma turbulence (Wesson 2011). Hence, it is reasonable to include the contribution of the enhanced perpendicular viscosity tensor to $\{r\,\nabla\cdot\boldsymbol{\pi}_i\cdot\mathbf{e}_\theta\}$. Our model form for $\{r\,\nabla\cdot\boldsymbol{\pi}_i\cdot\mathbf{e}_\theta\}$ is written

$$\{r\,\nabla\cdot\boldsymbol{\pi}_i\cdot\mathbf{e}_\theta\} = 4\pi^2\,R_0\left[\frac{\rho}{\tau_\theta}\,r^{\,3}\,(\Omega_\theta-\Omega_{\theta\,\mathrm{nc}}) - \frac{\partial}{\partial r}\left(\mu_\perp\,r^{\,3}\,\frac{\partial\Omega_\theta}{\partial r}\right)\right]. \tag{179}$$

Here, $\rho(r)$ is the equilibrium plasma mass density profile, $\tau_\theta(r)$ is the *poloidal flow-damping time* [which is generally of order $(a/q\,R_0)^2\,\tau_i$], $\Omega_{\theta\,\mathrm{nc}}(r)$ is the neoclassical poloidal angular velocity profile, and $\mu_\perp(r)$ is a phenomenological perpendicular viscosity due to plasma turbulence.

When evaluated with the zeroth-order ion flow, Equation (177) reduces to

$$4\pi^2\,R_0\left[\rho\,r^{\,3}\,\frac{\partial\Omega_\theta}{\partial t} + \frac{\rho}{\tau_\theta}\,r^{\,3}\,(\Omega_\theta-\Omega_{\theta\,\mathrm{nc}}) - \frac{\partial}{\partial r}\left(\mu_\perp\,r^{\,3}\,\frac{\partial\Omega_\theta}{\partial r}\right)\right] = T_{\theta\,s}\,\delta(r-r_s) + S_\theta, \tag{180}$$

where use has been made of Equation (179). Here, we have added a source term, $S_\theta(r)$, to the equation in order to account for the equilibrium poloidal flow. Let $\Omega_{\theta\,0}(r)$ be the unperturbed (by the tearing mode) ion poloidal angular velocity profile. It follows that

$$S_\theta = 4\pi^2\, R_0 \left[\frac{\rho}{\tau_\theta}\, r^{\,3}\, (\Omega_{\theta\,0} - \Omega_{\theta\,\rm nc}) - \frac{d}{dr}\left(\mu_\perp\, r^{\,3}\, \frac{d\Omega_{\theta\,0}}{dr}\right)\right]. \tag{181}$$

Hence, writing

$$\Omega_\theta(r,t) = \Omega_{\theta\,0}(r) + \Delta\Omega_\theta(r,t), \tag{182}$$

where $\Delta\Omega_\theta(r,t)$ is the modification to the ion poloidal angular velocity profile induced by the poloidal electromagnetic torque that develops at the resonant surface, Equation (180) yields

$$4\pi^2\, R_0 \left[\rho\, r^{\,3}\, \frac{\partial \Delta\Omega_\theta}{\partial t} + \frac{\rho}{\tau_\theta}\, r^{\,3}\, \Delta\Omega_\theta - \frac{\partial}{\partial r}\left(\mu_\perp\, r^{\,3}\, \frac{\partial \Delta\Omega_\theta}{\partial r}\right)\right] = T_{\theta\,s}\, \delta(r - r_s). \tag{183}$$

There is one further refinement that we can make to the previous equation. It turns out that neoclassical poloidal flow damping gives rise to an enhancement of poloidal ion inertia by a factor of $1 + 2\,q^{\,2}$ (Hirshman 1978). Hence, our final version of the perturbed plasma poloidal angular equation of motion becomes

$$4\pi^2\, R_0 \left[(1 + 2\,q^{\,2})\, \rho\, r^{\,3}\, \frac{\partial \Delta\Omega_\theta}{\partial t} + \frac{\rho}{\tau_\theta}\, r^{\,3}\, \Delta\Omega_\theta - \frac{\partial}{\partial r}\left(\mu_\perp\, r^{\,3}\, \frac{\partial \Delta\Omega_\theta}{\partial r}\right)\right] = T_{\theta\,s}\, \delta(r - r_s). \tag{184}$$

Taking the scalar product of $R_0\, \mathbf{e}_z$ with the plasma equation of motion, (176), and integrating around magnetic flux-surfaces, similar arguments to those just employed for the ion poloidal flow allow us to write the zeroth-order ion toroidal angular velocity profile in the form

$$\Omega_\varphi(r,t) = \Omega_{\varphi\,0}(r) + \Delta\Omega_\varphi(r,t), \tag{185}$$

where $\Omega_{\varphi\,0}(r)$ is the unperturbed (by the tearing mode) ion toroidal angular velocity profile, and $\Delta\Omega_\varphi(r,t)$ is the modification to this profile induced by the toroidal electromagnetic torque that develops at the resonant surface. The perturbed ion toroidal angular equation of motion is written

$$4\pi^2\, R_0^3 \left[\rho\, r\, \frac{\partial \Delta\Omega_\varphi}{\partial t} - \frac{\partial}{\partial r}\left(\mu_\perp\, r\, \frac{\partial \Delta\Omega_\varphi}{\partial r}\right)\right] = T_{\varphi\,s}\, \delta(r - r_s). \tag{186}$$

Note that the ion parallel viscosity tensor does not give rise to damping of the toroidal flow profile. Furthermore, there is no neoclassical enhancement of the plasma toroidal ion inertia.

Equations (184) and (186) are subject to the boundary conditions

$$\frac{\partial \Delta\Omega_\theta(0,t)}{\partial r} = \frac{\partial \Delta\Omega_\varphi(0,t)}{\partial r} = 0, \tag{187}$$

$$\Delta\Omega_\theta(a,t) = \Delta\Omega_\varphi(a,t) = 0. \tag{188}$$

The boundary conditions (187) merely ensure that the ion angular velocities remain finite at the magnetic axis. On the other hand, the boundary conditions (188) are a consequence of the action of *charge exchange* with electrically neutral particles emitted isotropically from the wall in the edge regions of the plasma (Brau, et al. 1983; Fitzpatrick 1993; Monier-Garbet, et al. 1997). Charge exchange with neutrals gives rise to dominant damping torques acting at the edge of the plasma that relax the edge ion angular velocities toward particular values. Moreover, the electromagnetic torques that develop at the resonant surface are not large enough, compared with the charge-exchange torques, to significantly modify the edge ion angular velocities (Fitzpatrick 1993).

3.12 Solution of Plasma Angular Equations of Motion

In most situations of interest, the perturbed angular velocity profiles, $\Delta\Omega_\theta(r,t)$ and $\Delta\Omega_\varphi(r,t)$, are localized in the vicinity of the resonant surface (Fitzpatrick 1993). Hence, it is reasonable to express the perturbed angular equations of motion, (184) and (186), in the simplified forms

$$4\pi^2\,R_0\left[(1+2\,q_s^2)\,\rho_s\,r^3\,\frac{\partial\Delta\Omega_\theta}{\partial t}+\frac{\rho_s}{\tau_{\theta\,s}}\,r^3\,\Delta\Omega_\theta-\mu_{\perp\,s}\,\frac{\partial}{\partial r}\left(r^3\,\frac{\partial\Delta\Omega_\theta}{\partial r}\right)\right]=T_{\theta\,s}\,\delta(r-r_s),\tag{189}$$

$$4\pi^2\,R_0^3\left[\rho_s\,r\,\frac{\partial\Delta\Omega_\varphi}{\partial t}-\mu_{\perp\,s}\,\frac{\partial}{\partial r}\left(r\,\frac{\partial\Delta\Omega_\varphi}{\partial r}\right)\right]=T_{\varphi\,s}\,\delta(r-r_s),\tag{190}$$

where $q_s=q(r_s)$, $\rho_s=\rho(r_s)$, $\tau_{\theta\,s}=\tau_\theta(r_s)$, and $\mu_{\perp\,s}=\mu_\perp(r_s)$.

Let us write

$$\Delta\Omega_\theta(r,t)=-\frac{1}{m}\sum_{p=1,\infty}\alpha_p(t)\,\frac{y_p(r/a)}{y_p(r_s/a)},\tag{191}$$

$$\Delta\Omega_\varphi(r,t)=\frac{1}{n}\sum_{p=1,\infty}\beta_p(t)\,\frac{z_p(r/a)}{z_p(r_s/a)},\tag{192}$$

where

$$y_p(r)=\frac{J_1(j_{1\,p}\,r/a)}{r/a},\tag{193}$$

$$z_p(r)=J_0(j_{0\,p}\,r/a).\tag{194}$$

Here, $J_m(z)$ is a Bessel function, and $j_{m\,p}$ denotes its pth zero. Note that Equations (191)–(194) automatically satisfy the boundary conditions (187) and (188).

It is easily demonstrated that

$$\frac{d}{dr}\left(r^3\,\frac{dy_p}{dr}\right)=-\frac{j_{1\,p}^2\,r^3\,y_p}{a^2},\tag{195}$$

$$\frac{d}{dr}\left(r\,\frac{dz_p}{dr}\right)=-\frac{j_{0\,p}^2\,r\,z_p}{a^2},\tag{196}$$

and

$$\int_0^a r^3\, y_p(r)\, y_q(r)\, dr = \frac{a^4}{2}\,[J_2(j_{1\,p})]^{\,2}\,\delta_{p,q}, \tag{197}$$

$$\int_0^a r\, z_p(r)\, z_q(r)\, dr = \frac{a^2}{2}\,[J_1(j_{0\,p})]^{\,2}\,\delta_{p,q}. \tag{198}$$

Equations (189) and (190) yield

$$(1+2\,q_s^2)\,\frac{d\alpha_p}{dt} + \left(\frac{1}{\tau_{\theta\,s}} + \frac{j_{1\,p}^2}{\tau_M}\right)\alpha_p = \frac{m^2\,[y_p(r_s/a)]^{\,2}}{\tau_A^2\,\epsilon_a^2\,[J_2(j_{1\,p})]^{\,2}}\,\mathrm{Im}(\Delta\hat{\Psi}_s\,\hat{\Psi}_s^*), \tag{199}$$

$$\frac{d\beta_p}{dt} + \frac{j_{0\,p}^2}{\tau_M}\,\beta_p = \frac{n^2\,[z_p(r_s/a)]^{\,2}}{\tau_A^2\,[J_1(j_{0\,p})]^{\,2}}\,\mathrm{Im}(\Delta\hat{\Psi}_s\,\hat{\Psi}_s^*). \tag{200}$$

Here,

$$\tau_M = \frac{\rho_s\,a^{\,2}}{\mu_{\perp\,s}}, \tag{201}$$

is the *momentum confinement time*,

$$\tau_A = \left(\frac{\mu_0\,\rho_s\,a^{\,2}}{B_z^2}\right)^{1/2} \tag{202}$$

is the *Alfvén time*,

$$\epsilon_a = \frac{a}{R_0} \ll 1 \tag{203}$$

is the *inverse aspect-ratio* of the plasma, and

$$\Delta\hat{\Psi}_s = \frac{\Delta\Psi_s}{R_0\,B_z}, \tag{204}$$

$$\hat{\Psi}_s = \frac{\Psi_s}{R_0\,B_z}. \tag{205}$$

Moreover, use has been made of Equations (163), (164), and (191)–(198).

3.13 No-Slip Constraint

The reconnected magnetic flux at the resonant surface is assumed to convected by the local plasma flow. (See Section 3.8.) Hence, changes in the plasma flow at the resonant surface induced by the electromagnetic torques that develop in the vicinity of this surface will modify the convection velocity. Consequently, the phase velocity of the tearing mode can be written

$$\omega(t) = \omega_0 + (\mathbf{k}\cdot\Delta\mathbf{V}_i)_{r=r_s} = \omega_0 + m\,\Delta\Omega_\theta(r_s,t) - n\,\Delta\Omega_\varphi(r_s,t), \tag{206}$$

where ω_0 is the unperturbed phase velocity. The previous expression is known as the *no-slip constraint* (Fitzpatrick 1993), and has been verified experimentally (Vahala, et al. 1980). It follows from Equations (191) and (192) that

$$\omega(t) = \omega_0 - \sum_{p=1,\infty} [\alpha_p(t) + \beta_p(t)]\,. \tag{207}$$

(See Section 7.4.)

3.14 Final Equations

Equations (125), (132), (135), (146)–(152), (199), (200), and (207) can be combined to give the following complete set of equations that determine the time evolution of the reconnected magnetic flux at the resonant surface:

$$\Delta\hat{\Psi}_s \equiv \tau_s \left(\frac{d\hat{\Psi}_s}{dt} + \mathrm{i}\,\omega\,\hat{\Psi}_s\right) = E_{ss}\,\hat{\Psi}_s + E_{sw}\,\hat{\Psi}_w, \tag{208}$$

$$\tau_w\,\frac{d\hat{\Psi}_w}{dt} = E_{sw}\,\hat{\Psi}_s + \tilde{E}_{ww}\,\hat{\Psi}_w + \hat{I}_c, \tag{209}$$

$$\omega(t) = \omega_0 - \sum_{p=1,\infty} [\alpha_p(t) + \beta_p(t)]\,, \tag{210}$$

$$(1+2\,q_s^2)\,\frac{d\alpha_p}{dt} + \left(\frac{1}{\tau_{\theta\,s}} + \frac{j_{1\,p}^2}{\tau_M}\right)\alpha_p = \frac{m^2\,[y_p(r_s/a)]^{\,2}}{\tau_A^2\,\epsilon_a^2\,[J_2(j_{1\,p})]^{\,2}}\,\mathrm{Im}(\Delta\hat{\Psi}_s\,\hat{\Psi}_s^*), \tag{211}$$

$$\frac{d\beta_p}{dt} + \frac{j_{0\,p}^2}{\tau_M}\,\beta_p = \frac{n^2\,[z_p(r_s/a)]^{\,2}}{\tau_A^2\,[J_1(j_{0\,p})]^{\,2}}\,\mathrm{Im}(\Delta\hat{\Psi}_s\,\hat{\Psi}_s^*). \tag{212}$$

Here,

$$\hat{I}_c = \left(\frac{r_w}{r_c}\right)^m \frac{\mu_0\,I_c}{R_0\,B_z}, \tag{213}$$

$$\tilde{E}_{ww} = E_{ww} + \frac{2m\,(r_w/r_c)^{2m}}{1-(r_w/r_c)^{2m}}. \tag{214}$$

4 Reduced Resonant Response Model

4.1 Introduction

Equations (208)–(212) contain two quantities—namely, the reconnection time, τ_s, and the unperturbed phase velocity, ω_0—that can only be determined by solving for the plasma response in the radially-thin resonant layer surrounding the resonant surface. Unfortunately, determining the resonant plasma response is not a straightforward task. The problem is that

the small characteristic lengthscale in the resonant region (i.e., the resonant layer width) causes the fundamental ordering parameters δ_e and δ_i (see Section 2.4) to take values that are of order unity. Consequently, most of the simplifications described in Section 2.5 are not applicable in the resonant layer. In particular, many of the terms in the Braginskii equations (see Section 2.3) that are negligible in the outer region (e.g., plasma resistivity) have to be taken into account in the resonant layer.

A tearing mode is a modified shear-Alfvén wave (Hazeltine & Meiss 1985), and has very little connection with a compressible-Alfvén wave. For instance, the resonance condition, $\mathbf{k}\cdot\mathbf{B} = 0$, which determines the position of the resonant surface, is identical to the resonance condition for a shear-Alfvén wave, but differs substantially from that of a compressible-Alfvén wave (Fitzpatrick 2015). Hence, one very effective way of simplifying the resonant layer equations is to remove the physics of compressible-Alfvén waves from them altogether, in the process converting a drift-magnetohydrodynamical[1](MHD) response model into a so-called *reduced* drift-MHD response model (Strauss 1976; Hazeltine, Kotschenreuther & Morrison 1985). The aim of this section is to describe the reduction process (which essentially boils down to arguing that the divergence of the plasma flow is small), and to derive the reduced drift-MHD equations that will subsequently be used to model the resonant response of the plasma.

4.2 Drift-MHD Equations

It is helpful to define the following parameters:

$$n_0 = n(r_s), \tag{215}$$

$$p_0 = p(r_s), \tag{216}$$

$$\eta_e = \left.\frac{d\ln T_e}{d\ln n}\right|_{r=r_s}, \tag{217}$$

$$\eta_i = \left.\frac{d\ln T_i}{d\ln n}\right|_{r=r_s}, \tag{218}$$

$$\tau = \left(\frac{T_e}{T_i}\right)_{r=r_s}\left(\frac{1+\eta_e}{1+\eta_i}\right), \tag{219}$$

where $n(r)$, $p(r)$, $T_e(r)$, and $T_i(r)$ refer to density, pressure, and temperature profiles that are unperturbed by the tearing mode.

Let us assume, for the sake of simplicity, that the perturbed electron and ion temperature profiles in the vicinity of the resonant layer are functions of the perturbed electron number density profile. In other words, $T_e = T_e(n)$ and $T_i = T_i(n)$. It follows that the perturbed total pressure profile is also a function of the perturbed electron number density profile: that

[1]The 'drift' appellation merely indicates that we are taking diamagnetic flows into account. However, this necessarily entails treating the ion and electron flows separately. In other words, a drift-MHD model is, by definition, also a 'two-fluid' model.

is, $p = p(n)$. Let us define

$$\mathbf{V}_* = \frac{\mathbf{b} \times \nabla p}{e\, n_0\, B_z}. \tag{220}$$

To lowest order, the electron and ion diamagnetic velocities take the respective forms

$$\mathbf{V}_{*\,e} = -\left(\frac{\tau}{1+\tau}\right) \mathbf{V}_*, \tag{221}$$

$$\mathbf{V}_{*\,i} = \left(\frac{1}{1+\tau}\right) \mathbf{V}_*. \tag{222}$$

(See Section 2.5.) The so-called *MHD velocity*, which is the velocity of a fictional 'MHD fluid', is defined

$$\mathbf{V} = \mathbf{V}_E + V_{\parallel\, i}\, \mathbf{b}, \tag{223}$$

where $\mathbf{V}_E$ is the $\mathbf{E} \times \mathbf{B}$ velocity, and $V_{\parallel\, i}$ is the parallel component of the ion fluid velocity. The lowest-order electron and ion fluid velocities take the respective forms:

$$\mathbf{V}_e = \mathbf{V} + \mathbf{V}_{*\,i} - \frac{\mathbf{j}}{n_0\, e}, \tag{224}$$

$$\mathbf{V}_i = \mathbf{V} + \mathbf{V}_{*\,i}. \tag{225}$$

(See Section 2.5.)

Following Hazeltine & Meiss 1992, if we neglect electron inertia and electron viscosity in the electron equation of motion, (9), then we obtain the *generalized Ohm's law*:

$$\mathbf{E} + \mathbf{V} \times \mathbf{B} + \frac{1}{e\, n_0}\left[\nabla p + \frac{1}{1+\tau}\left(\frac{0.71\, \eta_e\, \tau}{1+\eta_e} - 1\right)(\mathbf{b}\cdot\nabla p)\, \mathbf{b} - \mathbf{j} \times \mathbf{B}\right] = \eta_\parallel\, \mathbf{j}_\parallel + \eta_\perp\, \mathbf{j}_\perp. \tag{226}$$

Here, $\eta_\parallel = 1/\sigma_\parallel(r_s)$ and $\eta_\perp = 1/\sigma_\perp(r_s)$ are the parallel and perpendicular plasma resistivities, respectively, at the resonant surface. (See Section 2.3.) We have neglected the cross term in Equation (15) because it is a factor $(\Omega_e\, \tau_e)^{-1}$ smaller than ∇p. Incidentally, if we assume that all flow velocities are similar in magnitude to the diamagnetic velocity then the neglect of electron inertia and electron viscosity in the previous equation is justified because the corresponding terms are factors $(\rho_e/r_s)^2$ and $(\Omega_e\, \tau_e)\,(\rho_e/r_s)^2$, respectively, smaller than the leading order terms in the equation.

Next, we can add the electron and ion equations of motion, (9) and (12), again neglecting electron inertia and electron viscosity, to give the *plasma equation of motion*:

$$n_0\, m_i\left[\frac{\partial \mathbf{V}}{\partial t} + (\mathbf{V}\cdot\nabla)\mathbf{V} + \frac{1}{1+\tau}\,(\mathbf{V}_*\cdot\nabla)\mathbf{V}_E\right] + \nabla p + \nabla\cdot\boldsymbol{\pi}_i - \mathbf{j}\times\mathbf{B} = 0. \tag{227}$$

Here, $\nabla\cdot\boldsymbol{\pi}_i$ includes the contribution from the anomalous (i.e., enhanced due to the action of small-scale plasma turbulence) perpendicular viscosity tensor. The contribution from the gyroviscosity tensor, which is the same size as the ion inertial terms, has already been incorporated into the equation (Hazeltine & Meiss 1992). For the moment, we are neglecting

the contribution of the parallel viscosity tensor. The neglect of electron inertia and electron viscosity in the previous equation is justified because the corresponding terms are factors m_e/m_i and $(m_e/m_i)^{1/2}$, respectively, smaller than the leading order terms in the equation.

Finally, we can combine the electron and ion energy evolution equations, (10) and (13), to obtain a *plasma energy evolution equation*:

$$\frac{\partial p}{\partial t} + \mathbf{V}\cdot\nabla p + \Gamma\, p\,\nabla\cdot\mathbf{V} + \frac{2}{3}\,\nabla\cdot\mathbf{q} = 0, \tag{228}$$

where $\Gamma = 5/3$. Here, we have neglected a number of terms (e.g., the ohmic heating terms) because they are, at least, factors $(\Omega_e\,\tau_e)^{-1}$ or $(\Omega_i\,\tau_i)^{-1}$ smaller than $\nabla\cdot\mathbf{q}$. We have also neglected the viscous heating term because we expect the dominant contribution, which comes from the parallel viscosity, to be much smaller than its nominal magnitude in a large aspect-ratio tokamak plasma.

Equations (226)–(228) are known collectively as the *drift-MHD equations*, and contain both shear-Alfvén and compressible-Alfvén wave dynamics. The system of equations is completed by a subset of Maxwell's equations:

$$\nabla\cdot\mathbf{B} = 0, \tag{229}$$

$$\nabla\times\mathbf{E} = -\frac{\partial\mathbf{B}}{\partial t}, \tag{230}$$

$$\mu_0\,\mathbf{j} = \nabla\times\mathbf{B}. \tag{231}$$

4.3 Normalization Scheme

Let l be a typical variation lengthscale in the resonant layer. The *Alfvén velocity*, which is the typical phase velocity of compressible Alfvén waves, is defined

$$V_A = \frac{a}{\tau_A} = \frac{B_z}{\sqrt{\mu_0\,n_0\,m_i}}. \tag{232}$$

It is helpful to define the *collisionless ion skin-depth*:

$$d_i = \left(\frac{m_i}{n_0\,e^{\,2}\,\mu_0}\right)^{1/2}. \tag{233}$$

Note that $d_i = c/\omega_{p\,i}$, where c is the velocity of light in vacuum, and $\omega_{p\,i}$ is the ion plasma frequency (Fitzpatrick 2015).

It is convenient to adopt the following normalization scheme that renders all quantities in the drift-MHD equations dimensionless: $\hat{\nabla} = l\,\nabla$, $\hat{d}_i = d_i/l$, $\hat{t} = t/(l/V_A)$, $\hat{\mathbf{B}} = \mathbf{B}/B_z$, $\hat{\mathbf{E}} = \mathbf{E}/(B_z\,V_A)$, $\hat{\mathbf{j}} = \mathbf{j}/(B_z/\mu_0\,l)$, $\hat{\eta}_{\parallel,\perp} = \eta_{\parallel,\perp}/(\mu_0\,V_A\,l)$, $\hat{\mathbf{V}} = \mathbf{V}/V_A$, $\hat{\mathbf{V}}_{*,i} = \mathbf{V}_{*,i}/V_A$, $\hat{V}_{\parallel\,i} = V_{\parallel\,i}/V_A$, $\hat{p} = p/(B_z^2/\mu_0)$, $\hat{p}_0 = p_0/(B_z^2/\mu_0)$, $\hat{\boldsymbol{\pi}}_i = \boldsymbol{\pi}_i/(B_z^2/\mu_0)$, $\hat{\mathbf{q}} = \mathbf{q}/(B_z^2\,V_A/\mu_0)$. Equations (226)–(231) yield

$$\hat{\mathbf{E}} + \hat{\mathbf{V}}\times\hat{\mathbf{B}} + \hat{d}_i\left[\hat{\nabla}\hat{p} + \frac{1}{1+\tau}\left(\frac{0.71\,\eta_e\,\tau}{1+\eta_e} - 1\right)(\mathbf{b}\cdot\hat{\nabla}\hat{p})\,\mathbf{b} + \hat{\nabla}\cdot\hat{\boldsymbol{\pi}}_e - \hat{\mathbf{j}}\times\hat{\mathbf{B}}\right] = \hat{\eta}_\parallel\,\hat{\mathbf{j}}_\parallel + \hat{\eta}_\perp\,\hat{\mathbf{j}}_\perp, \tag{234}$$

$$\frac{\partial \hat{\mathbf{V}}}{\partial \hat{t}} + (\hat{\mathbf{V}}\cdot\hat{\nabla})\hat{\mathbf{V}} + \frac{1}{1+\tau}\,(\hat{\mathbf{V}}_*\cdot\hat{\nabla})\hat{\mathbf{V}}_E + \hat{\nabla}\hat{p} + \hat{\nabla}\cdot\hat{\boldsymbol{\pi}}_i - \hat{\mathbf{j}}\times\hat{\mathbf{B}} = 0, \tag{235}$$

$$\frac{\partial \hat{p}}{\partial \hat{t}} + \hat{\mathbf{V}}\cdot\hat{\nabla}\hat{p} + \Gamma\,\hat{p}\,\hat{\nabla}\cdot\hat{\mathbf{V}} + \frac{2}{3}\,\hat{\nabla}\cdot\hat{\mathbf{q}} = 0, \tag{236}$$

and

$$\hat{\nabla}\cdot\hat{\mathbf{B}} = 0, \tag{237}$$

$$\hat{\nabla}\times\hat{\mathbf{E}} = -\frac{\partial \hat{\mathbf{B}}}{\partial \hat{t}}, \tag{238}$$

$$\hat{\mathbf{j}} = \hat{\nabla}\times\hat{\mathbf{B}}. \tag{239}$$

Finally,

$$\hat{\mathbf{V}}_E = \hat{\mathbf{E}}\times\mathbf{b}, \tag{240}$$

$$\hat{\mathbf{V}} = \hat{\mathbf{V}}_E + \hat{V}_{\parallel\,i}\,\mathbf{b}, \tag{241}$$

$$\hat{\mathbf{V}}_* = \hat{d}_i\,\mathbf{b}\times\hat{\nabla}\hat{p}, \tag{242}$$

$$\hat{\mathbf{V}}_i = \hat{\mathbf{V}} + \frac{\hat{\mathbf{V}}_*}{1+\tau}. \tag{243}$$

4.4 Reduction Process

All variables in the resonant layer are assumed to be functions of $\hat{x} = (r - r_s)/l$,

$$\zeta = m\,\theta - n\,\varphi, \tag{244}$$

and $\hat{t}$, only. Let $\mathbf{n} = (0,\, \epsilon/q_s,\, 1)$, where $\epsilon = r/R_0$ and

$$q_s = q(r_s) = \frac{m}{n}. \tag{245}$$

It follows that $\mathbf{n}\cdot\nabla A = 0$ for any $A(\hat{x},\zeta,\hat{t})$. Let us write (Fitzpatrick & Waelbroeck 2009)

$$\hat{\mathbf{B}} \simeq (1+\delta b)\,\mathbf{n} + \hat{\nabla}\hat{\psi}\times\mathbf{n}, \tag{246}$$

which automatically satisfies Equation (237). Note that

$$\hat{\psi} = \frac{\psi}{r_s\,B_z}, \tag{247}$$

where ψ is defined in Equation (94). Here, $\delta b(\hat{x},\zeta,\hat{t})$ and $\hat{\psi}(\hat{x},\zeta,\hat{t})$ are assumed to be small compared to unity, which merely indicates that the perturbed magnetic field due to the tearing mode is small compared to the equilibrium magnetic field. We can write

$$\hat{\mathbf{E}} \simeq \left(\hat{E}_\parallel - \frac{\partial \hat{\psi}}{\partial \hat{t}}\right)\mathbf{n} + \hat{\nabla}\left(\frac{\partial \chi}{\partial \hat{t}}\right)\times\mathbf{n} + \hat{\nabla}\phi, \tag{248}$$

which automatically satisfies Equation (238) provided that

$$\hat{\nabla}^2 \chi = \delta b. \tag{249}$$

Here, $\hat{E}_\parallel = E_\parallel/(B_z\, V_A)$, where $E_\parallel$ represents the constant inductive parallel electric field that drives the equilibrium plasma current in the vicinity of the resonant surface. Moreover, $\partial/\partial\hat{t}$ and $\phi(\hat{x},\zeta,\hat{t})$ are assumed to be first order in small quantities, whereas $\hat{E}_\parallel$ is assumed to be second order. It follows that

$$\hat{\mathbf{V}}_E \simeq \hat{\nabla}\phi \times \mathbf{n}, \tag{250}$$

$$\hat{\mathbf{V}} \simeq \hat{V}_{\parallel\, i}\, \mathbf{n} + \hat{\nabla}\phi \times \mathbf{n} + \hat{\nabla}\Xi, \tag{251}$$

where $\hat{V}_{\parallel\, i}(\hat{x},\zeta,\hat{t})$ is assumed to be first order in small quantities, whereas $\Xi(\hat{x},\zeta,\hat{t})$ is assumed to be second order. We can write

$$\hat{p} = \frac{\beta}{\Gamma} + \delta p, \tag{252}$$

where

$$\beta = \Gamma\, \hat{p}_0 = \frac{\Gamma\, p_0\, \mu_0}{B_z^2}. \tag{253}$$

Here, $\delta p(\hat{x},\zeta,\hat{t})$ is assumed to be first order in small quantities. It follows that

$$\hat{\mathbf{V}}_* \simeq \hat{d}_i\, \mathbf{n} \times \hat{\nabla}\delta p, \tag{254}$$

$$\hat{\mathbf{V}}_i \simeq \hat{V}_{\parallel\, i}\, \mathbf{n} + \hat{\nabla}\left(\phi - \frac{\hat{d}_i\, \delta p}{1+\tau}\right) \times \mathbf{n}. \tag{255}$$

The normalized drift-MHD equations, (234)–(236), yield

$$\begin{aligned}
&\hat{d}_i\, \hat{\nabla}(\delta p + \delta b)\\
&+\left(\hat{E}_\parallel - \frac{\partial\hat{\psi}}{\partial\hat{t}} - [\hat{\psi},\phi] + \frac{\hat{d}_i\, [\hat{\psi},\delta p]}{1+\tau}\left(1 - \frac{0.71\,\eta_e\,\tau}{1+\eta_e}\right) + \hat{d}_i\, [\hat{\psi},\delta b] + \hat{\eta}_\parallel\, J\right)\mathbf{n}\\
&+\hat{\nabla}\left(\frac{\partial\chi}{\partial\hat{t}} + \Xi - \hat{\eta}_\perp\, \delta b\right) \times \mathbf{n} + \frac{\hat{d}_i}{2}\, \hat{\nabla}\delta b^2 - b_z\, \hat{\nabla}\phi + \hat{V}_{\parallel\, i}\, \hat{\nabla}\hat{\psi} + \hat{d}_i\, J\, \hat{\nabla}\hat{\psi} = 0,
\end{aligned} \tag{256}$$

$$\begin{aligned}
&\hat{\nabla}(\delta p + \delta b) + \left(\frac{\partial\hat{V}_{\parallel\, i}}{\partial\hat{t}} + [\hat{V}_{\parallel\, i},\phi] + [\hat{\psi},\delta b]\right)\mathbf{n}\\
&+\hat{\nabla}\left(\frac{\partial\phi}{\partial\hat{t}} - \frac{\hat{d}_i\, [\phi,\delta p]}{2\,(1+\tau)}\right) \times \mathbf{n} + \frac{1}{2}\, \hat{\nabla}\left(\hat{V}_\perp^{\,2} + \frac{\hat{\mathbf{V}}_* \cdot \hat{\mathbf{V}}_E}{1+\tau} + \delta b^2\right)\\
&-\hat{\nabla}^2\phi\, \hat{\nabla}\phi + \frac{\hat{d}_i}{2\,(1+\tau)}\left(\hat{\nabla}^2\phi\, \hat{\nabla}\delta p + \hat{\nabla}^2\delta p\, \hat{\nabla}\phi\right) + J\, \hat{\nabla}\hat{\psi} + \hat{\nabla}\cdot\hat{\boldsymbol{\pi}}_i = 0,
\end{aligned} \tag{257}$$

$$\frac{\partial \delta p}{\partial \hat{t}} + [\delta p, \phi] + \beta\, \hat{\nabla}^2 \Xi + \frac{2}{3}\, \hat{\nabla} \cdot \hat{\mathbf{q}} = 0, \tag{258}$$

where use has been made of Equation (239), and

$$[A, B] \equiv \hat{\nabla} A \times \hat{\nabla} B \cdot \mathbf{n}, \tag{259}$$

$$J = -\frac{2}{q_s\, \hat{R}_0} + \hat{\nabla}^2 \hat{\psi}, \tag{260}$$

with $\hat{R}_0 = R_0/l$. Here, $\hat{d}_i$ and β are assumed to be zeroth order in small quantities, J, $1/\hat{R}_0$, $\hat{\eta}_\parallel$, and $\hat{\eta}_\perp$ are assumed to be first order, while $\hat{\nabla} \cdot \hat{\boldsymbol{\pi}}_i$ and $\hat{\nabla} \cdot \hat{\mathbf{q}}$ are assumed to be second order.

To first order in small quantities, both Equations (256) and (257) yield

$$\delta b = -\delta p, \tag{261}$$

which is simply an expression of lowest-order equilibrium force balance. The scalar product of Equation (256) with $\mathbf{n}$ gives

$$\frac{\partial \hat{\psi}}{\partial \hat{t}} = [\phi, \hat{\psi}] + \hat{d}_i \left(\frac{\tau}{1+\tau}\right) \left(1 + \frac{0.71\, \eta_e}{1+\eta_e}\right) [\delta p, \hat{\psi}] + \hat{\eta}_\parallel\, J + \hat{E}_\parallel. \tag{262}$$

The scalar product of Equation (257) with $\mathbf{n}$ yields

$$\frac{\partial \hat{V}_{\parallel\, i}}{\partial \hat{t}} = [\phi, \hat{V}_{\parallel\, i}] - [\delta p, \hat{\psi}] - \mathbf{n} \cdot \hat{\nabla} \cdot \hat{\boldsymbol{\pi}}_i. \tag{263}$$

The scalar product of the curl of Equation (256) with $\mathbf{n}$ gives

$$\frac{\partial \delta p}{\partial \hat{t}} = [\phi, \delta p] + \hat{\nabla}^2 \Xi - [\hat{V}_{\parallel\, i}, \hat{\psi}] - \hat{d}_i\, [J, \hat{\psi}] + \hat{\eta}_\perp\, \hat{\nabla}^{\,2} \delta p. \tag{264}$$

Eliminating $\hat{\nabla}^2 \Xi$ between Equation (258) and the previous equation, we obtain

$$\frac{\partial \delta p}{\partial \hat{t}} = [\phi, \delta p] - c_\beta^2\, [\hat{V}_{\parallel\, i}, \hat{\psi}] - c_\beta^2\, \hat{d}_i\, [J, \hat{\psi}] - \frac{2}{3}\, (1 - c_\beta^2)\, \hat{\nabla} \cdot \hat{\mathbf{q}} + c_\beta^2\, \hat{\eta}_\perp \hat{\nabla}^2 \delta p, \tag{265}$$

where

$$c_\beta = \sqrt{\frac{\beta}{1+\beta}}. \tag{266}$$

Finally, the scalar product of the curl of Equation (257) with $\mathbf{n}$ gives

$$\frac{\partial U}{\partial \hat{t}} = [\phi, U] + \frac{\hat{d}_i}{2\,(1+\tau)} \left(\hat{\nabla}^2 [\phi, \delta p] + [\hat{\nabla}^2 \phi, \delta p] + [\hat{\nabla}^2 \delta p, \phi]\right) + [J, \hat{\psi}] + \mathbf{n} \cdot \hat{\nabla} \times \hat{\nabla} \cdot \hat{\boldsymbol{\pi}}_i, \tag{267}$$

where

$$U = \hat{\nabla}^2 \phi. \tag{268}$$

We can write

$$\hat{\nabla}\cdot\hat{\mathbf{q}} = -\left(\frac{\eta_e}{1+\eta_e}\,\frac{\tau}{1+\tau}\,\hat{\chi}_{\parallel\,e} + \frac{\eta_i}{1+\eta_i}\,\frac{1}{1+\tau}\,\hat{\chi}_{\parallel\,i}\right)[[\delta p,\hat{\psi}],\hat{\psi}]$$
$$-\left(\frac{\eta_e}{1+\eta_e}\,\frac{\tau}{1+\tau}\,\hat{\chi}_{\perp\,e} + \frac{\eta_i}{1+\eta_i}\,\frac{1}{1+\tau}\,\hat{\chi}_{\perp\,i}\right)\nabla_\perp^2\delta p, \tag{269}$$

where $\hat{\nabla}_\perp^2 \equiv \hat{\nabla}\cdot\hat{\nabla}_\perp$, $\chi_{\parallel\,e,i} = \kappa_{\parallel\,e,i}(r_s)/n_0$, $\chi_{\perp\,e,i} = \kappa_{\perp\,e,i}(r_s)/n_0$, $\hat{\chi}_{\parallel\,e,i} = \chi_{\parallel\,e,i}/(l\,V_A)$, $\hat{\chi}_{\perp\,e,i} = \chi_{\perp\,e,i}/(l\,V_A)$, and use has been made of Equations (20), (21), (217)–(219), and (246). We can also write

$$\hat{\nabla}\cdot\hat{\boldsymbol{\pi}}_i = -\hat{\chi}_\varphi\,\hat{\nabla}^2\hat{\mathbf{V}}_i, \tag{270}$$

where $\chi_\varphi = \mu_\perp(r_s)/(n_0\,m_i)$, $\hat{\chi}_\varphi = \chi_\varphi/(l\,V_A)$, and $\mu_\perp(r)$ is the anomalous ion perpendicular viscosity. Note that the previous equation is entirely phenomenological in nature. It is easily seen that

$$\mathbf{n}\cdot\hat{\nabla}\cdot\hat{\boldsymbol{\pi}}_i = -\hat{\chi}_\varphi\,\hat{\nabla}^2\hat{V}_{\parallel\,i}, \tag{271}$$

$$\mathbf{n}\cdot\hat{\nabla}\times\hat{\nabla}\cdot\hat{\boldsymbol{\pi}}_i = \hat{\chi}_\varphi\,\hat{\nabla}^4\left(\phi - \frac{\hat{d}_i\,\delta p}{1+\tau}\right). \tag{272}$$

4.5 Four-Field Model

Let us define $V = \hat{d}_i\,\hat{V}_{\parallel\,i}$ and $N = -\hat{d}_i\,\delta p$. Equations (260), (262)–(263), (265), (267)–(269), (271), and (272) yield the following closed set of equations (Fitzpatrick & Waelbroeck 2005):

$$\frac{\partial\hat{\psi}}{\partial\hat{t}} = [\phi,\hat{\psi}] - \left(\frac{\tau}{1+\tau}\right)(1+\lambda_e)\,[N,\hat{\psi}] + \hat{\eta}_\parallel\,J + \hat{E}_\parallel, \tag{273}$$

$$\frac{\partial U}{\partial\hat{t}} = [\phi,U] - \frac{1}{2\,(1+\tau)}\left(\hat{\nabla}^2[\phi,N] + [\hat{\nabla}^2\phi,N] + [\hat{\nabla}^2 N,\phi]\right) + [J,\hat{\psi}]$$
$$+\,\hat{\chi}_\varphi\,\hat{\nabla}^4\left(\phi + \frac{N}{1+\tau}\right), \tag{274}$$

$$\frac{\partial N}{\partial\hat{t}} = [\phi,N] + c_\beta^2\,[V,\hat{\psi}] + \hat{d}_\beta^2\,[J,\hat{\psi}] + \hat{D}_\parallel\,[[N,\hat{\psi}],\hat{\psi}] + \hat{D}_\perp\,\hat{\nabla}_\perp^2 N, \tag{275}$$

$$\frac{\partial V}{\partial\hat{t}} = [\phi,V] + [N,\hat{\psi}] + \hat{\chi}_\varphi\,\hat{\nabla}^2 V, \tag{276}$$

$$J = -\frac{2}{q_s\,\hat{R}_0} + \hat{\nabla}^2\hat{\psi}, \tag{277}$$

$$U = \hat{\nabla}^2\phi. \tag{278}$$

Here, the quantity

$$d_\beta = c_\beta\, d_i \tag{279}$$

is usually referred to as the *ion sound radius*, and $\hat{d}_\beta = d_\beta/l$. Moreover,

$$\lambda_e = 0.71\left(\frac{\eta_e}{1+\eta_e}\right), \tag{280}$$

and

$$\hat{D}_\parallel \equiv \frac{D_\parallel}{l\,V_A} = \frac{2}{3}\left(1-c_\beta^2\right)\left(\frac{\eta_e}{1+\eta_e}\,\frac{\tau}{1+\tau}\,\hat{\chi}_{\parallel\,e} + \frac{\eta_i}{1+\eta_i}\,\frac{1}{1+\tau}\,\hat{\chi}_{\parallel\,i}\right), \tag{281}$$

$$\hat{D}_\perp \equiv \frac{D_\perp}{l\,V_A} = c_\beta^2\,\hat{\eta}_\perp + \frac{2}{3}\left(1-c_\beta^2\right)\left(\frac{\eta_e}{1+\eta_e}\,\frac{\tau}{1+\tau}\,\hat{\chi}_{\perp\,e} + \frac{\eta_i}{1+\eta_i}\,\frac{1}{1+\tau}\,\hat{\chi}_{\perp\,i}\right). \tag{282}$$

4.6 Discussion

Equations (273)–(278) constitute our reduced drift-MHD resonant plasma response model. Our model is very similar to the original four-field model derived by Hazeltine, et al. (Hazeltine, Kotschenreuther & Morrison 1985). Equation (273) is the *generalized Ohm's law* that governs the time evolution of the (normalized) helical magnetic flux, $\hat{\psi}$. Equation (274) is the *parallel ion vorticity equation* that governs the time evolution of the (normalized) parallel ion vorticity, U. Equation (275) is the *electron number density continuity equation* that governs the time evolution of the (normalized) electron number density, N. Finally, Equation (276) is the *ion parallel equation of motion* that governs the time evolution of the (normalized) parallel ion velocity, V.

Strictly speaking, the four-field fluid model presented in this section is only valid when the ion gyroradius is smaller than the typical variation lengthscale in the resonant layer. If this is not the case then it is necessary to adopt a so-called *gyrofluid* approach in which the ion response is averaged over the ion gyro-orbits (Cowley, Kulsrud & Hahm 1986; Hammett, Dorland & Perkins 1992; Waelbroeck, Hazeltine & Morrison 2009).

Finally, the crucial element of the reduction process, by which our original drift-MHD response model is converted into a reduced drift-MHD model, is the set of ordering assumptions that render $\hat{\boldsymbol{\nabla}}\cdot\hat{\mathbf{V}} = \hat{\nabla}^2\Xi$ a second-order quantity while leaving $\hat{\mathbf{V}}$ a first-order quantity. This ordering implies that the MHD fluid is *incompressible* to lowest order. It should be noted, however, that the small, but finite, compressibility of the MHD fluid has a significant influence on the form of the continuity equation (275).

5 Linear Resonant Response Model

5.1 Introduction

The aim of this section is to employ the reduced resonant plasma response model derived in Section 4 to determine the *linear* response of the resonant layer to external perturbations.

It is convenient to set the normalization scale-length, l, in our four-field response model equal to the minor radius of the resonant surface, r_s. Recall that the four fields in question—namely, $\hat{\psi}$, ϕ, N, and V—have the following definitions:

$$\nabla\hat{\psi} = \frac{\mathbf{n}\times\mathbf{B}}{r_s\, B_z}, \tag{283}$$

$$\nabla\phi = \frac{\mathbf{n}\times\mathbf{V}}{r_s\, V_A}, \tag{284}$$

$$N = -\hat{d}_i\left(\frac{p-p_0}{B_z^2/\mu_0}\right), \tag{285}$$

$$V = \hat{d}_i\left(\frac{\mathbf{n}\cdot\mathbf{V}}{V_A}\right). \tag{286}$$

Our model also employs the auxiliary fields $J = -2\,\epsilon_s/q_s + r_s^2\,\nabla^2\hat{\psi}$ and $U = r_s^2\,\nabla^2\phi$. Here,

$$\epsilon_s = \frac{r_s}{R_0} \ll 1. \tag{287}$$

5.2 Plasma Equilibrium

The unperturbed plasma equilibrium is such that

$$\mathbf{B} = (0,\, B_\theta(r),\, B_z), \tag{288}$$

$$p = p(r), \tag{289}$$

$$\mathbf{V} = (0,\, V_E(r),\, V_z(r)), \tag{290}$$

where

$$V_E(r) \simeq \frac{E_r}{B_z} \tag{291}$$

is the (dominant θ-component of the) $\mathbf{E}\times\mathbf{B}$ velocity. Now, the resonant layer is assumed to have a radial thickness that is much smaller than r_s. (See Section 5.3.) Hence, we only need to evaluate plasma equilibrium quantities in the immediate vicinity of the resonant surface. Equations (283)–(290) suggest that

$$\hat{\psi} = \frac{\hat{x}^{\,2}}{2\,\hat{L}_s}, \tag{292}$$

$$\phi = -\hat{V}_E\,\hat{x}, \tag{293}$$

$$N = -\hat{V}_*\,\hat{x}, \tag{294}$$

$$V = \hat{V}_\parallel, \tag{295}$$

where

$$\hat{x} = \frac{r-r_s}{r_s}, \tag{296}$$

$\hat{L}_s = L_s/r_s$,

$$L_s = \frac{R_0\, q_s}{s_s} \tag{297}$$

is the *magnetic shear length*, $\hat{V}_E = V_E(r_s)/V_A$, $\hat{V}_* = V_*(r_s)/V_A$,

$$V_*(r) = \frac{1}{e\, n_0\, B_z}\,\frac{dp}{dr} \tag{298}$$

is the (dominant θ-component of the) diamagnetic velocity, and $\hat{V}_\parallel = \hat{d}_i\, V_z(r_s)/V_A$. We also have

$$J = -\left(\frac{2}{s_s} - 1\right)\frac{1}{\hat{L}_s}, \tag{299}$$

$$U = 0, \tag{300}$$

$$\hat{E}_\parallel = \left(\frac{2}{s_s} - 1\right)\frac{\hat{\eta}_\parallel}{\hat{L}_s}, \tag{301}$$

$$s_s = s(r_s). \tag{302}$$

Note that we are neglecting the radial shear of the equilibrium MHD velocity because, in conventional tokamak plasmas, such shear does not significantly affect the linear response of a resonant layer, due to the fact that the shear is comparatively weak (i.e., $|dV/dr| \ll V_A/a$) combined with the fact that a linear resonant layer is very narrow (Chen & Morrison 1990).

5.3 Derivation of Linear Layer Equations

Suppose that the system is perturbed by a tearing mode with m periods in the poloidal direction, and n periods in the toroidal direction. In accordance with Equations (292)–(295), and (299)–(300), we can write

$$\hat{\psi}(\hat{x},\zeta,\hat{t}) = \frac{\hat{x}^{\,2}}{2\,\hat{L}_s} + \tilde{\psi}(\hat{x})\,\mathrm{e}^{\,\mathrm{i}\,(\zeta - \hat{\omega}\,\hat{t})}, \tag{303}$$

$$\phi(\hat{x},\zeta,\hat{t}) = -\hat{V}_E\,\hat{x} + \tilde{\phi}(\hat{x})\,\mathrm{e}^{\,\mathrm{i}\,(\zeta - \hat{\omega}\,\hat{t})}, \tag{304}$$

$$N(\hat{x},\zeta,\hat{t}) = -\hat{V}_*\,\hat{x} + \left(\frac{1+\tau}{\tau}\right)\tilde{N}(\hat{x})\,\mathrm{e}^{\,\mathrm{i}\,(\zeta - \hat{\omega}\,\hat{t})}, \tag{305}$$

$$V(\hat{x},\zeta,\hat{t}) = \hat{V}_\parallel + \left(\frac{1+\tau}{\tau}\right)\tilde{V}(\hat{x})\,\mathrm{e}^{\,\mathrm{i}\,(\zeta - \hat{\omega}\,\hat{t})}, \tag{306}$$

$$J(\hat{x},\zeta,\hat{t}) = -\left(\frac{2}{s_s} - 1\right)\frac{1}{\hat{L}_s} + \hat{\nabla}^2\tilde{\psi}(\hat{x})\,\mathrm{e}^{\,\mathrm{i}\,(\zeta - \hat{\omega}\,\hat{t})}, \tag{307}$$

$$U(\hat{x},\zeta,\hat{t}) = \hat{\nabla}^2\tilde{\phi}(\hat{x})\,\mathrm{e}^{\,\mathrm{i}\,(\zeta - \hat{\omega}\,\hat{t})}, \tag{308}$$

where $\hat{t} = V_A\, t/r_s$, $\hat{\omega} = r_s\,\omega/V_A$, and ω is the phase velocity of the tearing mode in the laboratory frame. Substituting Equations (301)–(308) into the four-field model, (273)–(278), and only retaining terms that are first order in perturbed quantities, we obtain the following set of linear layer equations:

$$-\mathrm{i}\,[\omega - \omega_E - (1+\lambda_e)\,\omega_{*e}]\,\tau_H\,\tilde{\psi} = -\mathrm{i}\,\hat{x}\,[\tilde{\phi} - (1+\lambda_e)\,\tilde{N}] + S^{-1}\,\hat{\nabla}^2\tilde{\psi}, \tag{309}$$

$$-\mathrm{i}\,(\omega - \omega_E - \omega_{*i})\,\tau_H\,\hat{\nabla}^2\tilde{\phi} = -\mathrm{i}\,\hat{x}\,\hat{\nabla}^2\tilde{\psi} + S^{-1}\,P_\varphi\,\hat{\nabla}^4\left(\tilde{\phi} + \frac{\tilde{N}}{\tau}\right), \tag{310}$$

$$-\mathrm{i}\,(\omega - \omega_E)\,\tau_H\,\tilde{N} = -\mathrm{i}\,\omega_{*e}\,\tau_H\,\tilde{\phi} - \mathrm{i}\,c_\beta^2\,\hat{x}\,\tilde{V} - \mathrm{i}\left(\frac{\tau}{1+\tau}\right)\hat{d}_\beta^2\,\hat{x}\,\hat{\nabla}^2\tilde{\psi} \tag{311}$$

$$+ S^{-1}\,P_\parallel\left(m\,\omega_{*e}\,\tau_H\,\hat{x}\,\tilde{\psi} - \frac{m}{\hat{L}_s}\,\hat{x}^2\,\tilde{N}\right) + S^{-1}\,P_\perp\,\hat{\nabla}_\perp^2\tilde{N},$$

$$-\mathrm{i}\,(\omega - \omega_E)\,\tau_H\,\tilde{V} = \mathrm{i}\,\omega_{*e}\,\tau_H\,\tilde{\psi} - \mathrm{i}\,\hat{x}\,\tilde{N} + S^{-1}\,P_\varphi\,\hat{\nabla}^2\tilde{V}. \tag{312}$$

Here,

$$\tau_H = \frac{L_s}{m\,V_A} \tag{313}$$

is the *hydromagnetic time*,

$$\omega_E = \left(\frac{m}{r_s}\right)V_E(r_s) \tag{314}$$

the *E-cross-B frequency*,

$$\omega_{*e} = -\left(\frac{\tau}{1+\tau}\right)\left(\frac{m}{r_s}\right)V_*(r_s) \tag{315}$$

the *electron diamagnetic frequency*,

$$\omega_{*i} = \left(\frac{1}{1+\tau}\right)\left(\frac{m}{r_s}\right)V_*(r_s) \tag{316}$$

the *ion diamagnetic frequency*,

$$S = \frac{\tau_R}{\tau_H} \tag{317}$$

the *Lundquist number*,

$$\tau_R = \frac{\mu_0\,r_s^2}{\eta_\parallel} \tag{318}$$

the *resistive diffusion time*,

$$\tau_\varphi = \frac{r_s^2}{\chi_\varphi} = \frac{r_s^2\,n_0\,m_i}{\mu_\perp(r_s)} \tag{319}$$

the *toroidal momentum confinement time*, and

$$\tau_\perp = \frac{r_s^2}{D_\perp} \tag{320}$$

the *particle/energy confinement time*. Furthermore, $P_\varphi = \tau_R/\tau_\varphi$, $P_\perp = \tau_R/\tau_\perp$, $P_\parallel = \tau_R/\tau_\parallel$, and $\tau_\parallel = r_s^2/D_\parallel$.

In conventional tokamak plasmas, the Lundquist number, S, which is the nominal ratio of the plasma inertia term to the resistive diffusion term in the plasma Ohm's law, is very much greater than unity. In fact, S typically exceeds 10^8 (Wesson 2011). However, a resonant layer is characterized by a balance between plasma inertia and resistive diffusion (Furth, Killeen & Rosenbluth 1963). Such a balance is only possible if the layer is very narrow in the radial direction (because a narrow layer enhances radial derivatives, and, thereby, enhances resistive diffusion). Let us define the stretched radial variable (Ara, et al. 1978)

$$X = S^{1/3}\,\hat{x}. \tag{321}$$

Assuming that $X \sim \mathcal{O}(1)$ in the layer (i.e., assuming that the layer thickness is of order $S^{-1/3}\,r_s$), and making use of the fact that $S \gg 1$, we deduce that $\hat{\nabla}^2 \simeq \hat{\nabla}_\perp^2 \simeq S^{2/3}\,d^2/dX^2$. Hence, the linear layer equations, (309)–(312), reduce to (Cole & Fitzpatrick 2006)

$$-\mathrm{i}\,[Q - Q_E - (1+\lambda_e)\,Q_e]\,\tilde{\psi} = -\mathrm{i}\,X\left[\tilde{\phi} - (1+\lambda_e)\,\tilde{N}\right] + \frac{d^2\tilde{\psi}}{dX^2}, \tag{322}$$

$$-\mathrm{i}\,(Q - Q_E - Q_i)\,\frac{d^2\tilde{\phi}}{dX^2} = -\mathrm{i}\,X\,\frac{d^2\tilde{\psi}}{dX^2} + P_\varphi\,\frac{d^4}{dX^4}\left(\tilde{\phi} + \frac{\tilde{N}}{\tau}\right), \tag{323}$$

$$-\mathrm{i}\,(Q - Q_E)\tilde{N} = -\mathrm{i}\,Q_e\,\tilde{\phi} - \mathrm{i}\,c_\beta^2\,X\,\tilde{V} - \mathrm{i}\,D^2\,X\,\frac{d^2\tilde{\psi}}{dX^2} + P_\perp\,\frac{d^2\tilde{N}}{dX^2}, \tag{324}$$

$$-\mathrm{i}\,(Q - Q_E)\,\tilde{V} = \mathrm{i}\,Q_e\,\tilde{\psi} - \mathrm{i}\,X\,\tilde{N} + P_\varphi\,\frac{d^2\tilde{V}}{dX^2}. \tag{325}$$

Here, $Q = S^{1/3}\,\omega\,\tau_H$, $Q_E = S^{1/3}\,\omega_E\,\tau_H$, $Q_{e,i} = S^{1/3}\,\omega_{*\,e,i}\,\tau_H$, and $D = S^{1/3}\,[\tau/(1+\tau)]^{1/2}\,\hat{d}_\beta$. Note that the terms involving parallel transport have dropped out of Equation (324). The neglect of these terms is justified provided that the linear layer width is much less than the critical value,

$$w_c = \left(\frac{1}{\epsilon_s\,s_s\,n}\right)^{1/2}\left(\frac{D_\perp}{D_\parallel}\right)^{1/4} r_s, \tag{326}$$

below which parallel transport is unable to constrain the electron number density (and, by implication, the electron and ion temperatures) to be constant along magnetic field-lines (Fitzpatrick 1995). This condition is well satisfied in conventional tokamak plasmas. Note that all of the terms appearing in the normalized layer equations, (322)–(325), are assumed to be roughly the same order of magnitude.

5.4 Asymptotic Matching

The normalized linear layer equations, (322)–(325), possess independent *tearing parity* solutions, characterized by the symmetry $\tilde{\psi}(-X) = \tilde{\psi}(X)$, $\tilde{\phi}(-X) = -\tilde{\phi}(X)$, $\tilde{N}(-X) = -\tilde{N}(X)$, $\tilde{V}(-X) = \tilde{V}(X)$, and *twisting parity* solutions, characterized by the symmetry $\tilde{\psi}(-X) =$

$-\tilde{\psi}(X)$, $\tilde{\phi}(-X) = \tilde{\phi}(X)$, $\tilde{N}(-X) = \tilde{N}(X)$, $\tilde{V}(-X) = -\tilde{V}(X)$ (Fitzpatrick & Hender 1994). However, only the tearing parity solutions can be asymptotically matched to tearing mode solutions in the outer region. If we assume that the asymptotic behavior of the tearing parity layer solutions is

$$\tilde{\psi} \rightarrow \psi_0 \left[1 + \frac{\hat{\Delta}}{2} \, |X| + \mathcal{O}(X^2) \right] \tag{327}$$

as $|X| \rightarrow \infty$, where ψ_0 is an arbitrary constant, then asymptotic matching to the outer solution yields

$$\Delta \Psi_s = S^{1/3} \, \hat{\Delta} \, \Psi_s. \tag{328}$$

[See Equations (110) and (135).]

5.5 Fourier Transformation

Equations (322)–(325) are most conveniently solved in Fourier transform space (Cole & Fitzpatrick 2006). Let

$$\bar{\phi}(p) = \int_{-\infty}^{\infty} \tilde{\phi}(X) \, \mathrm{e}^{-\mathrm{i} \, p \, X} \, dX, \tag{329}$$

et cetera. The Fourier transformed linear layer equations become

$$-\mathrm{i} \left[Q - Q_E - (1 + \lambda_e) \, Q_e \right] \bar{\psi} = \frac{d}{dp} \left[\bar{\phi} - (1 + \lambda_e) \, \bar{N} \right] - p^2 \, \bar{\psi}, \tag{330}$$

$$-\mathrm{i} \, (Q - Q_E - Q_i) \, p^2 \, \bar{\phi} = \frac{d(p^2 \, \bar{\psi})}{dp} - P_\varphi \, p^4 \left(\bar{\phi} + \frac{\bar{N}}{\tau} \right), \tag{331}$$

$$-\mathrm{i} \, (Q - Q_E) \bar{N} = -\mathrm{i} \, Q_e \, \bar{\phi} + c_\beta^2 \, \frac{d\bar{V}}{dp} - D^2 \, \frac{d(p^2 \, \bar{\psi})}{dp} - P_\perp \, p^2 \bar{N}, \tag{332}$$

$$-\mathrm{i} \, (Q - Q_E) \, \bar{V} = \mathrm{i} \, Q_e \, \bar{\psi} + \frac{d\bar{N}}{dp} - P_\varphi \, p^2 \, \bar{V}, \tag{333}$$

where, for a tearing parity solution,

$$\bar{\phi}(p) \rightarrow \bar{\phi}_0 \left[\frac{\hat{\Delta}}{\pi \, p} + 1 + \mathcal{O}(p) \right] \tag{334}$$

as $p \rightarrow 0$.

Let us ignore the term $c_\beta^2 \, d\bar{V}/dp$ in Equation (332). This approximation can be justified *a posteriori*. It is equivalent to the neglect of the contribution of ion parallel dynamics to the linear plasma response in the resonant layer, and effectively decouples Equation (333) from Equations (330)–(332) (Waelbroeck, et al. 2012). Equations (330)–(332) reduce to (Cole & Fitzpatrick 2006)

$$\frac{d}{dp} \left[G(p) \, \frac{dY_e}{dp} \right] - \frac{A(p)}{B(p)} \, p^2 \, Y_e = 0, \tag{335}$$

where

$$G(p) = \frac{p^2}{-\mathrm{i}\,[Q - Q_E - (1+\lambda_e)\,Q_e] + p^2}, \tag{336}$$

$$A(p) = -(Q - Q_E)\,(Q - Q_E - Q_i) - \mathrm{i}\,(Q - Q_E - Q_i)\,(P_\varphi + P_\perp)\,p^2 + P_\varphi\,P_\perp\,p^4, \tag{337}$$

$$B(p) = -\mathrm{i}\,[Q - Q_E - (1+\lambda_e)\,Q_e] + \{P_\perp - \mathrm{i}\,(1+\lambda_e)\,(Q - Q_E - Q_i)\,D^2\}p^2 + [(1+\lambda_e) + 1/\tau]\,P_\varphi\,D^2\,p^4, \tag{338}$$

and $Y_e = \bar{\phi} - (1+\lambda_e)\,\bar{N}$. The boundary conditions are that $Y_e(p)$ is bounded as $p \rightarrow \infty$, and

$$Y_e(p) \rightarrow Y_0 \left[\frac{\hat{\Delta}}{\pi\,p} + 1 + \mathcal{O}(p)\right] \tag{339}$$

as $p \rightarrow 0$. In the following, we shall assume that $|Q| \sim |Q_E| \sim |Q_e| \sim |Q_i|$, $P_\varphi \sim P_\perp \sim P$, $\tau \sim \mathcal{O}(1)$, and $\lambda_e \sim \mathcal{O}(1)$, for the sake of simplicity.

5.6 Constant-ψ Approximation

Let us suppose that there are two layers in p space. In the small-p layer, suppose that Equation (335) reduces to

$$\frac{d}{dp}\left[\frac{p^2}{-\mathrm{i}\,[Q - Q_E - (1+\lambda_e)\,Q_e] + p^2}\,\frac{dY_e}{dp}\right] \simeq 0 \tag{340}$$

when $p \sim Q^{1/2}$. Integrating directly, we find that

$$Y_e(p) \simeq Y_0 \left[\frac{\hat{\Delta}}{\pi}\left(\frac{1}{p} + \frac{p}{\mathrm{i}\,[Q - Q_E - (1+\lambda_e)\,Q_e]}\right) + 1 + \mathcal{O}(p^2)\right] \tag{341}$$

for $p \lesssim \mathcal{O}(Q^{1/2})$, where use has been made of Equation (339). The two-layer approximation is equivalent to the well-known *constant-ψ approximation* (Furth, Killeen & Rosenbluth 1963).

In the large-p layer, for $p \gg \mathcal{O}(Q^{1/2})$, we obtain

$$\frac{d^2 Y_e}{dp^2} - \frac{A(p)}{B(p)}\,p^2\,Y_e \simeq 0, \tag{342}$$

with Y_e bounded as $p \rightarrow \infty$. Asymptotic matching to the small-p layer yields the boundary condition

$$Y_e(p) \simeq Y_0 \left\{1 + \frac{\hat{\Delta}}{\pi}\,\frac{p}{\mathrm{i}\,[Q - Q_E - (1+\lambda_e)\,Q_e]} + \mathcal{O}(p^2)\right\} \tag{343}$$

as $p \rightarrow 0$.

In the various constant-ψ linear response regimes considered in Section 5.7, Equation (342) reduces to an equation of the form

$$\frac{d^2 Y_e}{dp^2} - C\, p^m\, Y_e \simeq 0, \tag{344}$$

where m is real and non-negative, and C is a complex constant. Let $Y_e = \sqrt{p}\, Z$ and $q = \sqrt{C}\, p^n/n$, where $n = (m+2)/2$. The previous equation transforms into a modified Bessel equation of general order,

$$q^2\, \frac{d^2 Z}{dq^2} + q\, \frac{dZ}{dq} - (q^2 + \nu^2)\, Z = 0, \tag{345}$$

where $\nu = 1/(m+2)$. The solution that is bounded as $q \rightarrow \infty$ has the small-q expansion

$$K_\nu(z) = \frac{1}{\Gamma(1-\nu)} \left(\frac{2}{q}\right)^\nu - \frac{1}{\Gamma(1+\nu)} \left(\frac{q}{2}\right)^\nu + \mathcal{O}(q^{2-\nu}), \tag{346}$$

where $\Gamma(z)$ is a gamma function. A comparison of this expression with Equation (343) reveals that

$$\hat{\Delta} = \pi\, (-\mathrm{i}\, [Q - Q_E - (1+\lambda_e)\, Q_e])\, \frac{\Gamma(1-\nu)}{\Gamma(\nu)}\, \nu^{2\nu-1}\, C^{\,\nu}. \tag{347}$$

Note, finally, that $p_* \sim |C|^{-\nu}$, where p_* denotes the width of the large-p layer in p space. This width must be larger than $Q^{1/2}$ (i.e., the width of the small-p layer) in order for the constant-ψ approximation to hold.

5.7 Constant-ψ Linear Response Regimes

Suppose that $Q \gg P\, p^2$ and $D^2\, p^2 \ll 1$. It follows that $\nu = 1/4$ and

$$C = \frac{[-\mathrm{i}\, (Q - Q_E)]\, [-\mathrm{i}\, (Q - Q_E - Q_i)]}{-\mathrm{i}\, [Q - Q_E - (1+\lambda_e)\, Q_e]}. \tag{348}$$

Hence, we deduce that

$$\hat{\Delta} = \frac{2\pi\, \Gamma(3/4)}{\Gamma(1/4)}\, (-\mathrm{i}\, [Q - Q_E - (1+\lambda_e)\, Q_e])^{3/4}\, [-\mathrm{i}\, (Q - Q_E)]^{1/4}\, [-\mathrm{i}\, (Q - Q_E - Q_i)]^{1/4}. \tag{349}$$

This response regime is known as the *resistive-inertial regime*, because the layer response is dominated by resistivity and ion inertia (Furth, Killeen & Rosenbluth 1963; Ara, et al. 1976; Fitzpatrick 1998). The characteristic layer width is $p_* \sim Q^{-1/4}$, which implies that the regime is valid when $P \ll Q^{3/2}$, $Q \gg D^4$, and $Q \ll 1$.

Suppose that $Q \ll P\, p^2$ and $D^2\, p^2 \ll 1$. It follows that $\nu = 1/6$ and $C = P_\varphi$. Hence, we deduce that

$$\hat{\Delta} = \frac{6^{2/3}\, \pi\, \Gamma(5/6)}{\Gamma(1/6)}\, (-\mathrm{i}\, [Q - Q_E - (1+\lambda_e)\, Q_e])\, P_\varphi^{1/6}. \tag{350}$$

This response regime is known as the *visco-resistive regime*, because the layer response is dominated by resistivity and ion perpendicular viscosity (Bondeson & Persson 1986; Fitzpatrick 1993). The characteristic layer width is $p_* \sim P^{-1/6}$, which implies that the regime is valid when $P \gg Q^{3/2}$, $P \gg D^6$, and $P \ll Q^{-3}$.

Suppose that $Q \gg P\,p^2$ and $D^2\,p^2 \gg 1$. It follows that $\nu = 1/2$ and

$$C = \frac{-\mathrm{i}\,(Q - Q_E)}{(1+\lambda_e)\,D^2}. \tag{351}$$

Hence, we deduce that

$$\hat{\Delta} = \frac{\pi\,(-\mathrm{i}\,[Q - Q_E - (1+\lambda_e)\,Q_e])\,[-\mathrm{i}\,(Q-Q_E)]^{1/2}}{\sqrt{1+\lambda_e}\,D}. \tag{352}$$

This response regime is known as the *semi-collisional regime* (Drake & Lee 1977; Waelbroeck 2003). The characteristic layer width is $p_* \sim D\,Q^{-1/2}$, which implies that the regime is valid when $Q \ll D^4$, $P \ll Q^2/D^2$, and $Q \ll D$.

Suppose, finally, that $Q \ll P\,p^2$ and $D^2\,p^2 \gg 1$. It follows that $\nu = 1/4$ and

$$C = \frac{P_\perp}{[(1+\lambda_e) + 1/\tau]\,D^2}. \tag{353}$$

Hence, we deduce that

$$\hat{\Delta} = \frac{2\pi\,\Gamma(3/4)}{\Gamma(1/4)}\,\frac{(-\mathrm{i}\,[Q - Q_E - (1+\lambda_e)\,Q_e])\,P_\perp^{1/4}}{[(1+\lambda_e)+1/\tau]^{1/4}\,D^{1/2}}. \tag{354}$$

This response regime is known as the *Hall-resistive regime* (Cole & Fitzpatrick 2006). The characteristic layer width is $p_* \sim D^{1/2}\,P^{-1/4}$, which implies that the regime is valid when $P \gg Q^2/D^2$, $P \ll D^6$, and $P \ll D^2/Q^2$.

5.8 Nonconstant-ψ Regimes

Suppose that $p \ll Q^{1/2}$. In this limit, Equation (335) reduces to

$$\frac{d}{dp}\left(p^2\,\frac{dY_e}{dp}\right) - (-\mathrm{i}\,[Q - Q_E - (1+\lambda_e)\,Q_e])\,\frac{A(p)}{B(p)}\,p^2\,Y_e = 0. \tag{355}$$

In the various nonconstant-ψ regimes considered in this section, the previous equation takes the form

$$\frac{d}{dp}\left(p^2\,\frac{dY_e}{dp}\right) - C\,p^{m+2}\,Y_e = 0, \tag{356}$$

where m is real and non-negative, and C is a complex constant. Let $U = p\,Y_e$. The previous equation yields

$$\frac{d^2U}{dp^2} - C\,p^m\,U = 0. \tag{357}$$

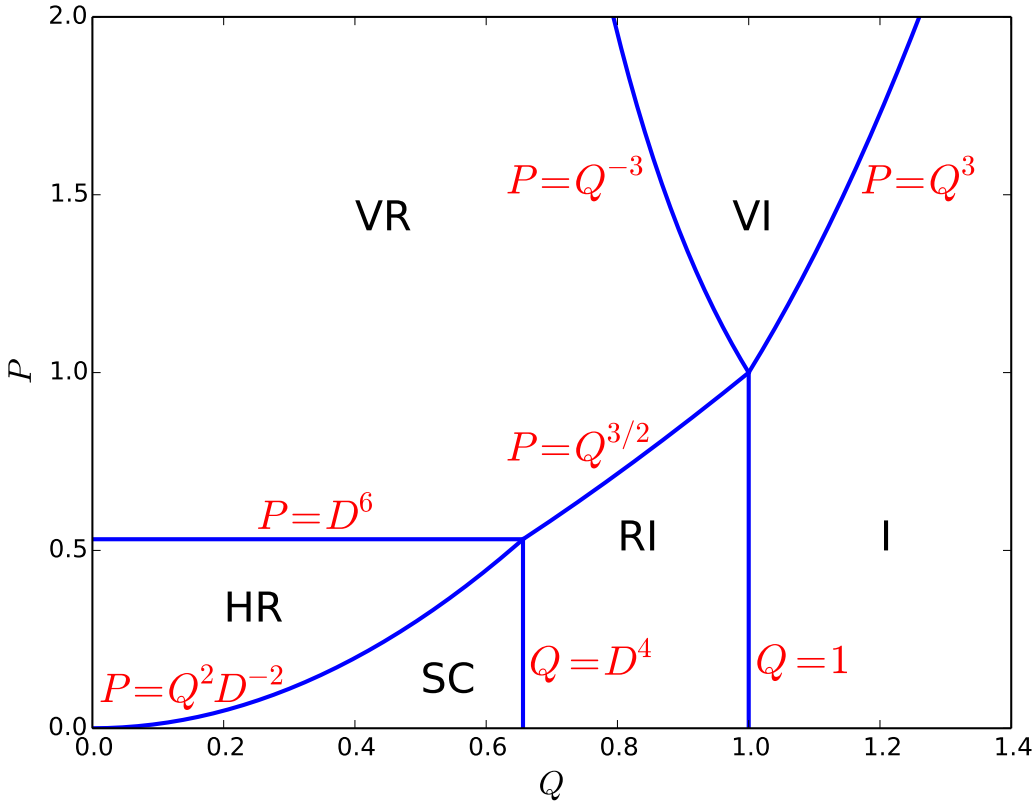

Figure 1: Linear resonant plasma response regimes in Q-P space for the case $D = 0.9$. The various regimes are the Hall-resisitive (HR), the semi-collisional (SC), the resistive-inertial (RI), the visco-resistive (VR), the visco-inertial (VI), and the inertial (I).

This equation is identical in form to Equation (344), which we have already solved. Indeed, the solution that is bounded as $p \to \infty$ has the small-p expansion (346), where $q = \sqrt{C}\, p^n/n$, $n = (m+2)/2$, and $\nu = 1/(m+2)$. Matching to Equation (339) yields

$$\hat{\Delta} = -\pi\, \frac{\Gamma(\nu)}{\Gamma(1-\nu)}\, \nu^{1-2\nu}\, C^{-\nu}. \tag{358}$$

The layer width in p-space again scales as $p_* \sim |C|^{-\nu}$. This width must be less that $Q^{1/2}$.

Suppose that $Q \gg P\, p^2$ and $D^2\, p^2 \ll 1$. It follows that $\nu = 1/2$ and

$$C = [-\mathrm{i}\,(Q - Q_E)]\,[-\mathrm{i}\,(Q - Q_E - Q_i)]. \tag{359}$$

Hence, we deduce that

$$\hat{\Delta} = -\frac{\pi}{[-\mathrm{i}\,(Q - Q_E)]^{1/2}\,[-\mathrm{i}\,(Q - Q_E - Q_i)]^{1/2}}. \tag{360}$$

This response regime is known as the *inertial regime*, because the layer response is dominated by ion inertia (Ara, et al. 1976; Fitzpatrick 1998). Note that the plasma response in the inertial regime is equivalent to that of two closely-spaced Alfvén resonances that straddle the resonant surface (Boozer 1996). The characteristic layer width is $p_* \sim Q^{-1}$, which implies that the regime is valid when $P \ll Q^3$, $Q \gg D$, and $Q \gg 1$.

Suppose that $Q \ll P\,p^2$ and $D^2\,p^2 \ll 1$. It follows that $\nu = 1/4$ and

$$C = (-\mathrm{i}\,[Q - Q_E - (1+\lambda_e)\,Q_e])\,P_\varphi. \tag{361}$$

Hence, we deduce that

$$\hat{\Delta} = -\frac{\pi}{2}\,\frac{\Gamma(1/4)}{\Gamma(3/4)}\,(-\mathrm{i}\,[Q - Q_E - (1+\lambda_e)\,Q_e])^{-1/4}\,P_\varphi^{-1/4}. \tag{362}$$

This response regime is known as the *visco-inertial regime*, because the layer response is dominated by ion perpendicular viscosity and ion inertia (Fitzpatrick 1998). The characteristic layer width is $p_* \sim Q^{-1/4}\,P^{-1/4}$, which implies that the regime is valid when $P \gg Q^3$, $P \gg D^4/Q$, and $P \gg Q^{-3}$.

Suppose, finally, that $Q \ll P\,p^2$ and $D^2\,p^2 \gg 1$. It follows that $\nu = 1/2$ and

$$C = \frac{(-\mathrm{i}\,[Q - Q_E - (1+\lambda_e)\,Q_e]\,P_\perp}{[(1+\lambda_e) + 1/\tau]\,D^2}. \tag{363}$$

Hence, we deduce that

$$\hat{\Delta} = -\frac{\pi\,[(1+\lambda_e) + 1/\tau]^{1/2}\,D}{(-\mathrm{i}\,[Q - Q_E - (1+\lambda_e)\,Q_e])^{1/2}\,P_\perp^{1/2}}. \tag{364}$$

This response regime is known as the *Hall-viscous regime*. The characteristic layer width is $p_* \sim D\,Q^{-1/2}\,P^{-1/2}$, which implies that the regime is valid when $Q \ll D$, $P \ll D^4/Q$, and $P \gg D^2/Q^2$.

5.9 Discussion

Figures 1 and 2 show the extents of the various different response regimes in Q-P space for the cases $D < 1$ and $D > 1$, respectively.

Let $\hat{\delta}_* \sim p_*^{-1}$ be the normalized radial thickness of the resonant layer. Of course, the true thickness is $\delta = S^{-1/3}\,\hat{\delta}_*\,r_s$. It follows from Equation (327) that the relative change in the perturbed helical flux, $\tilde{\psi}$, across the layer is

$$\left.\frac{d\ln\tilde{\psi}}{dX}\right|_{-\hat{\delta}/2}^{+\hat{\delta}/2} = \hat{\Delta}\;\hat{\delta}_* \sim \hat{\Delta}\;p_*^{-1}, \tag{365}$$

According to the analysis of Section 5.7, $\hat{\Delta}\,p_*^{-1}$ takes the respective values $Q^{1/2}$, $Q\,P^{1/3}$, Q^2/D^2, and $Q\,P^{1/2}/D$ in the resistive-inertial, visco-resistive, semi-collisional, and Hall-resistive response regimes. Moreover, it is clear from Figures 1 and 2 that these values

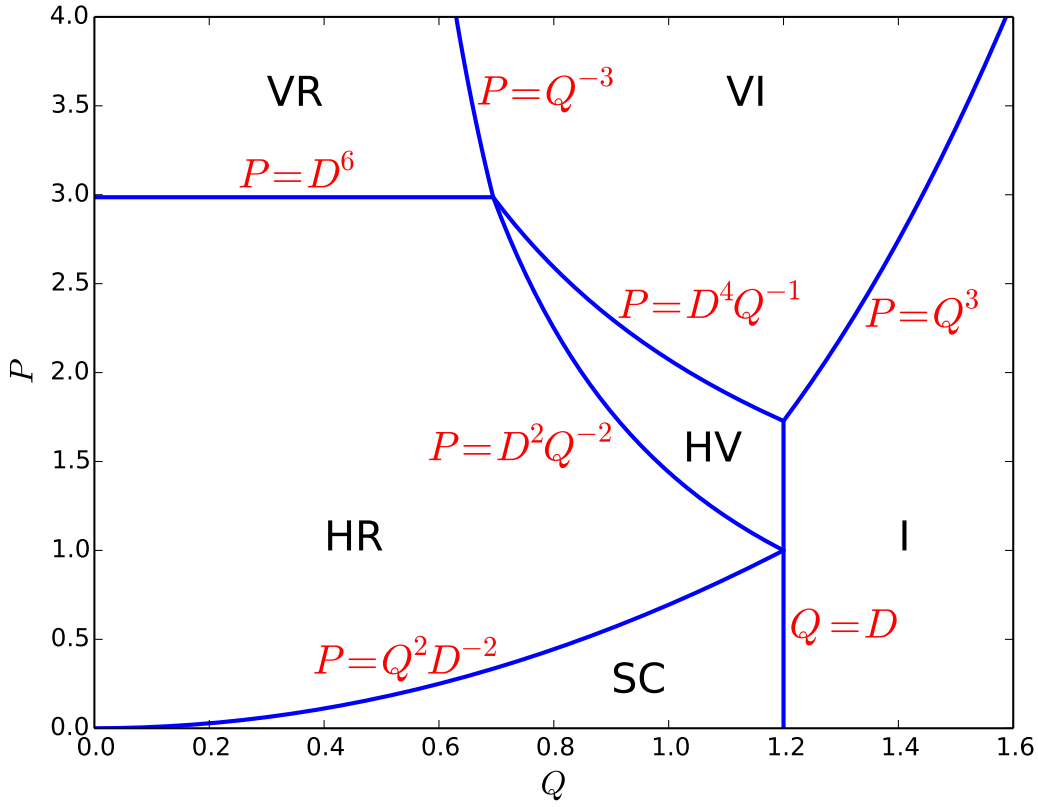

Figure 2: Linear resonant plasma response regimes in Q-P space for the case $D = 1.2$. The various regimes are the Hall-resisitive (HR), the semi-collisional (SC), the Hall-viscous (HV), the visco-resistive (VR), the visco-inertial (VI), and the inertial (I).

are all much less than unity. In other words, it is indeed the case that $\tilde{\psi}$ does not vary substantially across a 'constant-ψ' resonant layer. On the other hand, according to the analysis of Section 5.8, $\hat{\Delta}\, p_*^{-1} \sim 1$ in the inertial, visco-inertial, and Hall-viscous response regimes, which implies that $\tilde{\psi}$ does vary substantially across a 'nonconstant-ψ' layer.

Suppose that the resonant layer lies in a constant-ψ response regime. According to Equation (303), the perturbed magnetic flux in the layer takes the form:

$$\hat{\psi}(\hat{x},\zeta,\hat{t}) = \frac{\hat{x}^{\,2}}{2\,\hat{L}_s} + \tilde{\psi}\,\mathrm{e}^{\,\mathrm{i}\,(\zeta-\hat{\omega}\,\hat{t})}, \tag{366}$$

where $\tilde{\psi}$ is a complex constant. Of course, the physical flux is the real part of the previous expression; that is,

$$\hat{\psi}(\hat{x},\xi) = \frac{\hat{x}^{\,2}}{2\,\hat{L}_s} + |\tilde{\psi}|\,\cos\xi, \tag{367}$$

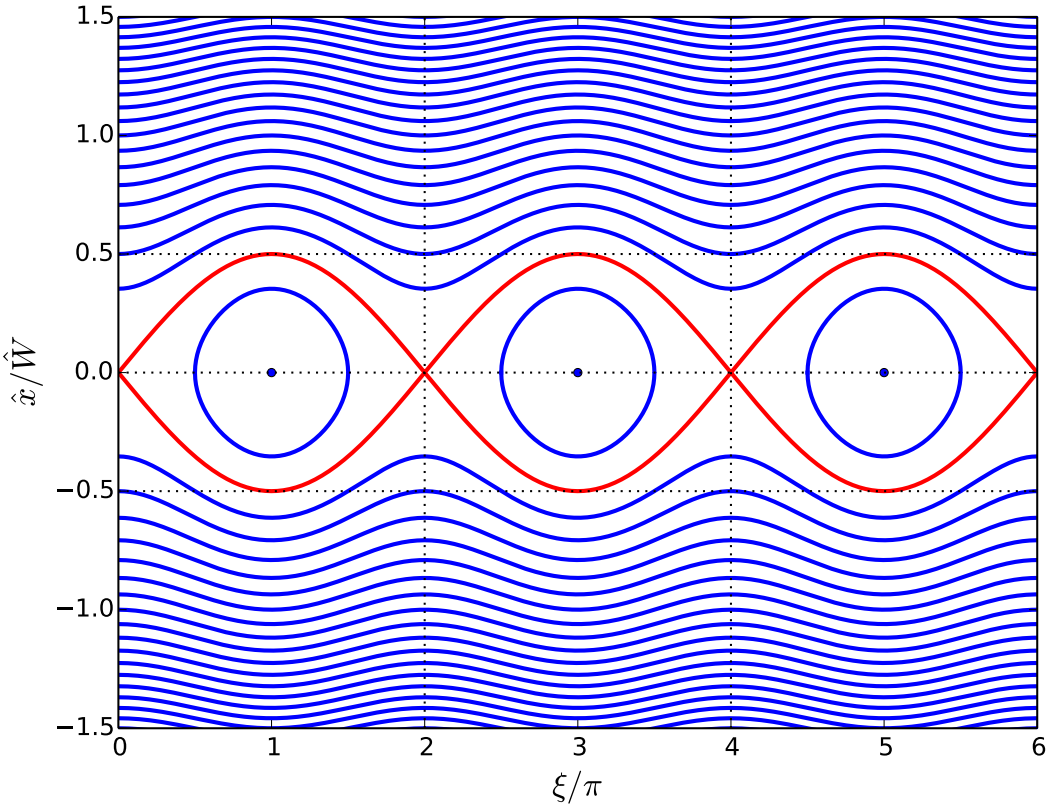

Figure 3: Equally-spaced contours of $\hat{\psi}(\hat{x},\xi)$. The magnetic separatrix is shown in red.

where

$$\xi = \zeta + \arg(\tilde{\psi}) - \hat{\omega}\,\hat{t} = m\,\theta - n\,\varphi + \arg(\tilde{\psi}) - \omega\,t. \tag{368}$$

Now, it is clear from Equation (283) that $\mathbf{B}\cdot\hat{\nabla}\hat{\psi} = 0$. In other words, the contours of $\hat{\psi}(\hat{x},\xi)$ map out the perturbed magnetic flux-surfaces in the vicinity of the resonant layer. Let $\hat{W} = 4\,(\hat{L}_s\,|\tilde{\psi}|)^{1/2}$. Equation (367) can be written

$$\frac{\hat{\psi}(\hat{x},\xi)}{|\tilde{\psi}|} = 8\left(\frac{\hat{x}}{\hat{W}}\right)^2 + \cos\xi. \tag{369}$$

Figure 3 shows the contours of $\hat{\psi}(\hat{x},\xi)$ specified by the previous equation. It can be seen that the tearing mode has reconnected magnetic field-lines to produce a *helical magnetic island chain* centered on the resonant surface ($\hat{x} = 0$). The chain has m periods in the poloidal direction, n periods in the toroidal direction, and propagates at the phase velocity ω. The maximum full (as opposed to half) radial width of the magnetic separatrix is

$$W = \hat{W}\,r_s = 4\,(\hat{L}_s\,|\tilde{\psi}|)^{1/2}\,r_s = 4\left(L_s\,R_0\,|\hat{\Psi}_s|\right)^{1/2}, \tag{370}$$

where $\Psi_s = r_s\, B_z\, \tilde{\psi}$ is the reconnected magnetic flux defined in Equation (100), and $\hat{\Psi}_s = \Psi_s/(R_0\, B_z)$.

Finally, our four-field resonant plasma response model, (273)–(278), contains many term of the general form $[\hat{\psi}, \tilde{A}]$, where $\tilde{A}(\hat{x}, \zeta, \hat{t})$ is a perturbed quantity. According to Equation (367), such terms can be written

$$[\hat{\psi}, \tilde{A}] = \mathrm{i}\, \frac{m}{r_s} \left(\frac{\hat{x}}{\hat{L}_s}\, \tilde{A} - \tilde{\psi}\, \frac{\partial \tilde{A}}{\partial \hat{x}} \right) \sim \mathrm{i}\, \frac{m}{r_s}\, \frac{\hat{\delta}}{\hat{L}_s}\, \tilde{A} - \mathrm{i}\, \frac{m}{r_s}\, \frac{\tilde{\psi}}{\hat{\delta}}\, \tilde{A}, \tag{371}$$

where $\delta = \hat{\delta}\, r_s$ is the width of the linear layer. Now, linear layer theory is only valid when the second term on the extreme right side of the previous equation is negligible compared to the first (because the second term is quadratic in perturbed quantities, whereas the first is linear). In other words, we require $\hat{\delta}^{\,2} \gg |\tilde{\psi}|\, \hat{L}_s$, which reduces to

$$\delta \gg W. \tag{372}$$

[See Equation (370).] We conclude that the linear resonant response theory presented in this section is only valid when the radial width of the magnetic island chain that develops in the vicinity of the resonant surface is *much less* than the radial width of the linear layer. Given that linear layers are very narrow in conventional tokamak plasmas, this is a stringent constraint.

6 Linear Tearing Mode Stability

6.1 Introduction

The aim of this section is to combine the analysis of Sections 3 and 5 to determine the linear stability of tearing modes in tokamak plasmas. In this study, we shall assume that the wall is perfectly conducting.

6.2 Linear Dispersion Relation

Let us write

$$\omega = \mathrm{i}\, \gamma + \omega_r, \tag{373}$$

where γ is the growth-rate of the tearing mode, whereas ω_r is the real phase velocity of the mode in the laboratory frame. We shall assume that $|\gamma| \ll |\omega_r|$. This assumption can easily be verified *a posteriori*. Asymptotic matching between the solution in the outer region and that in the thin linear layer surrounding the resonant surface yields a linear tearing mode dispersion relation of the form

$$S^{1/3}\, \hat{\Delta}(\gamma, \omega_r) = E_{ss}, \tag{374}$$

where use has been made of Equations (111) and (328). Here, E_{ss} is the real tearing stability index, whereas the complex layer matching parameter, $\hat{\Delta}$, is defined in Equation (327).

In a conventional tokamak plasma [assuming that $m \sim \mathcal{O}(1)$], $E_{ss} \sim \mathcal{O}(1)$,[2] and $S^{1/3} \gg 1$. Hence, the previous dispersion relation can only be satisfied if ω_r takes a value that renders $|\hat{\Delta}| \ll 1$. It is clear from Equations (349), (350), (352), and (354) that this goal can be achieved in all of the constant-ψ linear response regimes if

$$\omega_r = \omega_{\perp\, e}, \tag{375}$$

where

$$\omega_{\perp\, e} = \omega_E + (1+\lambda_e)\,\omega_{*\, e}. \tag{376}$$

According to Equations (375) and (376), the tearing mode co-rotates with the electron fluid at the resonant surface.[3]

6.3 Determination of Linear Growth-Rates

Reusing the analysis of Sections 5.6 and 5.7, let us again suppose that there are two layers in p space (i.e., Fourier space). The small-p layer turns out to be of width $|\hat{\gamma}|^{1/2}$, where $\hat{\gamma} = S^{1/3}\,\gamma\,\tau_H$. Given that we are effectively assuming that $|\hat{\gamma}| \ll 1$, the condition for the separation of the layer solution into two layers (i.e., that the width of the small-p layer is less than that of the large-p layer) is always satisfied. The large-p layer is governed by the equation

$$\frac{d^2 Y_e}{dp^2} - \frac{A(p)}{\tilde{B}(p)}\, Y_e = 0, \tag{377}$$

where

$$A(p) = (1+\lambda_e)\left(\frac{\tau}{1+\tau}\right)\left(1+\frac{\lambda_e\,\tau}{1+\tau}\right) Q_*^2 - \mathrm{i}\left(1+\frac{\lambda_e\,\tau}{1+\tau}\right) Q_*\,(P_\varphi + P_\perp)\,p^2 + P_\varphi\,P_\perp\,p^4, \tag{378}$$

$$\tilde{B}(p) = P_\perp - \mathrm{i}\,(1+\lambda_e)\left(1+\frac{\lambda_e\,\tau}{1+\tau}\right) Q_*\,D^2 + \left(\frac{1+\tau}{\tau}\right)\left(1+\frac{\lambda_e\,\tau}{1+\tau}\right) D^2\,P_\varphi\,p^2. \tag{379}$$

Here, $Q_* = S^{1/3}\,\omega_*\,\tau_H$, where

$$\omega_* = -\frac{m}{r_s}\,V_*(r_s) = -\frac{m}{r_s}\frac{1}{e\,n_0\,B_z}\left.\frac{dp}{dr}\right|_{r_s}. \tag{380}$$

In the following, ω_* is assumed to be positive. The boundary conditions on Equation (377) are that Y_e is bounded as $p \to \infty$, and

$$Y_e(p) = Y_0\left[1 - \frac{\hat{\Delta}\,p}{\pi\,\hat{\gamma}} + \mathcal{O}(p^2)\right] \tag{381}$$

[2]Note that we are neglecting $m = 1$ modes, for which $|E_{ss}| \gg 1$, because such modes are not really tearing modes (Wesson 1978).

[3]In fact, the mode rotates slightly faster than the electron fluid because of the influence of the thermal force, $\mathbf{F}_T$ [see Equation (43)], which generates the additional factor λ_e in Equation (376).

as $p \rightarrow 0$.

In the various constant-ψ linear response regimes considered in this section, Equation (377) reduces to an equation of the form

$$\frac{d^2 Y_e}{dp^2} - C\, p^m\, Y_e = 0, \tag{382}$$

where m is real and non-negative, and C is a complex constant. As described in Section 5.6, the solution of this equation that is bounded as $p \rightarrow \infty$ can be matched to the small-p asymptotic form (381) to give

$$\hat{\Delta} = \pi\, \hat{\gamma}\, \frac{\Gamma(1-\nu)}{\Gamma(\nu)}\, \nu^{2\nu-1}\, C^{\,\nu}, \tag{383}$$

where $\nu = 1/(m+2)$. The width of the large-p layer in p space is $C^{-\nu}$.

As before, we shall assume that $P_\varphi \sim P_\perp \sim P$, $\lambda_e \sim \mathcal{O}(1)$, and $\tau \sim \mathcal{O}(1)$, for the sake of simplicity. Suppose that $Q_* \gg P\, p^2$ and $P \gg Q_*\, D^2$. It follows that $\nu = 1/2$ and

$$C = \left(\frac{\tau}{1+\tau}\right)(1+\lambda_e)\left(1+\frac{\lambda_e\,\tau}{1+\tau}\right)\frac{Q_*^2}{P_\perp}. \tag{384}$$

Hence,

$$\hat{\Delta} = \pi\, \hat{\gamma}\left[\left(\frac{\tau}{1+\tau}\right)(1+\lambda_e)\left(1+\frac{\lambda_e\,\tau}{1+\tau}\right)\right]^{1/2}\frac{Q_*}{P_\perp^{1/2}}, \tag{385}$$

and $p_* \sim P^{1/2}/Q_*$. This so-called *resistive-inertial regime* is valid when $P \ll Q_*^{3/2}$ and $P \gg Q_*\, D^2$. Making use of Equation (374), the corresponding tearing mode growth-rate is

$$\gamma = \frac{E_{ss}}{\pi\left[\left(\frac{\tau}{1+\tau}\right)(1+\lambda_e)\left(1+\frac{\lambda_e\,\tau}{1+\tau}\right)\right]^{1/2}}\,\frac{1}{\omega_*\,\tau_H\,\tau_R^{1/2}\,\tau_\perp^{1/2}}. \tag{386}$$

Suppose that $Q_* \ll P\, p^2$ and $D^2\, p^2 \ll 1$. It follows that $\nu = 1/6$ and $C = P_\varphi$. Hence,

$$\hat{\Delta} = 6^{2/3}\,\pi\,\hat{\gamma}\,\frac{\Gamma(5/6)}{\Gamma(1/6)}\,P_\varphi^{1/6}, \tag{387}$$

and $p_* \sim P^{-1/6}$. This so-called *visco-resistive regime* is valid when $P \gg Q_*^{3/2}$ and $P \gg D^6$. The corresponding tearing mode growth-rate is

$$\gamma = \frac{E_{ss}}{6^{2/3}\,\pi\,[\Gamma(5/6)/\Gamma(1/6)]}\,\frac{\tau_\varphi^{1/6}}{\tau_H^{1/3}\,\tau_R^{5/6}}. \tag{388}$$

Suppose that $Q_* \gg P\, p^2$ and $P \ll Q_*\, D^2$. It follows that $\nu = 1/2$ and

$$C = \mathrm{i}\left(\frac{\tau}{1+\tau}\right)\frac{Q_*}{D^2}. \tag{389}$$

Hence,

$$\hat{\Delta} = \mathrm{e}^{\,\mathrm{i}\,\pi/4}\,\pi\,\hat{\gamma}\left(\frac{\tau}{1+\tau}\right)^{1/2}\,\frac{Q_*^{1/2}}{D}, \tag{390}$$

and $p_* \sim D/Q_*^{1/2}$. This so-called *semi-collisional regime* is valid when $P \ll Q_*^2/D^2$ and $P \ll Q_*\,D^2$. The corresponding tearing mode growth-rate is

$$\gamma = \frac{E_{ss}}{\sqrt{2}\,\pi}\,\frac{d_\beta/r_s}{\omega_*^{1/2}\,\tau_H\,\tau_R^{1/2}}. \tag{391}$$

Here, we have neglected the imaginary component of γ because it merely gives rise to a small correction to the phase velocity of the mode.

Suppose, finally, that $Q_* \ll P\,p^2$ and $D^2\,p^2 \gg 1$. It follows that $\nu = 1/4$ and

$$C = \frac{P_\perp\,[\tau/(1+\tau)]}{[1+\lambda_e\,\tau/(1+\tau)]\,D^2}. \tag{392}$$

Hence,

$$\hat{\Delta} = 2\pi\,\hat{\gamma}\,\frac{\Gamma(3/4)}{\Gamma(1/4)}\,\frac{[\tau/(1+\tau)]^{1/4}\,P_\perp^{1/4}}{[1+\lambda_e\,\tau/(1+\tau)]^{1/4}\,D^{1/2}}, \tag{393}$$

and $p_* \sim D^{1/2}/P^{1/4}$. This so-called *Hall-resistive regime* is valid when $P \gg Q_*^2/D^2$ and $P \ll D^6$. The corresponding tearing mode growth-rate is

$$\gamma = \frac{E_{ss}}{2\pi\,[\Gamma(3/4)/\Gamma(1/4)]\,[1+\lambda_e\,\tau/(1+\tau)]^{-1/4}}\,\frac{(d_\beta/r_s)^{1/2}\,\tau_\perp^{1/4}}{\tau_H^{1/2}\,\tau_R^{3/4}}. \tag{394}$$

6.4 Discussion

According to Equations (373), (375), (386), (388), (391), and (394), a linear tearing mode is unstable when the tearing stability index, E_{ss}, is positive, and is stable otherwise (Furth, Killeen & Rosenbluth 1963). Moreover, the perturbed magnetic field associated with the mode corotates with the electron fluid at the resonant surface (Ara, et al. 1978). Finally, the mode grows on a hybrid timescale that is much greater than the hydrodynamical timescale, τ_H, but much less than the resistive evolution timescale, τ_R. Note that, in all cases, the growth-rate goes to zero as $\tau_R \rightarrow \infty$. This is not surprising because, as is clear from Equation (309), the perturbed helical magnetic flux at the resonant surface, $\tilde{\psi}(\hat{x}=0,\zeta)$, is constrained to take the value zero in the limit that $S \rightarrow \infty$. In other words, magnetic reconnection at the resonant surface (which corresponds to a finite $\tilde{\psi}$ at $\hat{x}=0$) is impossible in the absence of plasma resistivity (Furth, Killeen & Rosenbluth 1963).

There are three main factors that affect the growth-rate of a tearing mode in a conventional tokamak plasma. First, the strength of diamagnetic flows in the plasma, which is parameterized by the diamagnetic frequency, ω_* (and by the normalized diamagnetic frequency, Q_*). Second, the anomalous perpendicular diffusion of momentum and particles,

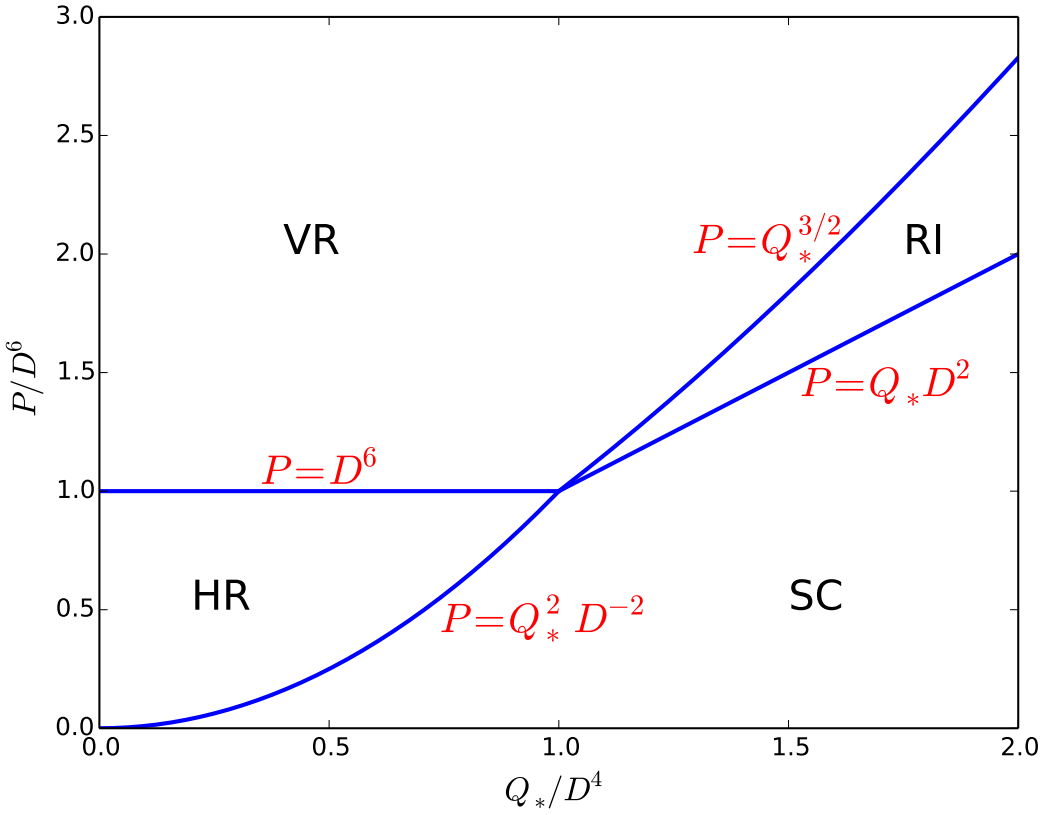

Figure 4: Linear tearing mode growth-rate regimes in Q_*-P space. The various regimes are the Hall-resisitive (HR), the semi-collisional (SC), the visco-resistive (VR), and the resistive-inertial (RI).

which is parameterized by the momentum and particle confinement timescales, τ_φ and $\tau_\perp$ (and by the magnetic Prandtl number, P). Third, finite ion sound radius effects, which are parameterized by the ion sound radius, d_β (and by the normalized ion sound radius D).

There are four tearing-mode growth-rate regimes—the resistive-inertial, the visco-resistive, the semi-collisional, and the Hall-resistive—and their extents in Q_*-P space are illustrated in Figure 4. Note that Figure 4 differs somewhat from Figures 1 and 2 because in the latter two figures it is assumed that $|Q-Q_E-(1+\lambda_e)\,Q_e| \sim |Q-Q_E| \sim |Q-Q_E-Q_i|$ whereas in the former figure it is assumed that $|Q-Q_E-(1+\lambda_e)\,Q_e| \ll |Q-Q_E| \sim |Q-Q_E-Q_i|$. This refined ordering eliminates the nonconstant-ψ response regimes, and significantly modifies the resistive-inertial response regime.

The absence of nonconstant-ψ response regimes in Figure 4 should come as no surprise. As we saw in Section 5.9, nonconstant-ψ resonant layers are characterized by $\hat{\Delta} \sim \hat{\delta}_*^{-1} = S^{-1/3}\,(r_s/\delta)$, where δ is the layer thickness. Hence, according to Equation (374), asymptotic matching of such a layer to the outer solution is only possible if $|E_{ss}| \sim r_s/\delta \gg 1$ (given

that resonant layers in tokamak plasmas are invariably very thin compared to the minor radius of the plasma). However, low-m tearing modes in conventional tokamak plasmas are characterized by $|E_{ss}| \sim \mathcal{O}(1)$ rather than $|E_{ss}| \gg 1$. (As before, we are neglecting $m = 1$ modes, which are characterized by $|E_{ss}| \gg 1$, because they are not really tearing modes.)

Diamagnetic flows modify the tearing mode growth-rate in the resistive-inertial and semi-collisional growth-rate regimes, but not in the Hall-resistive and visco-resistive regimes. Anomalous perpendicular transport modifies the growth-rate in all regimes except the semi-collisional regime. Finally, finite ion sound radius effects modify the growth-rate in the Hall-resistive and semi-collisional regimes, but not in the other two regimes.

Increasing the diamagnetic flow strength decreases the tearing mode growth-rate such that it eventually scales as $\omega_*^{-1/2}$. Increasing the anomalous perpendicular transport increases the growth-rate such that it eventually scales as $P_\varphi^{1/6}$. Increasing the ion sound radius increases the tearing mode growth-rate, but the increase eventually saturates (i.e., the growth-rate ends up scaling as d_β^0).

Finally, it is clear from Equation (374) that the layer solution can only be matched to the outer solution when ω_r takes a value that renders $|\hat{\Delta}| \ll 1$. We have seen that this is possible in all constant-ψ response regimes when $\omega_r = \omega_E + (1 + \lambda_e)\,\omega_{*e}$ (i.e., when the tearing perturbation corotates with the electron fluid at the resonant surface.) However, Equation (349) seems to suggest that in the resistive-inertial regime it might be possible to successfully match the layer solution to the outer solution when $\omega_r = \omega_E$ (i.e., $Q = Q_E$), or when $\omega_r = \omega_E + \omega_{*i}$ (i.e., $Q = Q_E + Q_i$), giving tearing mode perturbations that corotate with the MHD fluid and the ion fluid, respectively, at the resonant surface. In fact, we can see that this is not the case, because if we set $\omega_r = \omega_E$ or $\omega_r = \omega_E + \omega_{*i}$ then Equation (342) does not lead to a layer solution characterized by $|\hat{\Delta}| \ll 1$, as a consequence of finite anomalous perpendicular transport (Waelbroeck, et al. 2012). Likewise, Equation (352) seems to suggest that in the semi-collisional response regime it might be possible to successfully match the layer solution to the outer solution when $\omega_r = \omega_E$, giving rise to a tearing perturbation that corotates with the MHD fluid at the resonant surface. In fact, this possibility is also ruled out by finite anomalous perpendicular transport.

7 Error-Field Penetration in Tokamak Plasmas

7.1 Introduction

Tokamak plasmas are invariably subject to small amplitude, static, resonant magnetic perturbations—known as *error-fields*—which are primarily generated by field-coil misalignments and uncompensated coil feeds. Error-fields can drive magnetic reconnection, resulting in the formation of *locked* (i.e., non-rotating in the laboratory frame) magnetic island chains, in intrinsically tearing-stable plasmas. Low-density, ohmically-heated tokamak plasmas containing locked magnetic island chains often terminate in sudden violent events known as *disruptions* (Wesson, et al. 1989; Wesson 2011) (usually triggered when the external heating is turned on). Fortunately, error-field driven magnetic reconnection is strongly suppressed by

the naturally occurring rotation of ohmic plasmas. However, when the error-field amplitude rises above a certain critical amplitude, the rotation at the resonant surface is suddenly arrested, and error-field driven reconnection proceeds unhindered. This phenomenon is known as *error-field penetration* (Fitzpatrick 1993; Fitzpatrick 1998). The scenario just outlined has been observed in a number of tokamak experiments (Scoville, et al. 1991; Hender, et al. 1992; Fishpool & Haynes 1994; Wolfe, et al. 2005; Wolf, et al. 2005; Howell, Hender, & Cunningham 2007; Menard, et al. 2010; Wang, et al. 2014; Wang, et al. 2018).

In this section, we shall calculate the critical error-field amplitude required to trigger penetration on the assumption that, prior to penetration, the rotational suppression of error-field driven magnetic reconnection is sufficiently strong that the resonant plasma response is governed by linear layer physics (Fitzpatrick 1993; Fitzpatrick 1998; Cole & Fitzpatrick 2006).

7.2 Asymptotic Matching

It is convenient to parametrize the error-field in terms of the static current, I_c, that must be run through the magnetic field-coil introduced in Section 3.9 in order to generate it. Setting $d/dt = 0$ in Equations (208) and (209), we get

$$\Delta\hat{\Psi}_s = \Delta_{nw}\,\hat{\Psi}_s + \tilde{I}_c, \tag{395}$$

where

$$\Delta_{nw} = \Delta_{pw} + \frac{E_{sw}^2}{(-\tilde{E}_{ww})} \tag{396}$$

is the (real) tearing stability index in the absence of a wall,

$$\Delta_{pw} = E_{ss} \tag{397}$$

is the (real) tearing stability index in the presence of a perfectly conducting wall at $r = r_w$, and

$$\tilde{I}_c = \left(\frac{\Delta_{nw} - \Delta_{pw}}{E_{sw}}\right)\left(\frac{r_w}{r_c}\right)^m\left(\frac{\mu_0\, I_c}{R_0\, B_z}\right). \tag{398}$$

Here, the plasma-wall coupling parameter, $E_{sw} > 0$, is defined in Section 3.6. We expect $0 > \Delta_{nw} > \Delta_{pw}$ because the plasma is assumed to be tearing stable, and $\tilde{E}_{ww} < 0$.

In the resonant layer, Equation (328) yields

$$\Delta\hat{\Psi}_s = \Delta\;\hat{\Psi}_s, \tag{399}$$

where $\Delta = S^{1/3}\,\hat{\Delta}$, and the complex layer matching parameter, $\hat{\Delta}$, is defined in Equation (328). Hence, asymptotic matching between the inner and the outer regions yields

$$\hat{\Psi}_s = \frac{\tilde{I}_c}{(-\Delta_{nw}) + \Delta}, \tag{400}$$

where use has been made of Equations (395) and (399). The previous equation specifies the (normalized) reconnected magnetic flux, $\hat{\Psi}_s$, driven at the resonant surface by the (normalized) error-field coil current, $\tilde{I}_c$. The complex layer parameter, Δ, specifies the strength of a shielding current that is induced in the resonant layer, and acts to prevent driven magnetic reconnection.

7.3 Resonant Layer Response

Generally speaking, in an ohmically-heated tokamak, we do not expect the plasma flow at the resonant surface to be sufficiently large to cause a breakdown of the constant-ψ approximation. We also expect $P_\varphi, P_\perp \gg 1$. In other words, we expect the resistive evolution timescale to significantly exceed both the momentum and energy/particle confinement timescales (which it generally does by, at least, a factor of 10). Hence, consulting Figures 1 and 2, we can see that the appropriate linear resonant response regime is either the visco-resistive regime or the Hall-resistive regime.

According to the analysis of Section 5.7, and making use of the fact that $\omega = Q = 0$ for a static perturbation, in the visco-resistive response regime we have

$$\Delta_{\rm VR} = {\rm i}\,\tau_{\rm VR}\,(\omega_{\perp\,e} + \Delta\omega_E), \tag{401}$$

where $\tau_{\rm VR} = \tau_R\,\hat{\delta}_{\rm VR}$, and

$$\hat{\delta}_{\rm VR} = \frac{6^{2/3}\,\pi\,\Gamma(5/6)}{\Gamma(1/6)}\,\frac{\tau_H^{1/3}}{\tau_R^{1/6}\,\tau_\varphi^{1/6}} \tag{402}$$

is the visco-resistive layer width (normalized to r_s). Here, $\omega_{\perp\,e}$ is defined in Equation (376), and $\Delta\omega_E$ is the modification to the $\mathbf{E}\times\mathbf{B}$ frequency generated at the resonant surface by the electromagnetic torques that develop there in response to the error-field. Likewise, in the Hall-resistive regime we have

$$\Delta_{\rm HR} = {\rm i}\,\tau_{\rm HR}\,(\omega_{\perp\,e} + \Delta\omega_E), \tag{403}$$

where $\tau_{\rm HR} = \tau_R\,\hat{\delta}_{\rm HR}$, and

$$\hat{\delta}_{\rm HR} = \frac{2\pi\,\Gamma(3/4)}{\Gamma(1/4)\,[1+\lambda_e\,\tau/(1+\tau)]^{1/4}}\,\frac{\tau_H^{1/2}}{(d_\beta/r_s)^{1/2}\,\tau_R^{1/4}\,\tau_\perp^{1/4}} \tag{404}$$

is the Hall-resistive layer width (normalized to r_s).

We can combine the previous two results to give the composite layer response equation

$$\Delta = {\rm i}\,\tau_s\,(\omega_0 + \Delta\omega_E), \tag{405}$$

where $\tau_s = \tau_R\,\hat{\delta}$,

$$\hat{\delta} = \frac{\hat{\delta}_{\rm VR}\,\hat{\delta}_{\rm HR}}{\hat{\delta}_{\rm VR} + \hat{\delta}_{\rm HR}}, \tag{406}$$

and

$$\omega_0 = \omega_{\perp\, e}. \tag{407}$$

It can be seen, by comparison with the analysis of Section 3.7, that the resonant layer responds to the error-field perturbation in an analogous manner to a thin, rigid, resistive wall whose resistivity matches that of the plasma at the resonant surface, and whose radial thickness is $\delta = r_s\,\hat{\delta}$. Note, however, that the effective wall corotates with the electron fluid at the resonant surface. Moreover, it is the rotation of the effective wall that generates the shielding current.

Incidentally, the reason that a shielding current only develops in the vicinity of the resonant surface is that the plasma is not a rigid body. Under normal circumstances, the plasma responds to the error-field by displacing radially in such a manner as to eliminate the shielding current. The requisite displacement is (Freidberg 1987)

$$\xi_r(r,\zeta) = \frac{\tilde{\psi}(r,\zeta)}{B_\theta(r)\,[1 - q(r)/q_s]}. \tag{408}$$

However, this displacement becomes infinite at the resonant surface, where $q(r) = q_s$, which explains why a shielding current is only excited in the immediate vicinity of this surface.

Equations (400) and (405) yield

$$\hat{\Psi}_s = \frac{\tilde{I}_c}{(-\Delta_{nw}) + \mathrm{i}\,\tau_s\,(\omega_0 + \Delta\omega_E)}. \tag{409}$$

Now, in a conventional ohmically-heated tokamak plasma, $\tau_s\,\omega_0 \gg (-\Delta_{nw})$. Consequently, the shielding current that develops at the resonant surface, in response to the local plasma rotation, is strong enough to largely suppress error-field-driven magnetic reconnection [i.e., $|\hat{\Psi}_s| \ll |\tilde{I}_c|/(-\Delta_{nw})$]. However, the shielding current also gives rise to a localized electromagnetic torque at the resonant surface (see Section 3.10) that acts to slow the plasma rotation.

7.4 Torque Balance

According to Equations (206) and (207),

$$\Delta\omega_E = (\mathbf{k}\cdot\Delta\mathbf{V}_i)_{r=r_s} = -\sum_{p=1,\infty}(\alpha_p + \beta_p). \tag{410}$$

In other words, the shift in the $\mathbf{E}\times\mathbf{B}$ velocity at the resonant surface, in response to the electromagnetic torques that develop there, is mirrored by an equal shift in the ion fluid velocity. This is the essence of the no-slip constraint discussed in Section 3.13. The no-slip constaint follows from Equations (223) and (225) because the torques do not modify the diamagnetic velocity at the resonant surface.

Making use of Equations (193), (194), (211) and (212) (with $d/dt = 0$), (399), (405), (409), and (410), we arrive at the following torque balance equation (Fitzpatrick 1993; Fitzpatrick 1998):

$$T_{\rm VS}(v) = T_{\rm EM}(v), \tag{411}$$

where

$$v = \frac{\omega_0 + \Delta\omega_E}{\omega_0}, \tag{412}$$

$$T_{\rm VS}(v) = 1 - v, \tag{413}$$

$$T_{\rm EM}(v) = \frac{1}{4}\,\frac{v}{\zeta_s^2 + v^2}\left(\frac{|\tilde{I}_c|}{\tilde{I}_{c\,\rm crit}}\right)^2, \tag{414}$$

$$\zeta_s = \frac{(-\Delta_{nw})}{\tau_s\,\omega_0} \ll 1, \tag{415}$$

$$\tilde{I}_{c\,\rm crit} = (\epsilon_s\,s_s)\,(\omega_0\,\tau_H)\left/\left[\frac{q_s}{\epsilon_s}\left(\frac{\sqrt{\tau_\varphi\,\tau_i/\mu_{00}^i}}{\tau_s}\right) + 2\left(\frac{\tau_\varphi}{\tau_s}\right)\ln\left(\frac{a}{r_s}\right)\right]^{1/2}\right. . \tag{416}$$

Here, use has been made of the identities

$$\lim_{\epsilon\rightarrow 0}\sum_{p=1,\infty}\frac{\sqrt{\epsilon}\,[J_1(j_{1\,p}\,x)]^2}{[J_2(j_{1\,p})]^2\,(1+\epsilon\,j_{1\,p}^2)} = \frac{1}{4\,x}, \tag{417}$$

$$\sum_{p=1,\infty}\frac{[J_0(j_{0\,p}\,x)]^2}{[J_1(j_{0\,p}\,x)]^2\,j_{0\,p}^2} = \frac{1}{2}\,\ln\left(\frac{1}{x}\right). \tag{418}$$

We have also written

$$\frac{1}{\tau_{\theta\,s}} = \left(\frac{q_s}{\epsilon_s}\right)^2\,\left(\frac{\mu_{00}^i}{\tau_i}\right), \tag{419}$$

where τ_i is the ion collision time and μ_{00}^i is a dimensionless neoclassical viscosity coefficient defined in Fitzpatrick & Nelson 2020. Both quantities are evaluated at the resonant surface. Furthermore, we have assumed that $\tau_i/(\tau_\varphi\,\mu_{00}^i) \ll (q_s/\epsilon_s)^2$ (this turns out to be a very good approximation because the ion collision time, τ_i, is much less than the momentum confinement time, τ_φ, in conventional tokamak plasmas).

In Equation (411), the dimensionless parameter v takes the value unity when the plasma (i.e., electron fluid) rotation at the resonant surface is unmodified by the electromagnetic locking torque, and zero when the electromagnetic locking torque has reduced the rotation to zero. The electromagnetic torque itself is represented by the function $T_{\rm EM}(v)$, whereas the viscous restoring torque that acts to oppose changes in the plasma rotation is represented by the function $T_{\rm VS}(v)$. It can be seen from Figure 5 that, while the viscous restoring torque varies linearly with v, the electromagnetic locking torque varies with v in a nonmonotonic manner. The electromagnetic torque is zero when $v = 0$, because there is no plasma rotation

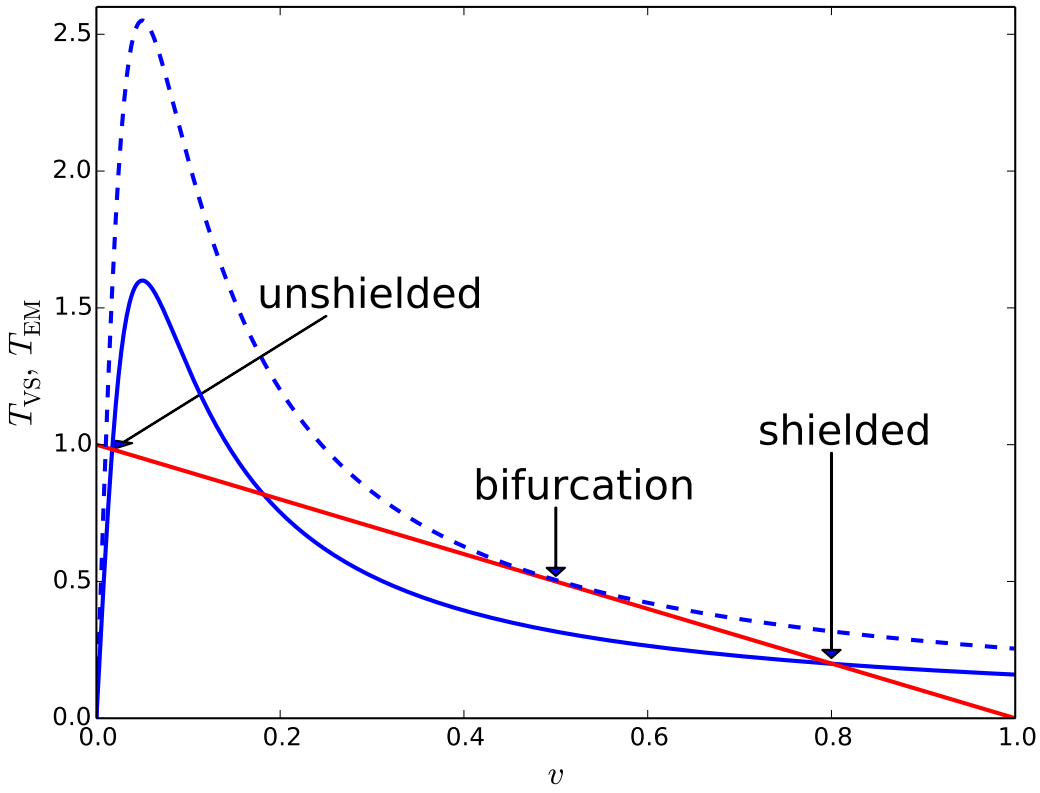

Figure 5: Torque balance. The red curve shows the normalized viscous restoring torque, $T_{\rm VS}(v)$. The solid and dashed blue curves show the normalized electromagnetic locking torque, $T_{\rm EM}(v)$, evaluated with $\zeta_s = 0.05$, and $|\tilde{I}_c|/\tilde{I}_{c\,\rm crit} = 0.8$ and 1.0, respectively.

to induce a shielding current. As v increases from zero, the torque initially increases linearly with v. However, the shielding current eventually becomes strong enough to expel the reconnected magnetic flux from the resonant layer. Consequently, because the torque is proportional to the product of the shielding current and the reconnected flux, the torque peaks, and ends up falling off as $1/v$ with increasing v (Gimblett & Peckover 1979; Fitzpatrick 1993).

The solutions of the torque balance equation (411) correspond to the crossing points of the viscous and electromagnetic torque curves. As is clear from Figure 5, if the normalized magnitude of the error-field coil current, $|\tilde{I}_c|$, lies below the critical value $\tilde{I}_{c\,\rm crit}$ then there are three crossing points. However, the intermediate crossing point corresponds to a dynamically unstable equilibrium. Hence, we deduce that there are two physical solution branches of the torque balance equation. The large-v solution branch corresponds to so-called *shielded* solutions in which the plasma rotation at the resonant surface is large enough to strongly suppress driven magnetic reconnection. The small-v solution branch corresponds to so-

called *unshielded* solutions in which the plasma rotation at the resonant surface is too weak to suppress driven magnetic reconnection. On the shielded solution branch, Equation (411) possesses the approximate solution

$$v \simeq \frac{1}{2}\left(1-\left[1-\left(\frac{|\tilde{I}_c|}{\tilde{I}_{c\,\rm crit}}\right)^2\right]^{1/2}\right). \tag{420}$$

It can be seen that as the error-field coil current increases the plasma rotation at the resonant surface decreases. However, when $|\tilde{I}_c|$ attains the critical value $\tilde{I}_{c\,\rm crit}$, and the rotation is reduced to *half* of its original value, the shielded solution branch ceases to exist, and there is a bifurcation to the unshielded solution branch (Fitzpatrick 1993; Fitzpatrick 1998). (See Figure 5.) The bifurcation is associated with a sudden decrease in the plasma rotation at the resonant surface, and a sudden increase in the driven reconnected magnetic flux, and is identified with the error-field penetration phenomenon observed in tokamak experiments. As is clear from Equation (416), the critical error-field coil current needed to trigger error-field penetration increases linearly with the unperturbed plasma rotation at the resonant surface, which is parameterized by ω_0. Once error-field penetration has occurred, the magnitude of the error-field coil current must be reduced to a value that is substantially less than $\tilde{I}_{c\,\rm crit}$ in order to trigger a reverse bifurcation to the unshielded solution branch (Fitzpatrick 1998).

Finally, the criterion for the validity of the theory presented in this section is that the width of the magnetic island chain driven at the resonant surface, just prior to mode penetration, is much less than the linear layer width (so that the resonant plasma response is governed by linear physics). This is the case provided that (Fitzpatrick 1998)

$$\hat{\delta} \gg 4\,S^{-2/5}\left(\frac{q_s}{\epsilon_s}\right)^{2/5}\left[\frac{q_s}{\epsilon_s}\left(\frac{\sqrt{\tau_\varphi\,\tau_i/\mu^i_{00}}}{\tau_R}\right)+2\left(\frac{\tau_\varphi}{\tau_R}\right)\ln\left(\frac{a}{r_s}\right)\right]^{-1/5}. \tag{421}$$

7.5 Scaling Analysis

The aim of this section is to use the previous analysis to predict the scaling of the error-field penetration threshold with the standard dimensionless scaling parameters (Connor & Taylor 1977)

$$\rho_* = \frac{T_0^{1/2}\,m_i^{1/2}}{e\,B_z\,L_s}, \tag{422}$$

$$\nu_* = \frac{L_s\,n_0\,e^2\,\eta_\parallel}{m_e^{1/2}\,T_0^{1/2}}, \tag{423}$$

$$\beta_* = \frac{\mu_0\,n_0\,T_0}{B_z^2}, \tag{424}$$

where $T_0 = p_0/n_0$. In the following, for the sake of simplicity, we shall assume that $T_i = T_e = T_0$, $\omega_0 = \omega_*$, and $-(d\ln p/dr)_{r_s} = 1/r_s$. We shall also neglect $\mathcal{O}(1)$ constants such as s_s, η_e, η_i, λ_e, τ, π, $\ln(r_s/a)$, et cetera.

Now, in an ohmically-heated tokamak plasma, the energy confinement timescale, τ_E, satisfies the constraint

$$\frac{n_0\,T_0}{\tau_E} = \eta_\parallel \left(\frac{B_z}{\mu_0\,L_s}\right)^2, \tag{425}$$

which is obtained by equating the energy loss rate to the ohmic heating rate. Let us assume that the momentum confinement time, τ_φ, and the particle/energy confinement time, $\tau_\perp$, are both equal to τ_E, as is generally (approximately) the case in ohmically-heated tokamak plasmas (ITER Physics Basis Editors 1999).

It is easily demonstrated that

$$\omega_0\,\tau_H \simeq \left(\frac{q_s}{\epsilon_s}\right)^2 \rho_*\,\beta_*^{1/2}, \tag{426}$$

$$\frac{\tau_H}{\tau_R} \simeq \left(\frac{q_s}{\epsilon_s}\right)^2 \left(\frac{m_e}{m_i}\right)^{1/2} \rho_*^2\,\nu_*\,\beta_*^{-1/2}, \tag{427}$$

$$\frac{\tau_\varphi}{\tau_R} = \frac{\tau_\perp}{\tau_R} \simeq \left(\frac{q_s}{\epsilon_s}\right)^2 \beta_*, \tag{428}$$

$$\frac{\tau_i}{\tau_R} \simeq \left(\frac{q_s}{\epsilon_s}\right)^2 \left(\frac{m_e}{m_i}\right)^{1/2} \rho_*^2\,\beta_*^{-1}, \tag{429}$$

$$\frac{d_\beta}{r_s} \simeq \left(\frac{q_s}{\epsilon_s}\right) \rho_*. \tag{430}$$

Hence, we deduce that

$$\hat{\delta}_{\rm VR} = \left(\frac{\tau_{\rm VR}}{\tau_R}\right) \simeq \left(\frac{\tau_H}{\tau_R}\right)^{1/3} \left(\frac{\tau_R}{\tau_\varphi}\right)^{1/6} \simeq \left(\frac{q_s}{\epsilon_s}\right)^{1/3} \left(\frac{m_e}{m_i}\right)^{1/6} \rho_*^{2/3}\,\nu_*^{1/3}\,\beta_*^{-1/3}, \tag{431}$$

$$\hat{\delta}_{\rm HR} = \left(\frac{\tau_{\rm HR}}{\tau_R}\right) \simeq \left(\frac{\tau_H}{\tau_R}\right)^{1/2} \left(\frac{\tau_R}{\tau_\perp}\right)^{1/4} \left(\frac{r_s}{d_\beta}\right)^{1/2} \simeq \left(\frac{m_e}{m_i}\right)^{1/4} \rho_*^{1/2}\,\nu_*^{1/2}\,\beta_*^{-1/2}, \tag{432}$$

$$\frac{\sqrt{\tau_\varphi\,\tau_i/\mu_{00}^i}}{\tau_R} \simeq \left(\frac{q_s}{r_s}\right)^2 \left(\frac{m_e}{m_i}\right)^{1/4} \rho_*. \tag{433}$$

Here, we have treated μ_{00}^i as an ignorable $\mathcal{O}(1)$ constant that is independent of ρ_*, ν_*, and β_* [as is indeed the case provided that the plasma at the resonant surface lies in the banana collisionality regime (Hirshman & Sigmar 1981)].

There are four error-field penetration regimes, depending on whether the plasma response in the resonant layer is in the visco-resistive or the Hall-resistive regime, and depending on whether the change in the ion rotation at the resonant surface, induced by the electromagnetic locking torque, is predominately toroidal or poloidal in nature. The plasma response in the resonant layer is in the visco-resisitive, rather than the Hall resistive, regime when $\tau_{\rm VR} < \tau_{\rm HR}$, or

$$\rho_* < \left(\frac{\epsilon_s}{q_s}\right)^2 \left(\frac{m_e}{m_i}\right)^{1/2} \nu_*\,\beta_*^{-1}, \tag{434}$$

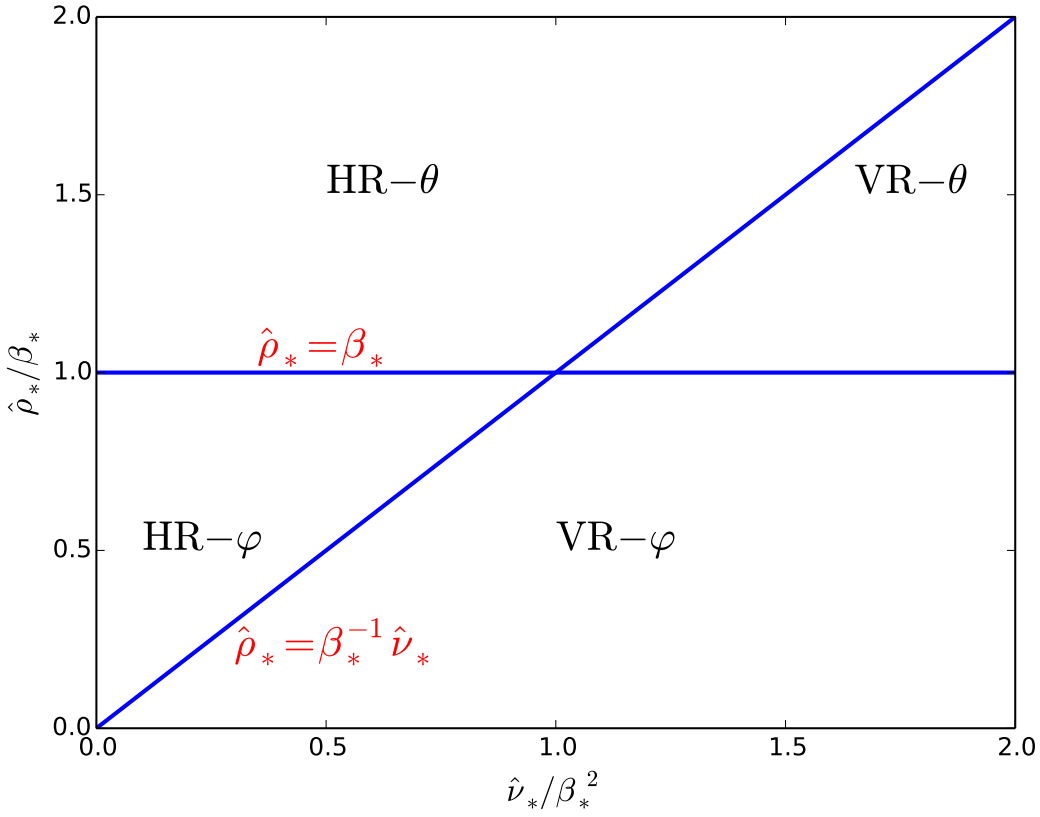

Figure 6: Error-field penetration regimes in $\hat{\nu}_*$-$\hat{\rho}_*$ space. The various regimes are the visco-resistive-toroidal (VR-φ), the visco-resistive-poloidal (VR-θ), the Hall-resistive-poloidal (HR-θ), and the Hall-resistive-toroidal (HR-φ).

and vice versa. The change in the ion rotation at the resonant surface is predominately toroidal, rather than poloidal, when

$$\rho_* < \left(\frac{\epsilon_s}{q_s}\right)\left(\frac{m_i}{m_e}\right)^{1/4}\beta_*, \tag{435}$$

and vice vera.

Let us define

$$\hat{\rho}_* = \left(\frac{q_s}{\epsilon_s}\right)\left(\frac{m_e}{m_i}\right)^{1/4}\rho_*, \tag{436}$$

$$\hat{\nu}_* = \left(\frac{\epsilon_s}{q_s}\right)\left(\frac{m_e}{m_i}\right)^{3/4}\nu_*. \tag{437}$$

As is illustrated in Figure 6, the *visco-resistive-toroidal regime* (i.e., a visco-resistive layer response combined with a predominately toroidal change in the ion rotation) corresponds

to $\hat{\rho}_* < \beta_*^{-1}\,\nu_*$ and $\hat{\rho}_* < \beta_*$, the *visco-resisitive-poloidal regime* corresponds to $\hat{\rho}_* < \beta_*^{-1}\,\nu_*$ and $\hat{\rho}_* > \beta_*$, the *Hall-resisitive-poloidal regime* corresponds to $\hat{\rho}_* > \beta_*^{-1}\,\nu_*$ and $\hat{\rho}_* > \beta_*$, and the *Hall-resistive-toroidal regime* corresponds to $\hat{\rho}_* > \beta_*^{-1}\,\nu_*$ and $\hat{\rho}_* < \beta_*$. It can be seen that higher/lower plasma collisionality (i.e., ν_*) favors the visco-resistive/Hall-resistive response regime, whereas a larger/smaller ion sound radius (i.e., ρ_*) favors poloidal/toroidal changes in the ion rotation. Finally, higher/lower plasma pressure (i.e., β_*) favors the Hall-resistive/visco-resistive response regime and toroidal/poloidal changes in the ion rotation.

In the visco-resistive-toroidal response regime, the critical vacuum (i.e., in the absence of shielding currents) radial magnetic field at the resonant surface required to trigger error-field penetration is (Cole & Fitzpatrick 2006)

$$\left(\frac{b_r}{B_z}\right)_{\mathrm{VR}-\varphi} \simeq \epsilon_s^{-1}\,\tilde{I}_{c\,\mathrm{crit}} \simeq \left(\frac{q_s}{\epsilon_s}\right)^{7/6} \left(\frac{m_e}{m_i}\right)^{1/12} \rho_*^{4/3}\,\nu_*^{1/6}\,\beta_*^{-1/6}, \tag{438}$$

where we have treated $-\Delta_{nw}$ as an ignorable $\mathcal{O}(1)$ parameter. Likewise, the critical field required to trigger penetration in the visco-resistive-poloidal regime is

$$\left(\frac{b_r}{B_z}\right)_{\mathrm{VR}-\theta} \simeq \left(\frac{q_s}{\epsilon_s}\right)^{2/3} \left(\frac{m_e}{m_i}\right)^{-1/24} \rho_*^{5/6}\,\nu_*^{1/6}\,\beta_*^{1/3}. \tag{439}$$

The critical field required to trigger penetration in the Hall-resistive-poloidal regime is

$$\left(\frac{b_r}{B_z}\right)_{\mathrm{HR}-\theta} \sim \left(\frac{q_s}{\epsilon_s}\right)^{1/2} \left(\frac{m_e}{m_i}\right)^{0} \rho_*^{3/4}\,\nu_*^{1/4}\,\beta_*^{1/4}. \tag{440}$$

Finally, the critical field required to trigger penetration in the Hall-resistive-toroidal regime is

$$\left(\frac{b_r}{B_z}\right)_{\mathrm{HR}-\varphi} \sim \left(\frac{q_s}{\epsilon_s}\right) \left(\frac{m_e}{m_i}\right)^{1/8} \rho_*^{5/4}\,\nu_*^{1/4}\,\beta_*^{-1/4}. \tag{441}$$

Generally speaking, ohmically-heated tokamak plasmas all have similar β_* values. However, both ν_* and ρ_* are smaller in devices of larger physical size. Hence, Equations (438)–(441) imply that the error-field penetration threshold is smaller in larger devices.

Let n, T, B, and R represent the typical electron number density, plasma temperature, toroidal magnetic field-strength, and physical dimension (i.e., major radius) of an ohmically-heated tokamak. Using $\rho_* \sim T^{1/2}\,B^{-1}\,R^{-1}$, $\nu_* \sim n\,T^{-2}\,R$, and $\beta_* \sim n\,T\,B^{-1}$ [see Equations (6), (18), and (422)–(424)], we deduce that

$$\left(\frac{b_r}{B_z}\right)_{\mathrm{VR}-\varphi} \propto n^0\,T^{\,1/6}\,B^{-1}\,R^{-7/6}, \tag{442}$$

$$\left(\frac{b_r}{B_z}\right)_{\mathrm{VR}-\theta} \propto n^{1/2}\,T^{\,5/12}\,B^{-3/2}\,R^{-2/3}, \tag{443}$$

$$\left(\frac{b_r}{B_z}\right)_{\mathrm{HR}-\theta} \propto n^{1/2}\,T^{\,1/8}\,B^{-5/4}\,R^{-1/2}, \tag{444}$$

$$\left(\frac{b_r}{B_z}\right)_{\rm HR-\varphi} \propto n^0\, T^{-1/8}\, B^{-3/4}\, R^{-1}. \tag{445}$$

It can be seen that the error-field penetration threshold exhibits no explicit dependence on the plasma density in regimes in which the change in the ion rotation at the resonant surface is predominately toroidal in nature (Fitzpatrick 1998; Cole & Fitzpatrick 2006). On the other hand, the penetration threshold scales as $n^{1/2}$ in regimes in which the change in the ion rotation at the resonant surface is predominately poloidal in nature. An $n^{1/2}$ scaling of the penetration threshold has been observed in a number of tokamak experiments (Hender, et al. 1999; Lazzaro, et al. 2002; Park, et al. 2012; Wang, et al. 2014; Wang, et al. 2018). On the other hand, some experiments have reported a linear scaling of the penetration threshold with n (Scoville, et al. 1991; Buttery, et al. 1999; Wolfe, et al. 2005; Wolf, et al. 2005; Howell, Hender, & Cunningham 2007; Menard, et al. 2010). The latter scaling is difficult to account for on the basis of the theory presented in this section.

In order to make further progress, we need to adopt a specific scaling model for the energy confinement timescale, τ_E. Let us adopt the following slightly modified version of the well-known neo-Alcator scaling law for low-density ohmically-heated tokamak plasmas (Goldston 1984; Simmet, et al. 1996; Fitzpatrick 2012):

$$\tau_E \propto n\, R^{\,13/4}. \tag{446}$$

[The modification is to ensure that the scaling law is consonant with the Connor-Taylor constraints (Connor & Taylor 1977).] It follows that

$$\nu_* \propto \rho_*^{2/3}\, \beta_*, \tag{447}$$

$$T \propto B^{\,4/5}\, R^{\,1/2}. \tag{448}$$

Hence, we deduce that

$$\left(\frac{b_r}{B_z}\right)_{\rm VR-\varphi} \propto n^0\, B^{-13/15}\, R^{-13/12}, \tag{449}$$

$$\left(\frac{b_r}{B_z}\right)_{\rm VR-\theta} \propto n^{1/2}\, B^{-7/6}\, R^{-11/24}, \tag{450}$$

$$\left(\frac{b_r}{B_z}\right)_{\rm HR-\theta} \propto n^{1/2}\, B^{-23/20}\, R^{-7/16}, \tag{451}$$

$$\left(\frac{b_r}{B_z}\right)_{\rm HR-\varphi} \propto n^0\, B^{-17/20}\, R^{-17/16}. \tag{452}$$

Equations (449)–(452) confirm the n^0 scaling of the error-field penetration threshold in regimes in which the change in the ion rotation at the resonant surface is predominately toroidal in nature, and the $n^{1/2}$ scaling when the change is predominately poloidal. All regimes exhibit a roughly linear inverse scaling with increasing magnetic field-strength. On

the other hand, the regimes in which the threshold scales as $n^{1/2}$ exhibit a weaker inverse scaling with machine size (roughly $R^{-1/2}$) than the regimes in which the threshold scales as n^0 (which exhibit an approximate R^{-1} scaling). [In fact, it is easily demonstrated, from the previous analysis, that if $b_r/B_z \propto n^{\alpha_n}\, B^{\alpha_B}\, R^{\alpha_R}$ then $\alpha_R = 2\,\alpha_n + 1.25\,\alpha_B$. (Buttery, et al. 1999).]

Note, finally, that the analysis presented in this section is only valid provided that the width of the magnetic island chain, W, driven at the resonant surface, just prior to error-field penetration, is less than the linear layer width, δ. The ratio of W to δ, just prior to penetration, in the four regimes discussed previously is

$$\left(\frac{W}{\delta}\right)_{\rm VR-\varphi} \simeq \left(\frac{q_s}{\epsilon_s}\right)^{7/12} \left(\frac{m_e}{m_i}\right)^{1/24} \rho_*^{1/6}\, \nu_*^{1/12}\, \beta_*^{-1/12}, \tag{453}$$

$$\left(\frac{W}{\delta}\right)_{\rm VR-\theta} \simeq \left(\frac{q_s}{\epsilon_s}\right)^{1/3} \left(\frac{m_i}{m_e}\right)^{1/48} \rho_*^{-1/12}\, \nu_*^{1/12}\, \beta_*^{1/6}, \tag{454}$$

$$\left(\frac{W}{\delta}\right)_{\rm HR-\theta} \simeq \left(\frac{q_s}{\epsilon_s}\right)^{3/4} \left(\frac{m_i}{m_e}\right)^{1/8} \rho_*^{1/8}\, \nu_*^{-1/8}\, \beta_*^{3/8}, \tag{455}$$

$$\left(\frac{W}{\delta}\right)_{\rm HR-\varphi} \simeq \left(\frac{q_s}{\epsilon_s}\right) \left(\frac{m_i}{m_e}\right)^{1/16} \rho_*^{3/8}\, \nu_*^{-1/8}\, \beta_*^{1/8}. \tag{456}$$

8 Nonlinear Resonant Response Model

8.1 Introduction

As was discussed in Section 5.9, the linear resonant response model derived in Section 5 is only valid when the width of the magnetic island chain that develops at the resonant surface is much less than the linear layer width. In the opposite limit, in which the island width greatly exceeds the layer width, a nonlinear approach is required. The aim of this section is to employ the reduced four-field resonant plasma response model derived in Section 4 to construct a suitable nonlinear resonant response model.

It is convenient to set the normalization scale-length, l, in the four-field model equal to the minor radius of the resonant surface, r_s. It is also convenient to work in a frame of reference that corotates with the island chain. In this reference frame, the normalized reconnected flux, $\hat{\Psi}_s(\hat{t})$, is assumed to be a positive real quantity. Furthermore, the four fields, $\hat{\psi}$, ϕ, N, and V, as well as the auxiliary field, J, are assumed to only be functions of the normalized radial coordinate, $\hat{x} = (r - r_s)/r_s$, the helical angle, $\zeta = m\,\theta - n\,\varphi$, and the normalized time, $\hat{t} = t\,V_A/r_s$.

It is helpful to define the reduced island width

$$w = \frac{W}{4} = (L_s\, R_0\, \hat{\Psi}_s)^{1/2}. \tag{457}$$

[See Equation (370).] It is assumed that $\delta \ll w \ll r_s$, where δ is the linear layer width. Let $\hat{w} = w/r_s$. Reusing the analysis of Section 5, in the limit $|\hat{x}|/\hat{w} \gg 1$ (i.e., many island widths from the resonant surface) we find that

$$\hat{\psi} \rightarrow \frac{\hat{x}^{\,2}}{2\,\hat{L}_s} + \hat{R}_0\,\hat{\Psi}_s\,\cos\zeta, \tag{458}$$

$$\phi \rightarrow \left(\frac{\hat{\omega}}{m} - \hat{V}_E\right)\hat{x} - \frac{s}{4}\,\hat{V}_E'\,\hat{x}^{\,2}, \tag{459}$$

$$N \rightarrow -\hat{V}_*\,\hat{x}, \tag{460}$$

$$V \rightarrow \hat{V}_\parallel, \tag{461}$$

$$J \rightarrow -\frac{2}{q_s\hat{R}_0} + \frac{1}{\hat{L}_s}. \tag{462}$$

Here, $\omega = \hat{\omega}\,V_A/r_s$ is the phase velocity of the island chain in the laboratory frame,

$$s = \mathrm{sgn}(\hat{x}), \tag{463}$$

and

$$\hat{V}_E' = \frac{1}{V_A}\left[r\,\frac{dV_E}{dr}\right]_{r_{s-}}^{r_{s+}}. \tag{464}$$

The parameter $\hat{V}_E'$ is introduced into the analysis in order to take into account the fact that the plasma rotation profile in the outer region develops a gradient discontinuity at the resonant surface in response to the nonlinear localized electromagnetic torque that emerges at the surface.

8.2 Rescaled Four-Field Model

Let

$$X = \frac{\hat{x}}{\hat{w}}, \tag{465}$$

$$T = \omega_*\,t. \tag{466}$$

It follows that $|X| \sim \mathcal{O}(1)$ in the immediate vicinity of the island chain. It is helpful to define the rescaled fields $\Psi(X,\zeta,T)$, $\Phi(X,\zeta,T)$, $\mathcal{N}(X,\zeta,T)$, $\mathcal{V}(X,\zeta,T)$, and $\mathcal{J}(X,\zeta,T)$, where

$$\hat{\psi} = \left(\frac{\hat{w}^{\,2}}{\hat{L}_s}\right)\Psi, \tag{467}$$

$$\phi = \left(\frac{\hat{\omega}_*\,\hat{w}}{m}\right)\Phi, \tag{468}$$

$$N = \left(\frac{\hat{\omega}_*\,\hat{w}}{m}\right)\mathcal{N}, \tag{469}$$

$$V = \hat{V}_\parallel + \left(\frac{\hat{L}_s\,\hat{\omega}_*^{\,2}}{m^2\,c_\beta^2}\right)\mathcal{V}, \tag{470}$$

$$J = -\frac{2}{q_s\hat{R}_0} + \frac{1}{\hat{L}_s} + \left(\frac{\hat{L}_s\,\hat{\omega}_*^{\,2}}{m^2\,\hat{w}^{\,2}}\right)\mathcal{J}. \tag{471}$$

The four-field model specified in Section 4.5 rescales to give

$$\frac{d(\ln\hat{w}^2)}{dT}\,\cos\zeta = \left\{\Phi - \left(\frac{\tau}{1+\tau}\right)(1+\lambda_e)\,\mathcal{N},\Psi\right\} + \epsilon_\beta\,\epsilon_d\,\epsilon_\eta\,\mathcal{J}, \tag{472}$$

$$\frac{\partial(\partial_X^2\,\Phi)}{\partial T} = \partial_X\left\{\Phi + \frac{\mathcal{N}}{1+\tau},\partial_X\Phi\right\} + \{\mathcal{J},\Psi\} + \epsilon_\chi\,\partial_X^4\left(\Phi + \frac{\mathcal{N}}{1+\tau}\right), \tag{473}$$

$$\begin{aligned}\frac{\partial\mathcal{N}}{\partial T} &= \{\Phi,\mathcal{N}\} + \{\mathcal{V},\Psi\} + \epsilon_d\,\epsilon_n\,\{\mathcal{J},\Psi\}\\ &\quad + \epsilon_D\left[\left(\frac{w}{w_c}\right)^4\,\{\{\mathcal{N},\Psi\},\Psi\} + \partial_X^2\mathcal{N}\right],\end{aligned} \tag{474}$$

$$\epsilon_d\,\frac{\partial\mathcal{V}}{\partial T} = \epsilon_d\,\{\Phi,\mathcal{V}\} + \{\mathcal{N},\Psi\} + \epsilon_d\,\epsilon_\chi\,\partial_X^2\mathcal{V}, \tag{475}$$

$$\partial_X^2\Psi = 1 + \epsilon_\beta\,\epsilon_d\,\mathcal{J}. \tag{476}$$

Here, $\partial_X \equiv \partial/\partial X$,

$$\{A,B\} \equiv \frac{\partial A}{\partial X}\,\frac{\partial B}{\partial\zeta} - \frac{\partial A}{\partial\zeta}\,\frac{\partial B}{\partial X}, \tag{477}$$

and we have set

$$\hat{E}_\parallel = \left(\frac{2}{q_s\hat{R}_0} - \frac{1}{\hat{L}_s}\right)\eta_\parallel. \tag{478}$$

Furthermore,

$$\epsilon_d = \left(\frac{L_s}{L_n}\right)^2\left(\frac{d_\beta}{w}\right)^2, \tag{479}$$

$$\epsilon_\beta = c_\beta^2, \tag{480}$$

$$\epsilon_n = \left(\frac{L_n}{L_s}\right)^2, \tag{481}$$

$$\epsilon_\eta = \frac{\eta_\parallel}{\mu_0\,\omega_*\,w^2}, \tag{482}$$

$$\epsilon_\chi = \frac{\chi_\phi}{\omega_*\,w^2}, \tag{483}$$

$$\epsilon_D = \frac{D_\perp}{\omega_*\,w^2}. \tag{484}$$

Finally,

$$\frac{1}{L_n} = -\frac{1}{\Gamma\,(1-c_\beta^2)}\left(\frac{d\ln n}{dr}\right)_{r_s} \tag{485}$$

is the *density gradient scalelength* at the resonant surface, and the critical reduced island width, w_c, is defined in Equation (326).

Equations (472)–(476) must be solved subject to the boundary conditions

$$\Psi \rightarrow \frac{X^2}{2} + \cos\zeta, \tag{486}$$

$$\Phi \rightarrow v\,X + \frac{s\,v'\,X^2}{2}, \tag{487}$$

$$\mathcal{N} \rightarrow X, \tag{488}$$

$$\mathcal{V} \rightarrow 0, \tag{489}$$

$$\mathcal{J} \rightarrow 0, \tag{490}$$

as $|X| \rightarrow \infty$. Here,

$$v(T) = \frac{\omega - \omega_E}{\omega_*}, \tag{491}$$

$$v'(T) = -\frac{\hat{w}}{2\,\omega_*}\left[r\,\frac{d\omega_E}{dr}\right]_{r_{s-}}^{r_{s+}}. \tag{492}$$

Note that Ψ, Φ, $\mathcal{N}$, $\mathcal{V}$, and $\mathcal{J}$ are all $\mathcal{O}(1)$ quantities. Note, further, that the boundary conditions (486)–(490), as well as the symmetry of the rescaled four-field equations, (472)–(476), ensure that Ψ, $\mathcal{V}$, and $\mathcal{J}$ are even functions of X, whereas Φ and $\mathcal{N}$ are odd functions.

8.3 Ordering Scheme

In the following, the dimensionless parameters ϵ_d, ϵ_β, ϵ_n, ϵ_η, ϵ_χ, and ϵ_D are all assumed to be of similar size, but much smaller than unity. The orderings $\epsilon_n \ll 1$ and $\epsilon_\beta \ll 1$ are consistent with the standard large-aspect ratio, low-β orderings used to describe conventional tokamak plasmas (Freidberg 1987). As will become apparent, the ordering $\epsilon_d \ll 1$ ensures that the island chain is sufficiently wide that ion acoustic waves propagating parallel to the magnetic field are able to smooth out any variations in the normalized electron number density, $\mathcal{N}$, around magnetic flux-surfaces (Scott, Hassam & Drake 1985). The fact that $\epsilon_d \ll 1$ implies that

$$w \gg \rho_\beta, \tag{493}$$

where

$$\rho_\beta = \left(\frac{L_s}{L_n}\right) d_\beta \tag{494}$$

is a characteristic lengthscale that is of order the ion poloidal gyroradius. The orderings $\epsilon_\eta \ll 1$, $\epsilon_\chi \ll 1$, and $\epsilon_D \ll 1$ ensure that the island chain is sufficiently wide that the

perpendicular diffusion of magnetic flux, momentum, and particles are not dominant effects in the rescaled four-field equations. We shall also assume that $w/w_c \sim \mathcal{O}(1)$. In other words, the island chain is sufficiently wide for the parallel diffusion of particles to compete with perpendicular diffusion.

Suppose that

$$\frac{\partial}{\partial T} \sim \mathcal{O}(\epsilon_d^3). \tag{495}$$

Let us expand the various fields in our model as follows:

$$\Psi = \Psi_0 + \epsilon_d^2 \Psi_2 + \epsilon_d^3 \Psi_3 + \cdots, \tag{496}$$

$$\Phi = \Phi_0 + \epsilon_d^2 \Phi_2 + \epsilon_d^3 \Phi_3 + \cdots, \tag{497}$$

$$\mathcal{N} = \mathcal{N}_0 + \epsilon_d^2 \mathcal{N}_2 + \epsilon_d^3 \mathcal{N}_3 + \cdots, \tag{498}$$

$$\mathcal{V} = \mathcal{V}_0. + \epsilon_d \mathcal{V}_1 + \cdots, \tag{499}$$

$$\mathcal{J} = \mathcal{J}_0 + \epsilon_d \mathcal{J}_1 + \cdots. \tag{500}$$

Here, Ψ_0, Ψ_1, et cetera are assumed to be $\mathcal{O}(1)$.

8.4 Lowest-Order Solution

To lowest order in ϵ_d, Equation (476) yields

$$\partial_X^2 \Psi_0 = 1. \tag{501}$$

Solving this equation subject to the boundary condition (486), we obtain

$$\Psi_0 = \Omega(X, \zeta) \equiv \frac{X^2}{2} + \cos\zeta. \tag{502}$$

Thus, we conclude that, to lowest order in our expansion, the magnetic flux-surfaces in the island region have the constant-ψ structure pictured in Figure 3. The island O-points correspond to $\Omega = -1$ and $\zeta = (2k-1)\,\pi$ (where k is an integer), the X-points correspond to $\Omega = +1$ and $\zeta = 2k\,\pi$, and the magnetic separatrix corresponds to $\Omega = +1$.

To lowest order in ϵ_d, Equation (475) yields

$$\{\mathcal{N}_0, \Omega\} = 0, \tag{503}$$

where use has been made of Equation (502). Given that $\mathcal{N}$ is an odd function of X, it follows that

$$\mathcal{N}_0(X, \zeta, T) = s\,\mathcal{N}_{(0)}(\Omega, T). \tag{504}$$

We conclude that parallel ion acoustic waves, whose dynamics are described by Equation (475), smooth out any variations in the lowest-order electron number density, $\mathcal{N}_0$, around magnetic flux-surfaces. By symmetry, $\mathcal{N}_0 = 0$ inside the magnetic separatrix of the island

chain. In other words, the electron number density profile (and, by implication, the electron and ion temperature profile) is completely flattened inside the separatrix.

It is helpful to define

$$L(\Omega, T) = \frac{d\mathcal{N}_{(0)}}{d\Omega}. \tag{505}$$

It follows that $L(\Omega < 1, T) = 0$. Furthermore, Equations (488) and (502) imply that

$$L(\Omega \rightarrow \infty, T) = \frac{1}{\sqrt{2\,\Omega}}. \tag{506}$$

To lowest order in ϵ_d, Equation (472) gives

$$\{\Phi_0, \Omega\} = 0, \tag{507}$$

where use has been made of Equations (502) and (504). Given that Φ is an odd function of X, it follows that

$$\Phi_0(X, \zeta, T) = s\,\Phi_{(0)}(\Omega, T). \tag{508}$$

We conclude that the lowest-order normalized electrostatic potential, Φ_0, is constant on magnetic flux-surfaces. By symmetry, $\Phi_0 = 0$ inside the magnetic separatrix of the island chain. In other words, the electrostatic potential profile is completely flattened inside the separatrix.

It is helpful to define

$$M(\Omega, T) = \frac{d\Phi_{(0)}}{d\Omega}. \tag{509}$$

It follows that $M(\Omega < 1, T) = 0$. Furthermore, Equations (487) and (502) imply that

$$M(\Omega \rightarrow \infty, T) = \frac{v}{\sqrt{2\,\Omega}} + v'. \tag{510}$$

To lowest order in ϵ_d, Equation (474) yields

$$\{\mathcal{V}_0, \Omega\} = 0, \tag{511}$$

where use has been made of Equations (502), (504), and (508). Given that $\mathcal{V}$ is an even function of X, we can write

$$\mathcal{V}_0(X, \zeta, T) = \mathcal{V}_{(0)}(\Omega, T). \tag{512}$$

In other words, the lowest-order normalized parallel ion velocity, $\mathcal{V}_0$, is also constant on magnetic flux-surfaces.

Finally, to lowest order in ϵ_d, Equation (473) yields

$$\{\mathcal{J}_0, \Omega\} = -\partial_X \left\{ \Phi_0 + \frac{\mathcal{N}_0}{1+\tau}, \partial_X \Phi_0 \right\} = \frac{1}{2} \left\{ d_\Omega \left[M \left(M + \frac{L}{1+\tau} \right) \right] X^2, \Omega \right\}, \tag{513}$$

where use has been made of Equations (502), (505), and (509). Moreover, $d_\Omega \equiv d/d\Omega$.

8.5 Flux-Surface Average Operator

The *flux-surface average operator*, $\langle\cdots\rangle$, is defined (Rutherford 1973)

$$\langle A(s,\Omega,\zeta)\rangle \equiv \begin{cases} \int_{\zeta_0}^{2\pi-\zeta_0} \frac{A(s,\Omega\,\zeta)+A(-s,\Omega,\zeta)}{2\,[2\,(\Omega-\cos\zeta)]^{1/2}}\,\frac{d\zeta}{2\pi} & 0\leq\Omega\leq 1 \\ \oint \frac{A(s,\Omega\,\zeta)}{[2\,(\Omega-\cos\zeta)]^{1/2}}\,\frac{d\zeta}{2\pi} & \Omega>1 \end{cases}, \tag{514}$$

where $\zeta_0=\cos^{-1}(\Omega)$ and $0\leq\zeta_0\leq\pi$. It follows that

$$\langle\{A,\Omega\}\rangle = 0 \tag{515}$$

for *any* $A(s,\Omega,\zeta,T)$. It is helpful to define

$$\tilde{A}\equiv A-\frac{\langle A\rangle}{\langle 1\rangle}. \tag{516}$$

It follows that

$$\langle\tilde{A}\rangle = 0 \tag{517}$$

for *any* $A(s,\Omega,\zeta,T)$.

Equation (513) yields

$$\mathcal{J}_0(\Omega,\zeta,T)=\frac{1}{2}\,d_\Omega\left[M\left(M+\frac{L}{1+\tau}\right)\right]\widetilde{X^2}+\overline{\mathcal{J}}_0(\Omega,T), \tag{518}$$

where $\overline{\mathcal{J}}_0(\Omega,T)$ is an undetermined flux-surface function.

8.6 Fluid Velocities

The flux-surface functions $M(\Omega,T)$ and $L(\Omega,T)$ are directly related to the lowest-order perpendicular velocities of the various fluid species in the island rest frame. In fact, as is clear from Sections 4.2, 4.3, and 8.2,

$$V_{\theta\,e}(X,\zeta,T)=-\frac{r_s\,\omega_*}{m}\,|X|\,Y_e(\Omega,T), \tag{519}$$

$$V_\theta(X,\zeta,T)=-\frac{r_s\,\omega_*}{m}\,|X|\,M(\Omega,T), \tag{520}$$

$$V_{\theta\,i}(X,\zeta,T)=-\frac{r_s\,\omega_*}{m}\,|X|\,Y_i(\Omega,T), \tag{521}$$

where

$$Y_e(\Omega,T)=M-\left(\frac{\tau}{1+\tau}\right)L, \tag{522}$$

$$Y_i(\Omega,T)=M+\left(\frac{1}{1+\tau}\right)L, \tag{523}$$

Here, $V_{\theta\,e}$, V_θ, and $V_{\theta\,i}$ refer to velocity components of the electron, MHD, and ion fluid, respectively. Note that Y_e and Y_i are both zero inside the magnetic separatrix of the island chain.

8.7 Need for Higher-Order Solution

To lowest order in our expansion scheme, the rescaled four-field model, (472)–(476), requires the density, temperature, and electrostatic potential profiles to be magnetic flux-surface functions. This should come as no surprise. In essence, a magnetic island chain is a helical magnetic equilibrium that evolves (in its local rest frame) on the very slow resistive timescale (Rutherford 1973). Hence, we would expect all of the results derived in Section 2.5 to apply to the plasma in the immediate region of the island chain, as is indeed the case. Note, however, that, while solving the rescaled four-field model (472)–(476) to lowest order tells us that $\mathcal{N} = s\,\mathcal{N}_{(0)}(\Omega, T)$, $\Phi_0 = s\,\Psi_{(0)}(\Omega, T)$, and $\mathcal{V}_0 = \mathcal{V}_{(0)}(\Omega, T)$, and that the lowest-order current density profile has the form (518), the lowest-order solution leaves the flux-surface functions $\mathcal{N}_{(0)}(\Omega, T)$, $\Phi_{(0)}(\Omega, T)$, $\mathcal{V}_{(0)}(\Omega, T)$, and $\overline{\mathcal{J}}_0(\Omega, T)$ undetermined. In fact, in order to determine the forms of these four functions it is necessary to solve the rescaled four-field model to higher order in our expansion. In particular, we need to include the terms that describe the perpendicular diffusion of magnetic flux, ion momentum, and particles in our analysis (Fitzpatrick & Waelbroeck 2005). The essential point is that the magnetic island chain persists in the plasma for a sufficiently long time that the relatively small perpendicular diffusion terms are able to relax the lowest-order profiles across the island region (and, in fact, across the whole plasma).

8.8 Higher-Order Solution

We need to evaluate Equation (472) to third order in ϵ_d in order to include the perpendicular transport term. Doing so, we obtain

$$\frac{d(\ln \hat{w}^{\,2})}{dT}\,\cos\zeta = \{F_e, \Omega\} + \epsilon_\beta\,\epsilon_d\,\epsilon_\eta\,\mathcal{J}_0, \tag{524}$$

where

$$F_e(\Omega, \zeta, T) = \epsilon_d^2\,(\Phi_2 + \epsilon_d\,\Phi_3) - \epsilon_d^2\left(\frac{\tau}{1+\tau}\right)(\mathcal{N}_2 + \epsilon_d\,\mathcal{N}_3) - \epsilon_d^2\,s\,Y_e(\Psi_2 + \epsilon_d\,\Psi_3), \tag{525}$$

and use has been made of Equations (496)–(498), (504), (505), (508), and (509). The flux-surface average of Equation (524) yields

$$\overline{\mathcal{J}}_0(\Omega, T) = \frac{1}{\epsilon_\beta\,\epsilon_d\,\epsilon_\eta}\frac{d(\ln \hat{w}^2)}{dT}\,\frac{\langle\cos\zeta\rangle}{\langle 1\rangle}, \tag{526}$$

where use has been made of Equations (515), (517), and (518). Hence, we can write

$$\mathcal{J}_0(\Omega, \zeta) = \frac{1}{2}\,d_\Omega(M\,Y_i)\,\widetilde{X^2} + \frac{1}{\epsilon_\beta\,\epsilon_d\,\epsilon_\eta}\frac{d(\ln \hat{w}^2)}{dT}\,\frac{\langle\cos\zeta\rangle}{\langle 1\rangle}, \tag{527}$$

where use has been made of Equation (523). The first term on the right-hand side of the previous equation represents the parallel return current driven by the perpendicular

polarization current associated with the acceleration of the ion fluid around the magnetic separatrix of the island chain (Smolyakov 1993; Smolyakov, et al. 1995). In fact, it is easily seen that if the ion fluid could pass freely through the separatrix (i.e., $\Phi_0 \propto X$ and $\mathcal{N}_0 \propto X$) then the term in question would be zero. The second term on the right-hand side of the previous equation represents the parallel current driven inductively when the reconnected flux at the resonant surfaces varies in time.

We need to evaluate Equation (474) to first order in ϵ_d in order to include the perpendicular transport term. Doing so, we obtain

$$0 = \epsilon_d \{\mathcal{V}_1, \Omega\} + \epsilon_D (X^2 \, d_\Omega L + L), \tag{528}$$

where use has been made of Equations (502), (504), and (505). The flux-surface average of the previous equation yields

$$\langle X^2 \rangle \, d_\Omega L + \langle 1 \rangle \, L = 0, \tag{529}$$

where use has been made of Equation (515). We can solve the previous equation, subject to the boundary condition (506), to give

$$L(\Omega) = \begin{cases} 0 & -1 \leq \Omega \leq 1 \\ 1/\langle X^2 \rangle & \Omega > 1 \end{cases}. \tag{530}$$

Here, we have taken into account the previously mentioned fact that $L = 0$ within the island separatrix. Note that L is discontinuous across the island separatrix, which implies that the density gradient—and, hence, the diamagnetic velocity—are both also discontinuous across the separatrix. Of course, there is not a real discontinuity. Given that the discontinuity in L is mandated by the ordering $\epsilon_d = (\rho_\beta/w)^2 \ll 1$, which requires L to be a flux-surface function—and, hence, zero, by symmetry, inside the separatrix—it is plausible that the discontinuity is resolved by a thin layer of characteristic thickness ρ_β on the island separatrix.

We need to evaluate Equation (473) to first order in ϵ_d in order to include the perpendicular transport term. Doing so, we obtain

$$0 = \epsilon_d \{\mathcal{J}_1, \Omega\} + \epsilon_\chi \, X \, d_\Omega \big[d_\Omega \big(X^3 \, d_\Omega Y_i \big) \big] . \tag{531}$$

where use has been made of Equations (502), (504), (505), (508), (509), and (523). The flux-surface average of the previous equation yields

$$d_\Omega^2 \big(\langle X^4 \rangle \, d_\Omega Y_i \big) = 0. \tag{532}$$

We can solve the previous equation, subject to the boundary conditions (506) and (510), to give

$$Y_i(\Omega, T) = \frac{v'(T)}{\int_1^\infty \frac{d\Omega}{\langle X^4 \rangle}} \begin{cases} 0 & -1 \leq \Omega \leq 1 \\ \int_1^\Omega \frac{d\Omega'}{\langle X^4 \rangle} & \Omega > 1 \end{cases} \tag{533}$$

(Fitzpatrick & Waelbroeck 2005). Here, we have rejected, as unphysical, the solution that blows up as $\Omega^{1/2}$ as $\Omega \rightarrow \infty$. We have also made use of the fact that $Y_i = 0$ within

the magnetic separatrix of the island chain. Finally, we have demanded that the ion fluid velocity—and, hence, the function Y_i—be continuous across the separatrix, because the ion fluid possesses finite perpendicular viscosity. Note, however, that the discontinuity in the function $L(\Omega)$ across the separatrix [see Equation (530)] implies that the electron and MHD fluid velocities are discontinuous across the separatrix. (See Section 8.6.) As previously mentioned, these discontinuities are resolved in a layer of characteristic thickness ρ_β.

We need to evaluate Equation (475) to second order in ϵ_d in order to include the perpendicular transport term. Doing so, we obtain

$$0 = \epsilon_d \{\mathcal{V}_1, \Omega\} + \epsilon_\chi (X^2 \, d_\Omega \mathcal{V}_{(0)} + \mathcal{V}_{(0)}), \tag{534}$$

where use has been made of Equations (502) and (512). The flux-surface average of the previous equation yields

$$\langle X^2 \rangle \, d_\Omega \mathcal{V}_{(0)} + \langle 1 \rangle \, \mathcal{V}_{(0)} = 0. \tag{535}$$

The previous equation can be solved, subject to the boundary condition (489), to give

$$\mathcal{V}_{(0)}(\Omega, T) = 0. \tag{536}$$

Hence, we conclude that the lowest-order ion parallel flow is unaffected by the presence of the island chain.

8.9 Asymptotic Matching

Now that we have solved the four-field model in the immediate vicinity of the magnetic island chain, it is necessary to asymptotically match this solution to the solution in the outer region. In the island rest frame, the reconnected magnetic flux, defined in Equation (100), can be written

$$\Psi_s = R_0 \, B_z \, \hat{\Psi}_s \, (\cos\zeta + \mathrm{i} \, \sin\zeta), \tag{537}$$

where $\hat{\Psi}_s$ is real and positive. It follows from Equations (110), (204), and (247) that

$$\begin{aligned} \mathrm{Re}\left(\frac{\Delta\hat{\Psi}_s}{\hat{\Psi}_s}\right) &= \frac{2\, r_s}{R_0 \, B_z \, \hat{\Psi}_s} \int_{r_{s-}}^{r_{s+}} \oint \frac{\partial^2 \psi}{\partial r^2} \, \cos\zeta \, \frac{d\zeta}{2\pi} \, dr \\ &= \frac{2}{\hat{w} \, \hat{R}_0 \, \hat{\Psi}_s} \int_{-\infty}^{\infty} \oint \frac{\partial^2 \hat{\psi}}{\partial X^2} \, \cos\zeta \, \frac{d\zeta}{2\pi} \, dX, \end{aligned} \tag{538}$$

$$\begin{aligned} \mathrm{Im}\left(\frac{\Delta\hat{\Psi}_s}{\hat{\Psi}_s}\right) &= -\frac{2\, r_s}{R_0 \, B_z \, \hat{\Psi}_s} \int_{r_{s-}}^{r_{s+}} \oint \frac{\partial^2 \psi}{\partial r^2} \, \sin\zeta \, \frac{d\zeta}{2\pi} \, dr \\ &= -\frac{2}{\hat{w} \, \hat{R}_0 \, \hat{\Psi}_s} \int_{-\infty}^{\infty} \oint \frac{\partial^2 \hat{\psi}}{\partial X^2} \, \sin\zeta \, \frac{d\zeta}{2\pi} \, dX. \end{aligned} \tag{539}$$

Making use of Equations (457) and (467), we obtain

$$\mathrm{Re}\left(\frac{\Delta\hat{\Psi}_s}{\hat{\Psi}_s}\right) = \frac{2}{\hat{w}} \int_{-\infty}^{\infty} \oint \partial_X^2 \Psi \, \cos\zeta \, \frac{d\zeta}{2\pi} \, dX, \tag{540}$$

$$\mathrm{Im}\left(\frac{\Delta\hat{\Psi}_s}{\hat{\Psi}_s}\right) = -\frac{2}{\hat{w}}\int_{-\infty}^{\infty}\oint \partial_X^2\Psi\,\sin\zeta\,\frac{d\zeta}{2\pi}\,dX. \tag{541}$$

However, according to Equations (476) and (500),

$$\partial_X^2\Psi = 1 + \epsilon_\beta\,\epsilon_d\,\mathcal{J}_0 + \epsilon_\beta\,\epsilon_d^2\,\mathcal{J}_1. \tag{542}$$

Moreover, it is clear from Equations (527) and (531) that $\mathcal{J}_0$ has the symmetry of $\cos\zeta$, whereas $\mathcal{J}_1$ has the symmetry of $\sin\zeta$. Hence, we deduce that

$$\mathrm{Re}\left(\frac{\Delta\hat{\Psi}_s}{\hat{\Psi}_s}\right) = \frac{2\,\epsilon_\beta\,\epsilon_d}{\hat{w}}\int_{-\infty}^{\infty}\oint \mathcal{J}_0\,\cos\zeta\,\frac{d\zeta}{2\pi}\,dX, \tag{543}$$

$$\mathrm{Im}\left(\frac{\Delta\hat{\Psi}_s}{\hat{\Psi}_s}\right) = -\frac{2\,\epsilon_\beta\,\epsilon_d^2}{\hat{w}}\int_{-\infty}^{\infty}\oint \mathcal{J}_1\,\sin\zeta\,\frac{d\zeta}{2\pi}\,dX. \tag{544}$$

The previous two equations can also be written

$$\mathrm{Re}\left(\frac{\Delta\hat{\Psi}_s}{\hat{\Psi}_s}\right) = \frac{4\,\epsilon_\beta\,\epsilon_d}{\hat{w}}\int_{-1}^{\infty}\langle\mathcal{J}_0\,\cos\zeta\rangle\,d\Omega, \tag{545}$$

$$\mathrm{Im}\left(\frac{\Delta\hat{\Psi}_s}{\hat{\Psi}_s}\right) = -\frac{4\,\epsilon_\beta\,\epsilon_d^2}{\hat{w}}\int_{-1}^{\infty}\langle\mathcal{J}_1\,\sin\zeta\rangle\,d\Omega = -\frac{4\,\epsilon_\beta\,\epsilon_d^2}{\hat{w}}\int_{-1}^{\infty}\langle X\,\{\mathcal{J}_1,\Omega\}\rangle\,d\Omega. \tag{546}$$

Equations (531) and (546) can be combined to give (Fitzpatrick & Waelbroeck 2005)

$$\begin{aligned}\mathrm{Im}\left(\frac{\Delta\hat{\Psi}_s}{\hat{\Psi}_s}\right) &= \frac{4\,\epsilon_\beta\,\epsilon_d\,\epsilon_\chi}{\hat{w}}\int_1^{\infty}\left\langle X^2\,d_\Omega\left[d_\Omega(X^3\,d_\Omega Y_i)\right]\right\rangle d\Omega\\ &= \frac{4\,\epsilon_\beta\,\epsilon_d\,\epsilon_\chi}{\hat{w}}\int_1^{\infty} d_\Omega\left(-\langle X\rangle\,Y_i + 2\,\langle X^3\rangle\,d_\Omega Y_i + \langle X^5\rangle\,d_\Omega^2 Y_i\right) d\Omega\\ &= \frac{4\,\epsilon_\beta\,\epsilon_d\,\epsilon_\chi}{\hat{w}}\lim_{\Omega\to\infty}\left(-\langle X\rangle\,Y_i + 2\,\langle X^3\rangle\,d_\Omega Y_i + \langle X^5\rangle\,d_\Omega^2 Y_i\right),\end{aligned} \tag{547}$$

where use has been made of the facts that Y_i is zero inside the island separatrix, and Y_i is continuous across the separatrix. Combining the previous equation with Equation (533), we obtain (Fitzpatrick & Waelbroeck 2005)

$$\mathrm{Im}\left(\frac{\Delta\hat{\Psi}_s}{\hat{\Psi}_s}\right) = -\frac{4\,\epsilon_\beta\,\epsilon_d\,\epsilon_\chi\,v'}{\hat{w}}. \tag{548}$$

The previous equation yields

$$\left[r\,\frac{d\omega_E}{dr}\right]_{r_{s-}}^{r_{s+}} = \left(\frac{\tau_\varphi\,\hat{w}^4}{2\,\tau_H^2}\right)\mathrm{Im}\left(\frac{\Delta\hat{\Psi}_s}{\hat{\Psi}_s}\right), \tag{549}$$

where use has been made of Equation (492). The same relation can be obtained by integrating Equation (184) across the resonant surface, making use of Equation (163), as well as the identification

$$\left[r \frac{d\omega_E}{dr} \right]_{r_{s-}}^{r_{s+}} = m \left[r \frac{\partial \Delta\Omega_\theta}{\partial r} \right]_{r_{s-}}^{r_{s+}}. \tag{550}$$

The previous identification merely states that the discontinuity in the MHD fluid velocity gradient that develop at the resonant surface is mirrored by an equal discontinuity in the ion fluid velocity gradient (because the discontinuity is ultimately due to a discontinuity in the $\mathbf{E} \times \mathbf{B}$ velocity gradient).

Equations (527) and (545) can be combined to give

$$\mathrm{Re}\left(\frac{\Delta\hat{\Psi}_s}{\hat{\Psi}_s} \right) = \frac{2\,\epsilon_\beta\,\epsilon_d}{\hat{w}} \int_{1+}^{\infty} d_\Omega(M\,Y_i) \left\langle \widetilde{X^2}\,\cos\zeta \right\rangle d\Omega + \frac{4}{\epsilon_\eta\,\hat{w}} \frac{d(\ln \hat{w}^2)}{dT} \int_{-1}^{\infty} \frac{\langle \cos\zeta \rangle^2}{\langle 1 \rangle}\, d\Omega \tag{551}$$

Making use of Equations (523), (530), and (533), the previous equation yields

$$\begin{aligned} \mathrm{Re}\left(\frac{\Delta\hat{\Psi}_s}{\hat{\Psi}_s} \right) &= -\frac{2\,\epsilon_\beta\,\epsilon_d\,v'}{(1+\tau)\,\hat{w}} \int_1^{\infty} d_\Omega\left(\frac{F_i}{\langle X^2 \rangle} \right) \left\langle \widetilde{X^2}\,\cos\zeta \right\rangle d\Omega \\ &\quad + \frac{2\,\epsilon_\beta\,\epsilon_d\,v'^2}{\hat{w}} \int_1^{\infty} d_\Omega\big(F_i^2\big) \left\langle \widetilde{X^2}\,\cos\zeta \right\rangle d\Omega \\ &\quad + \frac{4}{\epsilon_\eta\,\hat{w}} \frac{d(\ln \hat{w}^2)}{dT} \int_{-1}^{\infty} \frac{\langle \cos\zeta \rangle^2}{\langle 1 \rangle}\, d\Omega, \end{aligned} \tag{552}$$

where

$$F_i(\Omega) = \int_1^{\Omega} \frac{d\Omega'}{\langle X^4 \rangle} \Big/ \int_1^{\infty} \frac{d\Omega}{\langle X^4 \rangle} \tag{553}$$

Finally, Equations (548) and (552) can be combined to give (Waelbroeck & Fitzpatrick 1997; Fitzpatrick & Waelbroeck 2005a)

$$\begin{aligned} \mathrm{Re}\left(\frac{\Delta\hat{\Psi}_s}{\hat{\Psi}_s} \right) &= I_1\,\tau_R \frac{d}{dt}\left(\frac{4\,w}{r_s} \right) - \frac{I_2}{4} \left(\frac{c_\beta}{1+\tau} \right) \left(\frac{\rho_\beta}{r_s} \right) \left(\frac{\tau_\varphi}{\tau_H} \right) \left(\frac{w}{r_s} \right)^2 \mathrm{Im}\left(\frac{\Delta\hat{\Psi}_s}{\hat{\Psi}_s} \right) \\ &\quad - \frac{I_3}{16} \left(\frac{\tau_\varphi}{\tau_H} \right)^2 \left(\frac{w}{r_s} \right)^7 \left[\mathrm{Im}\left(\frac{\Delta\hat{\Psi}_s}{\hat{\Psi}_s} \right) \right]^2, \end{aligned} \tag{554}$$

where

$$I_1 = 2 \int_{-1}^{\infty} \frac{\langle \cos\zeta \rangle^2}{\langle 1 \rangle}\, d\Omega = 0.8227, \tag{555}$$

$$I_2 = \int_1^{\infty} d_\Omega\left(\frac{F_i}{\langle X^2 \rangle} \right) \left(\langle X^4 \rangle - \frac{\langle X^2 \rangle^2}{\langle 1 \rangle} \right) d\Omega = 0.1955, \tag{556}$$

$$I_3 = \int_1^\infty d_\Omega\big(F_i^{\,2}\big)\left(\langle X^4\rangle - \frac{\langle X^2\rangle^2}{\langle 1\rangle}\right) d\Omega = 0.4711. \tag{557}$$

Here, use has been made of Equations (318), (319), (482), and (483). Note that d/dt in Equation (554) represents a time derivative in the island rest frame.

9 Isolated Magnetic Island Chains

9.1 Introduction

Suppose that the wall surrounding the plasma is perfectly conducting (i.e. $\tau_w \rightarrow \infty$), and that there is no current flowing through the external magnetic field-coil (i.e., $\hat{I}_c = 0$). In this case, Equations (208), (209), and (397), yield

$$\frac{\Delta\hat{\psi}_s}{\hat{\psi}_s} = \Delta_{pw}, \tag{558}$$

where Δ_{pw} is the (real) perfect-wall tearing stability index. It is clear from the previous equation that

$$\mathrm{Im}\left(\frac{\Delta\hat{\psi}_s}{\hat{\psi}_s}\right) = 0, \tag{559}$$

which implies that zero electromagnetic torque is exerted at the resonant surface. (See Section 3.10.) In this respect, the magnetic island chain that develops at the resonant surface can be termed 'isolated'.

9.2 Rutherford Island Width Evolution Equation

Equation (558) implies that

$$\mathrm{Re}\left(\frac{\Delta\hat{\psi}_s}{\hat{\psi}_s}\right) = \Delta_{pw}. \tag{560}$$

Equations (457), (554), (559), and (560) yield the *Rutherford island width evolution equation* (Rutherford 1973):

$$I_1\,\tau_R\,\frac{d}{dt}\left(\frac{W}{r_s}\right) = \Delta_{pw}, \tag{561}$$

where d/dt represents a time derivative in the island rest frame. According to the Rutherford equation, if the perfect-wall tearing stability index is positive then the width of the magnetic island chain at the resonant surface grows *algebraically* on the resistive evolution timescale, τ_R.

9.3 Saturated Island Width

Equation (561) gives the impression that if $\Delta_{pw} > 0$ then the width of the magnetic island chain grows without limit. In fact, this is not the case. Instead, the width of the island chain eventually stops growing, and the tearing mode attains a saturated steady state. In order to model this effect, it is necessary to perform the asymptotic matching between the inner and outer regions to higher order, taking into account the finite width of the island chain (White, et al. 1977; Thyagaraja 1981; Escande & Ottaviani 2004; Militello & Porcelli 2004).

For the case of an island chain that is sufficiently wide to flatten the density and temperature profiles within its magnetic separatrix, the appropriate saturation theory is given in Hastie, Militello, and Porcelli 2005. According to this theory, Δ_{pw} in Equation (561) must be replaced by

$$\Delta_{pw}(0) - \left(0.8\,\alpha_s^2 - 0.27\,\beta_s - 0.09\,\alpha_s\right)\frac{W}{r_s}, \tag{562}$$

where $\Delta_{pw}(0)$ denotes the zero-island-width tearing stability index, α_s is defined in Equation (108), and

$$\beta_s = -\left(\frac{r\,q\,J_z''}{s}\right)_{r=r_s}. \tag{563}$$

Equations (561) and (562) can be combined to give

$$I_1\,\tau_R\,\frac{d}{dt}\left(\frac{W}{r_s}\right) = \Delta_{pw}(0) - \left(0.8\,\alpha_s^2 - 0.27\,\beta_s - 0.09\,\alpha_s\right)\frac{W}{r_s}. \tag{564}$$

If we define

$$W_{\rm sat} = \frac{\Delta_{pw}(0)\,r_s}{0.8\,\alpha_s^2 - 0.27\,\beta_s - 0.09\,\alpha_s}, \tag{565}$$

$$\tau_{\rm sat} = \frac{I_1\,\tau_R}{\Delta_{pw}(0)}\,\frac{W_{\rm sat}}{r_s}, \tag{566}$$

then Equation (564) reduces to

$$\tau_{\rm sat}\,\frac{d}{dt}\left(\frac{W}{W_{\rm sat}}\right) = 1 - \frac{W}{W_{\rm sat}}. \tag{567}$$

The previous equation can be solved to give

$$W(t) = W_{\rm sat}\left(1 - {\rm e}^{-t/\tau_{\rm sat}}\right), \tag{568}$$

assuming that the island width is zero at $t = 0$. It follows that the width of the island chain does not grow without limit, but instead eventually attains the saturated value $W_{\rm sat}$. Moreover, the time required to attain saturation, $\tau_{\rm sat}$, is of order $\tau_R\,(W_{\rm sat}/r_s)$.

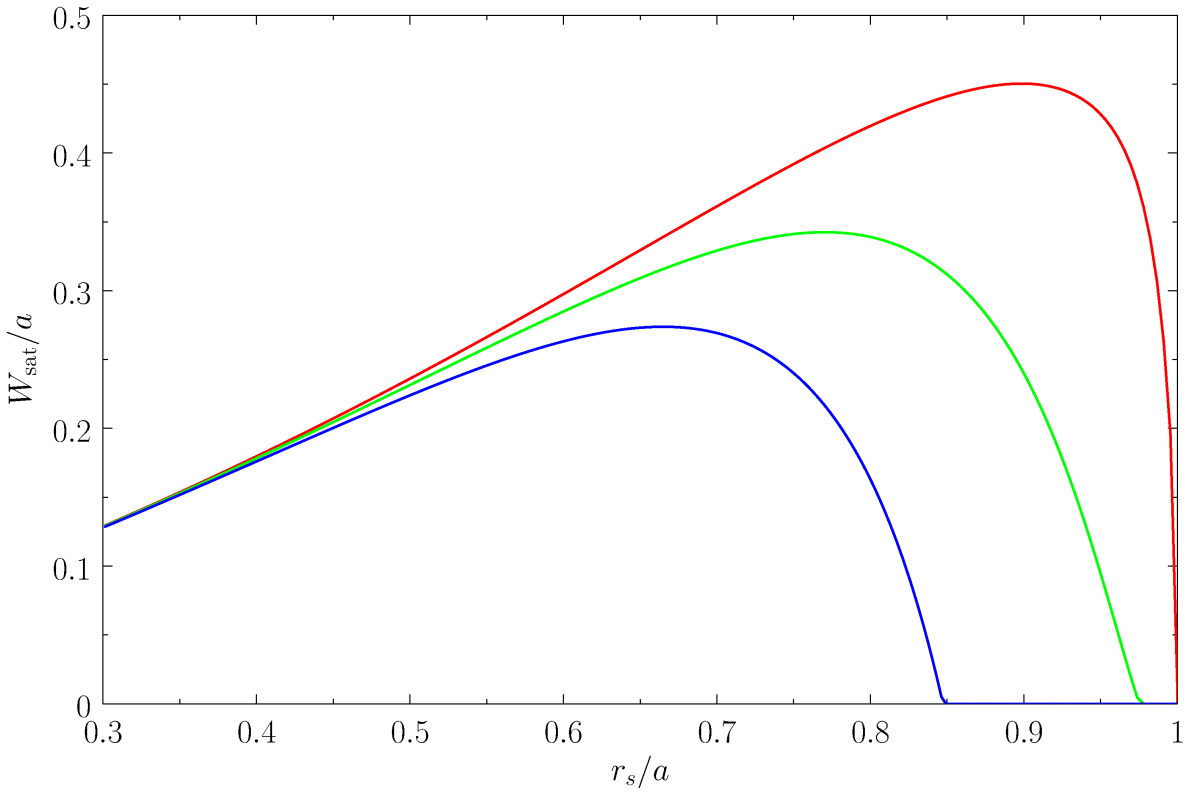

Figure 7: Saturated island width of the $m = 2/n = 1$ tearing mode for a Wesson equilibrium in which $q(0) = 0.8$ and $q(a)$ is varied. The blue, green, and red curves correspond to $r_w/a = 1.0$, 1.1, and 1.2, respectively.

Figure 7 shows the saturated island width of an $m = 2/n = 1$ tearing mode[4] in a so-called 'Wesson' equilibrium (Wesson 1978) characterized by

$$J_z(r) = \frac{2}{q(0)}\left(1 - \frac{r^2}{a^2}\right)^{\nu}, \tag{569}$$

$$q(r) = \frac{q(a)\,(r/a)^2}{1 - (1 - r^2/a^2)^{1+\nu}}, \tag{570}$$

where $\nu = q(a)/q(0) - 1$. Here, $q(0)$ and $q(a)$ are the safety-factor values at the magnetic axis and the plasma boundary, respectively. In the calculation shown in Figure 7, $\Delta_{pw}(0)$ is determined by solving the cylindrical tearing mode equation, subject to suitable boundary conditions, as described in Section 3.5. Moreover, $q(0)$ is given the plausible value 0.8 (Wesson 2011), while $q(a)$ is varied in order to shift the position of the resonant surface within the plasma. It can be seen that if the resonant surface lies far from the plasma boundary then the 2/1 island chain saturates at relatively small width (i.e., $W_{\rm sat}/a \ll 1$). On the other hand, if the resonant surface lies close to the plasma boundary then the island

[4]This is, generally, the most unstable tearing mode in conventional tokamak plasmas (Wesson 1978).

chain saturates at a much higher width. However, the presence of a close-fitting perfectly conducting wall can mitigate this effect to some extent.

9.4 Island Phase Velocity

Equations (548) and (559) imply that

$$v' = 0 \tag{571}$$

for an isolated magnetic island chain. It follows from Equations (522), (523), (530), and (533) that the stream functions for the electron, MHD, and ion fluids take the respective forms

$$Y_e(\Omega) = \begin{cases} 0 & -1 \leq \Omega \leq 1 \\ -1/\langle X^2\rangle & \Omega > 1 \end{cases}, \tag{572}$$

$$M(\Omega) = \left(\frac{1}{1+\tau}\right) \begin{cases} 0 & -1 \leq \Omega \leq 1 \\ -1/\langle X^2\rangle & \Omega > 1 \end{cases}, \tag{573}$$

$$Y_i(\Omega) = 0, \tag{574}$$

in the vicinity of the island chain. Equations (491), (510), (571), and (573) yield $v = -1/(1+\tau)$, or

$$\omega = \omega_{\perp\, i}, \tag{575}$$

where

$$\omega_{\perp\, i} = \omega_E + \omega_{*\, i}, \tag{576}$$

and

$$\omega_{*\, i} = -\left(\frac{1}{1+\tau}\right)\omega_*. \tag{577}$$

We conclude that, unlike a linear tearing mode, which is convected by the electron fluid at the resonant surface (see Section 6.2), a nonlinear tearing mode is convected by the *ion* fluid (Fitzpatrick & Waelbroeck 2005).

Figure 8 shows the normalized velocity profiles of the electron, MHD, and ion fluids across the O-point of an isolated magnetic island chain in the island rest frame, as determined from Equations (519)–(521) and (572)–(574) (Fitzpatrick & Waelbroeck 2005). Here, $\hat{V}_\theta = (m/r_s)\, V_\theta/\omega_*$. It can be seen that all three fluids co-rotate with the island chain inside the magnetic separatrix. The ion fluid velocity profile is completely unaffected by the presence of the chain. On the other hand, the electron and the MHD fluid velocity profiles are modified by the island chain. In particular, both profiles are discontinuous across the magnetic separatrix. As has already been mentioned, these discontinuities are resolved in a thin layer of thickness ρ_β on the separatrix. It is clear from the figure that the island chain rotates in the ion (i.e., negative) direction with respect to the unperturbed $\mathbf{E}\times\mathbf{B}$ frame at the resonant surface (Fitzpatrick & Waelbroeck 2005).

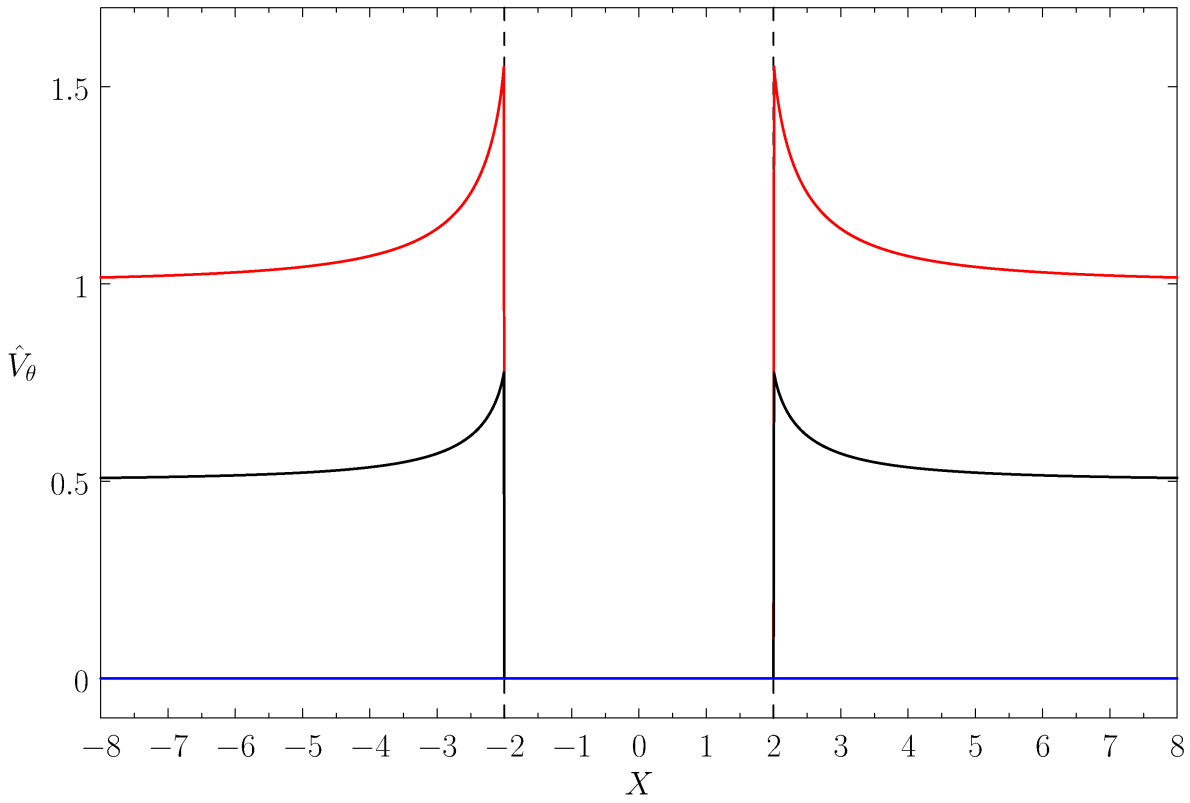

Figure 8: Normalized velocity profiles across the O-point of an isolated magnetic island chain in the island rest frame. The red, black, and blue curves correspond to the electron, MHD, and ion fluid, respectively. Here, $\tau = 1$.

9.5 Discussion

The phase velocity of an isolated tearing mode is determined by the equilibrium plasma flow at the resonant surface. Now, a magnetic island chain is a helical pattern in the magnetic field generated by a helical current perturbation that is localized in the vicinity of the resonant surface. Given that plasma current is predominately carried by the electrons, it is natural to suppose that a magnetic island chain (as well as the magnetic perturbation away from the resonant surface) is convected by the electron fluid in the immediate vicinity of the resonant surface. This is indeed the case in the linear regime. (See Section 6.2.) Of course, as a consequence of diamagnetic flows, if the island chain is convected by the electron fluid at the resonant surface then it propagates with respect to the local ion fluid. However, this is not a problem because a linear layer is sufficiently thin that the magnetic field can diffuse through the plasma very rapidly, which implies that the ion fluid is not tied to the magnetic structure of the island chain (Fitzpatrick 2020).

The situation is very different in the nonlinear regime. The region inside the magnetic separatrix of a sufficiently wide nonlinear magnetic island chain is governed by a combination of flux-freezing and perturbed force balance. This implies that both the electron and the

ion fluids are trapped inside the separatrix, and are, therefore, forced to co-rotate with the island chain. There is no such constraint outside the separatrix, so the electron and ion fluids rotate at different speeds in this region, as a consequence of diamagnetism. It follows that one or other of the electron and the ion fluid rotation profiles must exhibit a strong gradient across the separatrix. The island phase velocity is determined by which of the two fluids is most resistant to the formation of such a gradient. Of course, it is the ion fluid which is more resistant because of its much greater perpendicular viscosity. Hence, a nonlinear magnetic island chain is convected by the ion fluid in the vicinity of the resonant surface, because this choice of phase velocity minimizes the ion fluid velocity gradient across the separatrix (Fitzpatrick 2000). Incidentally, there is clear experimental evidence that wide magnetic island chains in tokamak plasmas rotate in the ion diamagnetic direction relative to the unperturbed $\mathbf{E}\times\mathbf{B}$ frame at the resonant surface (La Haye, et al. 2003; Burratti, et al. 2016).

Finally, it is reasonable to suppose that the critical island width that must be exceeded before a magnetic island chain switches from rotating in the electron direction, with respect to the unperturbed local $\mathbf{E}\times\mathbf{B}$ frame, to rotating in the ion direction, is that above which the density and temperature profiles flatten within the separatrix (Scott, Hassam & Drake 1985).

10 Mode Locking in Tokamak Plasmas

10.1 Introduction

Mode locking is a process by which the rotation of a slowly growing tearing mode is braked due to electromagnetic interaction with the resistive wall surrounding the plasma, causing the mode to eventually *lock* (i.e., become stationary in the laboratory frame) to an error-field (Nave & Wesson 1990; Berge, Sandal & Wesson 1989; Zohm, et al. 1990; Fitzpatrick 1993; Waelbroeck & Fitzpatrick 1997). Locked tearing modes are one of the principal causes of disruptions in tokamaks (de Vries, et al. 2011).

10.2 Resistive-Wall Rotation Braking

Let us, first of all, investigate the braking of tearing mode rotation due to electromagnetic interaction with the resistive wall, in the absence of the error-field. Assuming that the tearing mode possesses the phase velocity ω, and that $\hat{I}_c = 0$, Equation (209) yields

$$\hat{\Psi}_w = \frac{E_{sw}/(-\tilde{E}_{ww})}{1-\mathrm{i}\,\omega\,\tau_{LR}}, \tag{578}$$

where

$$\tau_{LR} = \frac{\tau_w}{(-\tilde{E}_{ww})} \tag{579}$$

is the effective L/R time of the wall. Equation (208) then gives

$$\frac{\Delta\hat{\Psi}_s}{\hat{\Psi}_s} = \Delta_{pw} + (\Delta_{nw} - \Delta_{pw})\left(\frac{1 + \mathrm{i}\,\omega\,\tau_{LR}}{1 + \omega^2\,\tau_{LR}^2}\right), \tag{580}$$

where use has been made of Equations (396) and (397). It follows that

$$\mathrm{Re}\left(\frac{\Delta\hat{\Psi}_s}{\hat{\Psi}_s}\right) = \Delta_{pw} + (\Delta_{nw} - \Delta_{pw})\left(\frac{1}{1 + \omega^2\,\tau_{LR}^2}\right), \tag{581}$$

$$\mathrm{Im}\left(\frac{\Delta\hat{\Psi}_s}{\hat{\Psi}_s}\right) = (\Delta_{nw} - \Delta_{pw})\left(\frac{\omega\,\tau_{LR}}{1 + \omega^2\,\tau_{LR}^2}\right). \tag{582}$$

Finally, making use of the island saturation theory presented in Section 9.3, we obtain

$$\mathrm{Re}\left(\frac{\Delta\hat{\Psi}_s}{\hat{\Psi}_s}\right) = \Delta_{pw}(0)\left(1 - \frac{w}{w_{pw}}\right) + [\Delta_{nw}(0) - \Delta_{pw}(0)]\left(\frac{1}{1 + \omega^2\,\tau_{LR}^2}\right), \tag{583}$$

$$\mathrm{Im}\left(\frac{\Delta\hat{\Psi}_s}{\hat{\Psi}_s}\right) = [\Delta_{nw}(0) - \Delta_{pw}(0)]\left(\frac{\omega\,\tau_{LR}}{1 + \omega^2\,\tau_{LR}^2}\right), \tag{584}$$

where $w_{pw} = W_{pw}/4$, and

$$W_{pw} = \frac{\Delta_{pw}(0)\,r_s}{0.8\,\alpha_s^2 - 0.27\,\beta_s - 0.09\,\alpha_s} \tag{585}$$

is the saturated island width when the wall is perfectly conducting.

Equations (554), (583), and (584) yield the following modified Rutherford island width evolution equation:

$$\begin{aligned} I_1\,\tau_R\,\frac{d}{dt}\left(\frac{4\,w}{r_s}\right) &= \Delta_{pw}(0)\left(1 - \frac{w}{w_{pw}}\right) + [\Delta_{nw}(0) - \Delta_{pw}(0)]\left(\frac{1}{1 + \omega^2\,\tau_{LR}^2}\right) \\ &+ \frac{I_2}{4}\,[\Delta_{nw}(0) - \Delta_{pw}(0)]\left(\frac{c_\beta}{1+\tau}\right)\left(\frac{\rho_\beta}{r_s}\right)\left(\frac{\tau_\varphi}{\tau_H}\right)\left(\frac{w}{r_s}\right)^2\left(\frac{\omega\,\tau_{LR}}{1 + \omega^2\,\tau_{LR}^2}\right) \\ &+ \frac{I_3}{16}\,[\Delta_{nw}(0) - \Delta_{pw}(0)]^2\left(\frac{\tau_\varphi}{\tau_H}\right)^2\left(\frac{w}{r_s}\right)^7\left(\frac{\omega\,\tau_{LR}}{1 + \omega^2\,\tau_{LR}^2}\right)^2. \end{aligned} \tag{586}$$

The first term on the right-hand side of the previous equation governs the growth and saturation of the tearing mode when the wall is perfectly conducting. The second term describes the loss of wall stabilization when the phase velocity of the mode is sufficiently small that the associated perturbed magnetic field can penetrate through the wall. The third and fourth terms represent the destabilizing effect of the ion polarization current induced in the vicinity of the island chain when the ion fluid flows around the chain's magnetic

separatrix (Waelbroeck & Fitzpatrick 1997; Fitzpatrick & Waelbroeck 2005a). Unlike the case of an isolated island chain, the polarization effect is non-zero because, according to Equation (521), (533), (548), and (584), the electromagnetic braking torque exerted on the plasma in the immediate vicinity of the island chain, due to interaction with the resistive wall, generates finite ion flow in the island rest frame.

Equations (210) and (575) imply that

$$\omega = \omega_0 - \sum_{p=1,\infty} (\alpha_p + \beta_p), \tag{587}$$

where $\omega_0 = \omega_{\perp\, i}$ is the island phase velocity in the absence of the resistive wall. In the following, ω_0 is assumed to be positive for the sake of definiteness. The modifications to the analysis when ω_0 is negative are trivial. The previous equation can be combined with Equations (211), (212), (417), (418), (457), and (584) to give the following torque balance equation:

$$\omega_0 - \omega = \frac{1}{4}\left[\Delta_{nw}(0) - \Delta_{pw}(0)\right]\left(\frac{\epsilon_s}{q_s}\right)^2\left(\frac{\tau_V}{\tau_H^2}\right)\left(\frac{w}{r_s}\right)^4\left(\frac{\omega\,\tau_{LR}}{1+\omega^2\,\tau_{LR}^2}\right), \tag{588}$$

where

$$\tau_V = 2\,\ln\left(\frac{a}{r_s}\right)\tau_\varphi + \left(\frac{q_s}{\epsilon_s}\right)\left(\frac{\tau_i\,\tau_\varphi}{\mu_{00}^i}\right)^{1/2}. \tag{589}$$

The left-hand side of Equation (588) represents the viscous restoring torque that acts to prevent changes in the island chain's phase velocity. The right-hand side represents the electromagnetic braking torque acting on the island chain due to eddy currents induced in the resistive wall.

Let

$$x = \frac{x}{x_{pw}}, \tag{590}$$

$$y = \frac{\omega}{\omega_0}, \tag{591}$$

$$T = \frac{t}{\tau_{pw}}, \tag{592}$$

$$\tau_{pw} = \frac{I_1\,\tau_R}{\Delta_{pw}(0)}\,\frac{W_{pw}}{r_s}. \tag{593}$$

The modified Rutherford equation, (586), and the torque balance equation, (588), can be written in the nondimensional forms (Waelbroeck & Fitzpatrick 1997)

$$\frac{dx}{dT} = 1 - x + \beta_l\left(\frac{1}{1+\alpha_l^2\,y^2}\right) + \gamma_l\left(\frac{1-y}{x^2}\right) + \delta_l\left[\frac{(1-y)^2}{x}\right], \tag{594}$$

$$1 - y = \epsilon_l\left(\frac{x^4\,y}{1+\alpha_l^2\,y^2}\right), \tag{595}$$

respectively, where

$$\alpha_l = \omega_0\,\tau_{LR}, \tag{596}$$

$$\beta_l = 1 - \frac{\Delta_{pw}(0)}{\Delta_{nw}(0)}, \tag{597}$$

$$\gamma_l = \frac{I_2}{\Delta_{nw}(0)}\left(\frac{q_s}{\epsilon_s}\right)^2\left(\frac{c_\beta}{1+\tau}\right)\left(\frac{\rho_\beta}{r_s}\right)\left(\frac{\tau_\varphi\,\tau_H\,\omega_0}{\tau_V}\right)\left(\frac{r_s}{w_{pw}}\right)^2, \tag{598}$$

$$\delta_l = \frac{I_3}{\Delta_{nw}(0)}\left(\frac{q_s}{\epsilon_s}\right)^4\left(\frac{\tau_\varphi\,\tau_H\,\omega_0}{\tau_V}\right)^2\left(\frac{r_s}{w_{pw}}\right), \tag{599}$$

$$\epsilon_l = \frac{\beta_l}{4\,\Delta_{pw}(0)}\left(\frac{\epsilon_s}{q_s}\right)^2\left(\frac{\tau_{LR}\,\tau_V}{\tau_H^2}\right)\left(\frac{w_{pw}}{r_s}\right)^4. \tag{600}$$

In conventional tokamaks, it is generally the case that $\alpha_l \gg 1$. In other words, in the absence of wall braking, tearing modes rotate sufficiently rapidly that the associated perturbed magnetic fields do not penetrate through the wall. It is easily demonstrated that if α_l exceed the critical value $\sqrt{27}$ then the normalized torque balance equation, (595), possesses two branches of solutions (Fitzpatrick 1993). The *high-rotation solution branch* is characterized by $1/2 \leq y \leq 1$, and is such that

$$y \simeq \frac{1}{2}\left(1 - \left[1 - \left(\frac{x}{x_h}\right)^4\right]^{1/2}\right), \tag{601}$$

where

$$x_h = \left(\frac{\alpha_l^2}{4\,\epsilon_l}\right)^{1/4}. \tag{602}$$

The high-rotation solution branch ceases to exist when the normalized island width, x, exceeds the critical value, x_h—at which point the island phase velocity has been reduced to *half* of its original value—and there is a bifurcation to the low-rotation solution branch. The low-rotation solution branch is characterized by $0 \leq y \leq 1/\alpha_l$, and is such that

$$y \simeq \frac{1}{\alpha_l}\left\{\left(\frac{x}{x_l}\right)^4 - \left[\left(\frac{x}{x_l}\right)^8 - 1\right]^{1/2}\right\}, \tag{603}$$

where

$$x_l = \left(\frac{2\,\alpha_l}{\epsilon_l}\right)^{1/4}. \tag{604}$$

The low-rotation solution branch ceases to exist when the normalized island width falls below the critical value x_l, and there is a bifurcation to the high-rotation solution branch. Note that $x_h \gg x_l$, which indicates that once the island chain has grown sufficiently to

trigger a high-rotation to low-rotation bifurcation it is unlikely to ever attain a high-rotation state again (because it would have to shrink by a considerable factor to trigger the reverse bifurcation). Note that, in the presence of a resistive wall, there is a forbidden band of island phase velocities: $\omega_0/\alpha_l < \omega < \omega_0/2$. The existence of this forbidden band has been verified experimentally (Gates & Hender 1996).

It is clear from Equation (594) that rotation braking due to eddy currents induced in the resistive wall has a *destabilizing* effect on a tearing mode. In fact, if there is no substantial braking then the normalized modified Rutherford equation (594) reduces to

$$\frac{dx}{dT} \simeq 1 - x, \tag{605}$$

indicating that the normalized island width, x, saturates at its perfect-wall value, unity. On the other hand, on the low-rotation solution branch, Equation (594) reduces to

$$\frac{dx}{dT} \simeq 1 - x + \beta_l + \frac{\gamma_l}{x^2} + \frac{\delta_l}{x}, \tag{606}$$

indicating that the normalized island width saturates at a value that is greater than unity. (Because β_l, γ_l, and δ_l are all positive.) The tearing mode is destabilized by the loss of wall stabilization, and also by the ion polarization effect associated with rotation braking.

10.3 Locking to Static Error-Field

Rotation braking due to interaction with a resistive wall can reduce the phase velocity of a tearing mode by a large factor, but it cannot reduce the velocity to zero (because the braking torque is zero when $\omega = 0$). The later goal can be achieved by locking to a static error-field, a process that is greatly facilitated once the phase velocity of the tearing mode has been reduced to a comparatively small value by wall braking.

Suppose that the tearing mode has locked to a static error-field generated by running a steady current I_c in the external field-coil. Without loss of generality, we can suppose that I_c is a real quantity. Because the mode is locked (i.e., $\omega = 0$), Equations (208) and (209) yield

$$\frac{\Delta\hat{\Psi}_s}{\hat{\Psi}_s} = \Delta_{pw} + (\Delta_{nw} - \Delta_{pw}) + \left(\frac{\Delta_{nw} - \Delta_{pw}}{E_{sw}}\right)\frac{\hat{I}_c}{\hat{\Psi}_s}. \tag{607}$$

Let $\Psi_s = |\Psi_s|\,\mathrm{e}^{-\mathrm{i}\,\varphi_s}$. It is convenient to define the normalized vacuum flux,

$$\hat{\Psi}_v = \frac{\beta_l}{E_{sw}}\left(\frac{r_w}{r_c}\right)^m \frac{\mu_0\, I_c}{R_0\, B_z}, \tag{608}$$

and the reduced vacuum island width,

$$w_v = (L_s\, R_0\, \hat{\Psi}_v)^{1/2}. \tag{609}$$

[See Equation (457).] The vacuum island width $W_v = 4\, w_v$ is the width of the magnetic island chain that would be driven at the resonant surface by the error-field in the absence

of shielding. The quantity φ_s is the helical phase shift between the actual magnetic island chain at the resonant surface and the vacuum magnetic island chain. Making use of the island saturation theory presented in Section 9.3, we deduce that

$$\mathrm{Re}\left(\frac{\Delta\hat{\Psi}_s}{\hat{\Psi}_s}\right) = \Delta_{pw}(0)\left[1 - \frac{w}{w_{pw}} + \beta_l + \left(\frac{w_v}{w}\right)^2 \cos\varphi_s\right], \tag{610}$$

$$\mathrm{Im}\left(\frac{\Delta\hat{\Psi}_s}{\hat{\Psi}_s}\right) = \Delta_{pw}(0)\left(\frac{w_v}{w}\right)^2 \sin\varphi_s. \tag{611}$$

Using similar analysis to that employed in Section 10.2, we obtain the nondimensional modified Rutherford equation,

$$\frac{dx}{dT} = 1 - x + \beta_l + \frac{\gamma_l}{x^2} + \frac{\delta_l}{x} + \left(\frac{x_v}{x}\right)^2 \cos\varphi_s, \tag{612}$$

and the nondimensional torque balance equation,

$$x_u^4 = x_v^2\, x^2\, \sin\varphi_s. \tag{613}$$

Here, $x_u = w_u/w_{pw}$, and

$$w_u = \left[\frac{4}{\Delta_{pw}(0)}\left(\frac{q_s}{\epsilon_s}\right)^2\left(\frac{\tau_H^2\,\omega_0}{\tau_V}\right)\right]^{1/4} r_s. \tag{614}$$

The left-hand side of Equation (613) represents the viscous restoring torque that acts to prevent changes in the island chain's phase velocity. The right-hand side represents the electromagnetic locking torque exerted on the island chain by the error-field. It is clear from Equation (613) that the error-field is only able to lock the island chain when $x_v\, x > x_u^2$, or, equivalently,

$$w_v\, w > w_u^2. \tag{615}$$

When the previous criterion is satisfied, the relative phase of the island chain lies in the range $0 \leq \varphi_s \leq \pi/2$. Note that the island chain unlocks from the error-field, and spins up under the influence of the viscous restoring force, if φ_s exceeds the critical value $\pi/2$. Finally, a comparison between Equations (606) and (612) reveals that when the island chain locks to the error-field it is further destabilized (because $\cos\varphi_s > 0$).

10.4 Discussion

Magnetic island chains in tokamak plasmas that remain rotating tend to be fairly benign. On the other hand, magnetic island chains that slow down, due to interaction with a resistive wall, and lock to an error-field, often attain sufficiently large widths to trigger disruptions (de Vries, et al. 2011). As described in Sections 10.2 and 10.3, the slowing down and locking of a magnetic island chain gives rise to three additional destabilizing terms in the chain's

island width evolution equation. The first is due to the loss of wall stabilization. The second is due to the ion polarization current generated by by the velocity gradient discontinuity that develops at the resonant surface when the island chain slows down. The third is due to the error-field. Hence, we can understand why tokamak plasmas containing locked magnetic island chains are more disruption-prone than those that contain rotating island chains.

Bibliography

Ara, A., et al. 1978. *Magnetic Reconnection and m = 1 Oscillations in Current Carrying Plasmas.* Ann. Physics (NY) **112**, 443.

Berge, G., Sandal, L.K., and Wesson, J.A. 1989. *Rotation and Mode Locking in Tokamaks.* Phys. Scr. **40**, 173.

Bondeson, A., and Persson, M. 1986. *Resistive Tearing Modes in the Presence of Equilibrium Flows.* Phys. Fluids **29**, 2997.

Boozer, A.H. 1996. *Shielding of Resonant Magnetic Perturbations by Rotation.* Phys. Plasmas **3**, 4620.

Buttery, R.J., et al. 1999. *Error Field Mode Studies on JET, COMPASS-D and DIII-D, and Implications for ITER.* Nucl. Fusion **39**, 1827.

Braginskii, S.I. 1965. *Transport Processes in a Plasma.* In *Reviews of Plasma Physics.* Vol. 1, 205. Consultants Bureau, New York NY.

Brau, K., et al. 1983. *Plasma Rotation in the PDX Tokamak.* Nucl. Fusion **23**, 1643.

Buratti, P., et al. 2016. *Diagnostic Application of Magnetic Islands Rotation in JET.* Nucl. Fusion **56**. 076004.

Chapman, S., and Cowling, T.G. 1953. *The Mathematical Theory of Non-Uniform Gases.* Cambridge University Press, Cambridge UK.

Chen, X.L., and Morrison, P.J. 1990. *Resistive Tearing Instability with Equilibrium Shear Flow.* Phys. Plasmas **2**, 495.

Cole, A., and Fitzpatrick, R. 2006. *Drift-Magnetohydrodynamical Model of Error-Field Penetration in Tokamak Plasmas.* Phys. Plasmas **13**, 032503.

Connor, J.W., and Taylor, J.B. 1977. *Scaling Laws for Plasma Confinement.* Nucl. Fusion **17**, 1047.

Cowley, S.C., Kulsrud, R.M., and Hahm, T.S. 1986. *Linear Stability of Tearing Modes.* Phys. Fluids **29**, 3230.

de Vries, P.C., et al. 2011. *Survey of Disruption Causes at JET.* Nucl. Fusion **51**, 053018.

Drake, J.F., and Lee, Y.C. 1977. *Kinetic Theory of Tearing Instabilities.* Phys. Fluids **20**, 1341.

Escande, D.F., and Ottaviani, M. 2004. *Simple and Rigorous Solution for the Nonlinear Tearing Mode.* Phys. Lett. A **323**, 278.

Fishpool, G.M., and Haynes, P.S. 1994. *Field Error Instabilities in JET*. Nucl. Fusion **34**, 109.

Fitzpatrick, R. 1993. *Interaction of Tearing Modes with External Structures in Cylindrical Geometry*. Nucl. Fusion **33**, 1049.

Fitzpatrick, R. 1995. *Helical Temperature Perturbations Associated with Tearing Modes in Tokamak Plasmas*. Phys. Plasmas **2**, 825.

Fitzpatrick, R. 1998. *Bifurcated States of a Rotating Tokamak Plasma in the Presence of a Static Error-Field*. Phys. Plasmas **5**, 3325.

Fitzpatrick, R. 2008. *Maxwell's Equations and the Principles of Electromagnetism*. Jones & Bartlett, Burlington MA.

Fitzpatrick, R. 2012. *Nonlinear Error-Field Penetration in Low Density Ohmically Heated Tokamak Plasmas*. Plasma Phys. Control. Fusion **54**, 094002.

Fitzpatrick, R. 2015. *Plasma Physics: An Introduction*. Taylor & Francis, CRC Press, Boca Raton FL.

Fitzpatrick, R. 2020. *Modeling q95 Windows for the Suppression of Edge Localized Modes by Resonant Magnetic Perturbations in the DIII-D Tokamak*. Phys. Plasmas **27**, 102511.

Fitzpatrick, R., and Hender, T.C. 1994. *Effect of a Static External Magnetic Perturbation on Resistive Mode Stability in Tokamaks*. Phys. Plasmas **1**, 3337.

Fitzpatrick, R., and Nelson, A.O. 2020. *An Improved Theory of the Response of DIII-D H-mode Discharges to Static Resonant Magnetic Perturbations and its Implications for the Suppression of Edge Localized Modes*. Phys. Plasmas **27**, 072501.

Fitzpatrick, R., and Waelbroeck, F.L. 2005. *Two-Fluid Magnetic Island Dynamics in Slab Geometry. I. Isolated Islands*.

Fitzpatrick, R., and Waelbroeck, F.L. 2005a. *Two-Fluid Magnetic Island Dynamics in Slab Geometry. II. Islands Interacting with Resistive Walls or Resonant Magnetic Perturbations*. Phys. Plasmas **12**, 022308.

Fitzpatrick, R., and Waelbroeck, F.L. 2009. *Effect of Flow Damping on Drift-Tearing Magnetic Islands in Tokamak Plasmas*. Phys. Plasmas **16**, 072507.

Freidberg, J.P. 1987. *Ideal Magnetohydrodynamics*. Plenum, New York NY.

Furth, H.P., Killeen, J., and Rosenbluth, M.N. 1963. *Finite-Resistivity Instabilities of a Sheet Pinch*. Phys. Fluids **6**, 459.

Gates, D.A., and Hender, T.C. 1996. *Resistive Wall Induced Forbidden Bands of Mode Rotation Frequency on the COMPASS-D Tokamak*. Nucl. Fusion **36**, 273.

Gimblett, C.G., and Peckover, R.S. 1979. *On the Mutual Interaction Between Rotation and Magnetic Fields for Axisymmetric Bodies.* Proc. Roy. Soc. London **369**, 1732.

Goldston, R.J. 1984. *Energy Confinement Scaling in Tokamaks: Some Implications of Recent Experiments with Ohmic and Strong Auxiliary Heating.* Plasma Phys. Control. Fusion **26**, 87.

Hammett, G.W., Dorland, W., and Perkins, F.W. 1992. *Fluid Models of Phase Mixing, Landau Damping, and Nonlinear Gyrokinetic Dynamics.* Phys. Fluids B **4**, 2052.

Hastie, R.J., Militello, F., and Porcelli, F. 2005. *Nonlinear Saturation of Tearing Mode Islands.* Phys. Rev. Lett. **95**, 065001.

Hazeltine, R.D., Kotschenreuther, M., and Morrison, P.G. 1985. *A Four-Field Model for Tokamak Plasma Dynamics.* Phys. Fluids **28**, 2466.

Hazeltine, R.D., and Meiss, J.D. 1985. *Shear-Alfvén Dynamics of Toroidally Confined Plasmas.* Physics Reports **121**, 1.

Hazeltine, R.D., and Meiss, J.D. 1992. *Plasma Confinement.* Addison-Wesley, Redwood City CA.

Hender, T.C., et al. 1992. *Effect of Resonant Magnetic Perturbations on COMPASS-C Tokamak Discharges.* Nucl. Fusion **32**, 2091.

Hirshman, S.P. 1978. *The Ambipolarity Paradox in Toroidal Diffusion, Revisited.* Nucl. Fusion **18**, 917.

Hirshman, S.P., and Sigmar, D.J. 1981. *Neoclassical Transport of Impurities in Tokamak Plasmas.* Nucl. Fusion **21**, 1079.

Howell, D.F., Hender, T.C., and Cunningham, G. 2007. *Locked Mode Thresholds on the MAST Spherical Tokamak.* Nucl. Fusion **47**, 1336.

ITER Physics Basis Editors 1999. *Plasma Confinement and Transport.* Nucl. Fusion **39**, 2175.

La Haye, R.J., et al. 2003. *Propagation of Magnetic Islands in the $E_r = 0$ Frame of Co-Injected Neutral Beam Driven Discharges in the DIII-D Tokamak.* Phys. Plasmas **10**, 3644.

Lazzaro, E., et al. 2002. *Error Field Locked Modes Thresholds in Rotating Plasmas, Anomalous Braking and Spin-Up.* Phys. Plasmas **9**, 3906.

Menard, J.E., et al. 2010. *Progress in Understanding Error-Field Physics in NSTX Spherical Torus Plasmas.* Nucl. Fusion **50**, 045008.

Militello, F., and Porcelli, F. 2004. *Simple Analysis of the Nonlinear Saturation of the Tearing Mode*. Phys. Plasmas **11**, L13.

Monier-Garbet, P., et al. 1997. *Effects of Neutrals on Plasma Rotation in DIII-D*. Nucl. Fusion **37**, 403.

Nave, M.F.F., and Wesson, J.A., 1990. *Mode Locking in Tokamaks*. Nucl. Fusion **30**, 2575.

Park, J.-K., et al. 2012. *Sensitivity to Error Fields in NSTX High β Plasmas*. Nucl. Fusion **52**, 023004.

Reif, F. 1965. *Fundamentals of Statistical and Thermal Physics*. McGraw-Hill, New York NY.

Richardson, A.S. 2019. *2019 NRL Plasma Formulary*. Naval Research Laboratory, Washington DC.

Rutherford, P.H. 1973. *Nonlinear Growth of the Tearing Mode*. Phys. Fluids **16**, 1903.

Scott, B.D., Hassam, A.B., and Drake, J.F. 1985. *Nonlinear Evolution of Drift-Tearing Modes*. Phys. Fluids **28**, 275.

Scoville, J.T., et al. 1991. *Locked Modes in DIII-D and a Method for Prevention of the Low Density Mode*. Nucl. Fusion **31**, 875.

Simmet, E.E., et al. 1996. *Statistical Analysis of the Global Energy Confinement Time in Ohmic Discharges in the ASDEX Tokamak*. Plasma Phys. Control. Fusion **38**, 689.

Smolyakov, A.I. 1993. *Nonlinear Evolution of Tearing Modes in Inhomogeneous Plasmas*. Plasma Phys. Contol. Fusion **35**, 657.

Smolyakov, A.I., et al. 1995. *Rotating Nonlinear Magnetic Islands in a Tokamak Plasma*. Phys. Plasmas **2**, 1581.

Stix, T.H. 1973. *Decay of Poloidal Rotation in a Tokamak Plasma*. Phys. Fluids **16**, 1260.

Strauss, H.R. 1976. *Nonlinear, Three-Dimensional Magnetohydrodynamics of Noncircular Tokamaks*. Phys. Fluids **19**, 134.

Thyagaraja, A. 1981. *Perturbation Analysis of a Simple Model of Magnetic Island Structures*. Phys. Fluids **24**, 1716.

Vahala, G., et al. 1980. *Perturbed Magnetic-Field Phase Slip for Tokamaks*. Nucl. Fusion **20**, 17.

Waelbroeck, F.L. 2003. *Shielding of Resonant Magnetic Perturbations in the Long Mean-Free Path Regime*. Phys. Plasmas **10**, 4040.

Waelbroeck, F.L., and Fitzpatrick, R. 1997. *Rotation and Locking of Magnetic Islands*. Phys. Rev. Lett. **78**, 1703.

Waelbroeck, F.L., Hazeltine, R.D., and Morrison, P.J. 2009. *A Hamiltonian Electromagnetic Gyrofluid Model*. Phys. Plasmas **16**, 032109.

Waelbroeck, F.L., et al. 2012. *Role of Singular Layers in the Plasma Response to Resonant Magnetic Perturbations*. Nucl. Fusion **52**, 074004.

Wang, H.-H., et al. 2018. *Density Scaling on $n = 1$ Error Field Penetration in Ohmically Heated Discharges in EAST*. Nucl. Fusion **58**, 056024.

Wang, N., et al. 2014. *Study of the Penetration of Resonant Magnetic Perturbations in J-TEXT*. Nucl. Fusion **54**, 064014.

Wesson, J.A. 1978. *Hydrodynamic Stability of Tokamaks*. Nucl. Fusion **18**, 87.

Wesson, J.A. 2011. *Tokamaks*. Oxford University Press, Oxford UK.

Wesson, J.A., et al. 1989. *Disruptions in JET*. Nucl. Fusion **29**, 641.

White, R.A., et al. 1977. *Saturation of the Tearing Mode*. Phys. Fluids **20**, 800.

Wolf, R.C., et al. 2005. *Effect of the Dynamic Ergodic Divertor in the TEXTOR Tokamak on MHD Stability, Plasma Rotation and Transport*. Nucl. Fusion **45**, 1700.

Wolfe, S.M., et al. 2005. *Nonaxisymmetric Field Effects on Alcator C-Mod*. Phys. Plasmas **12**, 056110.

Zohm, H., et al. 1990. *Plasma Angular-Momentum Loss by MHD Mode Locking*. Europhys. Lett. **11**, 745.